Molecular Cloning, Expression, Purification and Functional Implications of Recombinant Cytokines

A Thesis by Nidhi Chaubey

2/18/2014

Thesis Supervisor

Siddhartha Sankar Ghosh

Dedicated to my family for their unconditional love, encouragement and support

DEPARTMENT OF BIOTECHNOLOGY

INDIAN INSTITUTE OF TECHNOLOGY GUWAHATI

STATEMENT

I, hereby, declare that the matter embodied in this thesis entitled "***Molecular Cloning, Expression, Purification and Functional Implications of Recombinant Cytokines***" is the result of investigations carried out by me under the supervision of Prof. Siddhartha Sankar Ghosh, Department of Biotechnology, Indian Institute of Technology Guwahati, India for the award of degree of Doctor of Philosophy. This work has not been submitted elsewhere for any degree, diploma, associateship or membership etc. of any institute or university to the best of my knowledge and belief.

February, 2014

Nidhi Chaubey
Roll No. 08610617

DEPARTMENT OF BIOTECHNOLOGY

INDIAN INSTITUTE OF TECHNOLOGY GUWAHATI

CERTIFICATE

This is to certify that the thesis entitled "***Molecular Cloning, Expression, Purification and Functional Implications of Recombinant Cytokines***" being submitted to the Indian Institute of Technology Guwahati by NIDHI CHAUBEY for the award of the degree of Doctor of Philosophy in Department of Biotechnology, is a bonafide record of research work carried out by her. The contents of this thesis have not been submitted to any other University or Institute for the award of any degree or diploma.

Prof. Siddhartha Sankar Ghosh
(Supervisor)

ACKNOWLEDGEMENTS

I pay my gratitute to all those people who have played a very important role during the path of my Ph.D journey. When I joined IIT Guwahati, there were few dreams in my eyes but the success and final outcome required a lot of guidance and assistance. I am extremely fortunate to get the same throughout my Ph.D work tenure. I have been nurtured here mentally, personally and professionaly. Thus I would like to express my gratitude to my guide and mentor; Prof. Siddharta Sankar Ghosh who provided me with this golden opportunity to work in such a wonderful milieu. Here I could not only freely execute my ideas but also realize my dreams and thus do research in an amicable way. Thank you Sir, for your guidance which allowed me to stay focused and also motivated all throughout. Your words of encouragement and faith, always helped me to keep my moral high. I am indeed fortunate to have a teacher like you.

I would also like to express my heartfelt gratitude to my doctoral committee Chairperson Dr. Aiyagari Ramesh and my committee members, Dr. Anil Mukund Limaye and Dr. Bhubaneswar Mandal for evaluating my work, giving critical comments, valuable guidance and inspirations. I am also very grateful to Dr. Biplab Bose and Prof. Arun Chattopadhyay for their scientific advice, knowledge, insightful discussions and suggestions.

I am heavily indebted to my lab members Kohila, Chokalingam, Subhamoy, Archita, Sharmila, Asif, Neha, Amaresh, Upashi, Bandhan, Amit, Shilpa and Deepanjali who have provided me ongoing support, inspiration and enjoyable working environment. I am especially thankful to Amaresh, for providing me with a deeper insight about Nanotechnology. A special thank you to Archita, Sharmila and Asif for giving me suggestions while writing my papers and thesis. I also want to thank my senior lab members Gopinath, Vinod, Pallab whose constant support and guidance played an important role for understanding the work.

I take this opportunity to thank all my seniors and friends Manab, Sudeep, Thyahoo, Sandipan, Mitun, Asim, Pojul, Ashok, Rishikesh, Shraddha, Gauri, Nivedita, Saravanan, Ankana, Priyamvada, Babina. I am especially grateful to Debamitra for her unassessable fondness; she made my stay at IITG a gratifying and memorable one.

I owe my gratitude to the Department of Biotechnology, Centre for Nanotechnology, and Central Instrument Facility, IIT Guwahati for providing me all supports and necessary facilities.

My sincere thanks to our Department Technical Assistants (Mr. Sharan, Mr. Nurul, Mr. Indrajit, Mrs. Anita, Mrs. Prathana and Mrs. Rashmi).

I dedicate this work to my family members, my brother Nitish, sister Nishi, husband Ajay, mother Smt. Rita Chaubey and my father Sri Narottam Chaubey. I am also indebted to my parent in-laws Smt. Prema Tripathi and Sri S.N. Tripathi. There are many names which need to mentioned here because every person who come in our life, teach us something, which help us to be ,"What we are today". My heartfelt thank you to all.

My final words of acknowledgements to the Almighty God for giving me the strength for establishing me in such a way so that I could complete my work properly.

Nidhi

Abstract

An eventful outcome of recombinant technology is generation of recombinant proteins, among which, therapeutic proteins cloned from human origin have gained considerable importance for their reduced host antagonistic responses. New cloning strategies and efficient purification procedures are being investigated to obtain functional proteins. In this context, cytokines, the small glycoproteins known to regulate cell and tissue functions, have immense therapeutic potential. Human granulocyte macrophage colony stimulating factor (hGMCSF) is a FDA approved cytokine for the treatment of primary immunodeficiency of acute myeloid leukemia, myeloid reconstitution and bone marrow transplantation. Similarly, IFNγ, a naturally occurring cytokine produced and secreted by the immune cells, is also a FDA approved cytokine, which exerts tumoricidal and antimicrobial activity. However, therapeutic application of IFNγ is limited due to its shorter life time and rapid clearance from the body. Therefore, prolonged sustainability of IFNγ would be a viable option for exploiting maximum therapeutic benefits by its possible integration with nanoparticles. Hence, it is important to purify, characterize and study the recombinant hGMCSF and IFNγ, and their effects on cancer cells alone or in combination with chemotherapeutic drugs.

The thesis illustrates cloning of two important cytokines, GMCSF and IFNγ, in bacterial and mammalian expression systems and their applications on cancer cell growth. **Chapter 1** covers introduction and review of literature for recombinant therapeutic proteins, cloning strategy, purification procedure and their applications. The chapter also illustrates important polymeric nanoparticles for protein stabilization, the role of cytokines as adjuvant and immune surveillance and their therapeutic importance in combination therapy. **Chapter 2** describes cloning, purification of recombinant GMCSF and its functional characterization, as well as dose dependent cell proliferative activity on various cell types. **Chapter 3** describes cloning, purification and anti-cell proliferative affect of IFNγ. It also describes development of biodegradable PLGA composite nanoparticles loaded with silver nanoparticles as a suitable carrier for IFNγ protein. Further, it illustrates that the composite nanoparticle interacts with cell surface, to augment cancer cell killing by cell cycle arrest and apoptosis. In **Chapter 4,** the combined effects of recombinant GMCSF and IFNγ cytokines on MCF-7 cell death using activated macrophages producing reactive oxygen species (ROS) are described. **Chapter 5** reports generation of the cell lines over-expressing GMCSF and IFNγ, testing their sensitivity to chemotherapeutic drugs, followed by cell cycle analysis and cyclin expression profiling. Finally, **Chapter 6** summarizes Conclusion and Future Prospects of the cell proliferative effects of recombinant GMCSF, anticancer effects of recombinant IFNγ and their potential applications in cancer therapeutics.

Flow Diagram of Thesis Organization

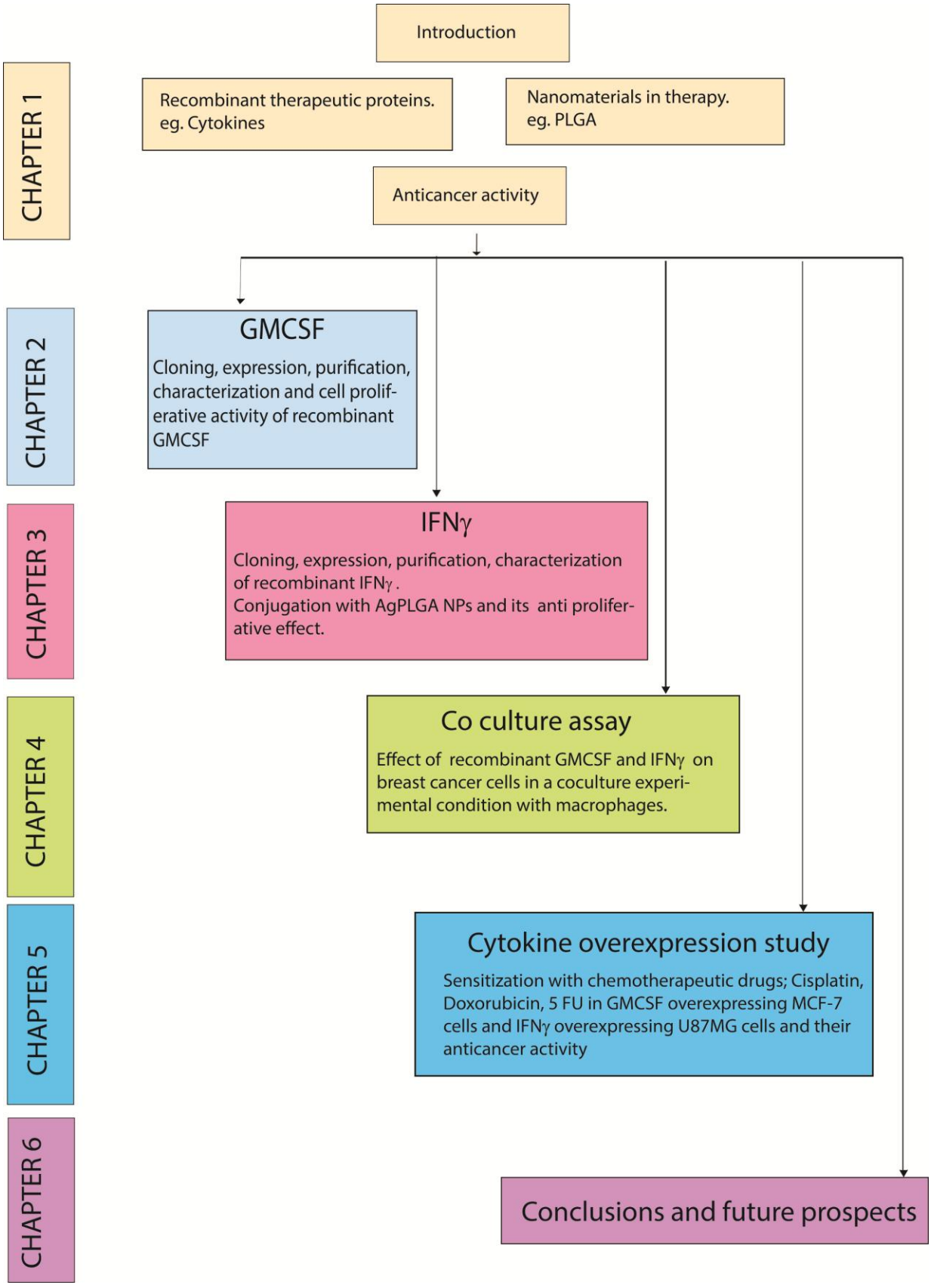

Contents

Chapter 5: Overexpression of cytokines in mammalian cells

Abbreviations

5 FU- 5 Fluorouracil

ACN- Acetonitrile

Ag NPs- Silver nanoparticles

Ag PLGA NPs- Silver nanoparticle loaded PLGA composite nanoparticle

AO- Acridine orange

APC- Antigen presenting cells

BSA- Bovine serum albumin

CD- Circular dichroism

CHCA- α cyano-4-hydroxycinnamic acid

CO2- Carbon di oxide

CSF- Colony stimulating factor

DAB- 3,3'diaminobenzidine

DEPC- Diethyl pyrocarbonate

DMEM- Dulbecco's Modified Eagle's Medium

DNA- Deoxyribonucleic acid

dNTPs- Deoxyneucleotide triphosphate

EB- Ethidium bromide

EDTA- Ehylene diamine tetra acetate

FACS- Fluorescence activated cell sorting

FBS- Fetal bovine serum

FDA- US food and drug administration

FITC- Fluorescein isothiocyanate

GMCSF- Granulocyte macrophage colony stimulating factor

GST- Glutathione S transferase

h- Hours

HRP- Horse radish peroxidase

IPTG- Isopropyl-1-thio-P-D galactopyranoside

MALDI TOF- Matrix assisted laser desorption ionization; time of flight

min- Minutes

mRNA- Messenger RNA

ms-milisecond

MTT- 3-(4, 5-dimethylthiazol-2-yl)-2, 5-diphenyltetrazolium bromide

NPs- Nanoparticles

OD- Optical density

PBS- Phosphate buffer saline

PCR- Polymerase chain reaction

PI- Propidium iodide

PLGA- Poly lactide co glycolide

PVA- Poly vinyl alcohol

RNA- Ribonucleic acid

SDS PAGE- Sodium dodecyl sulphate; polyacrylamide gel electrophoresis

TAE- Tris acetate EDTA

X gal- 5-bromo-4-chloro-3-indolyl-β-D-galactopyranoside

XTT- 2, 3-bis-(2-methoxy-4-nitro-5-sulfophenyl)-2H-tetrazolium-5-carboxanilide

CHAPTER 1

This chapter briefly describes about recombinant DNA technology, cancer therapy, benefits of combination therapy in cancer and importance of cytokines as adjuvant therapy.

CHAPTER 1

Introduction

1.1 Recombinant proteins:

Emergence of recombinant DNA (rDNA) technology has great impact on developing recombinant proteins since last few decades, mainly due to its cost effective, time saving and easy regulation from laboratory to scale-up stages. The pharmaceutical products are no longer solely dependent on the biological sources; rather rDNA technology is now in routine practice for making sufficient quantity of proteins. Hence, production of therapeutically important protein has gained importance because of evolving expression technology. Human insulin is the first therapeutic protein produced by rDNA technology. Insulin expressed in *Escherichia coli* is now used for insulin dependent diabetic patients (Reference no. 71, Website 1). This approach has replaced the whole market of pig and cattle based formation of insulin (Gualandi *et al*, 2001). A few other recombinant products are chymosin (Reference no. 72, Website 2), growth hormone soomatotropin (Von Fange *et al*, 2008), blood clotting factor VIII (Manco-Johnson *et al*, 2010), hepatitis B vaccine, recombinant HIV proteins for HIV infection kit. Many other recombinant products such as, golden rice, insect and herbicide resistant crops are in trial phases. Clinically important proteins, like cytokines, are required in ample amount for their applications. However, expression profile of cytokines vary substantially depending on the physiological state of the body (Sakai *et al*, 1987; Reference no. 73, Website 3).

The level of biologically significant cytokines is too low in human to be considered as a beneficial source of clinical use. The only way to resolve this issue is the generation of recombinant cytokines, where desired cytokine genes can be cloned into suitable expression vectors, such as, yeast (*Saccharomyces cerevisiae* expression system), bacteria (*Escherichia coli* expression system), mammalian cells (Chinese hamster ovary cells) or baculovirus expression system (Andersen *et al*, 2002). The major obstacle in purification of the recombinant proteins is to make them in soluble form. In the recent years, several efforts have been made by various research groups to address this issue either by genetic engineering of laboratory strains or by tedious search for new strains, which can adopt easily in laboratory conditions (Chen *et al*, 2012). Efforts are also being made to resolve the problem related to glycosylation of eukaryotic proteins. The discovery of N-linked glycosylation in Gram negative

Campylobacter jejuni bacteria, paved the avenue for synthesizing glycosylated proteins using *E.coli* system (Wacker *et al*, 2002). Recombinant proteins produced by rDNA technology provide a platform to investigate structural and functional relationships of the proteins (Toren *et al*, 2002; Whiles *et al*, 2002; Pappachan *et al*, 2008).

1.2 Combination therapy:

The recombinant proteins have several therapeutic applications for many dreadful diseases. Cancer is one of the most disastrous disease and WHO mortality survey showed that cancer is second leading cause of death in the world (Reference no. 74 and 75; Website 4 and 5). There are several methods available for cancer treatment, which include surgery, chemotherapy, hormone therapy, laser therapy, mastectomy, cryosurgery, cancer vaccination, radiotherapy, bone marrow transplantation and adjuvant therapy. The main drawback in single drug therapy emerges with frequent mutations in cancer, which lead to drug resistant population. This effect could be minimized by multiple therapies, in other words combination therapy, which increases the chance of effective treatment (Komarova *et al*, 2013). Other than this, therapeutic modules like mastectomy, bone marrow transplantation and chemotherapy can be supported by combination therapy, to overcome their side effects and rescue normal cells from the harmful effect of therapy. Recently, an application of recombinant proteins in cancer therapy has gained much importance (Pastan *et al*, 1991; Kreitman *et al*, 2003; Pastan 2003; Vázquez *et al*, 2009). Recombinant proteins used as adjuvant not only increase the efficacy, but may increase the chance of long term survival of the patients. In case of breast cancer therapy, adjuvant therapy is well acceptable. Although it has some side effects, they are outweighed by the benefits of adjuvant therapy. Scheme 1.1 shows different approaches of cancer therapy (Reference no. 76, Website 6).

Scheme 1.1. Different approaches for cancer therapy

Combination therapy is preferred over single therapeutic module for reducing the tumour load (Miles *et al*, 2002). A recent report showed that combination therapy not only reduced cancer recurrence (Reference no. 77, Website 7), but also significantly improved survival rate of metastatic melanoma patient in treatment with GMCSF (Reference no. 78, Website 8). Scheme 2 illustrates the benefit of combination therapy.

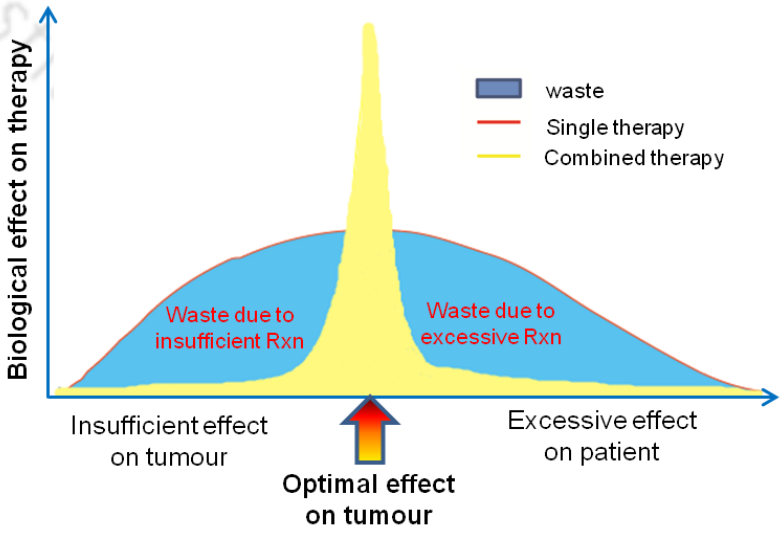

Scheme 1.2. Diagram showing the effect of combination therapy

The biological molecules, like cytokines, elicit controlled immune response in combination therapy. Cytokines are small soluble glycoprotein molecules secreted by the cells of innate and adaptive immune system and they act as chemical messenger, regulate homeostasis, and behave as hormonal regulators to co-ordinate with other cells to exert proper immune response through cell signaling. For example, interleukin 2 (IL-2) controls the cell mediated immunity by triggering the production of T cells (Reference no. 79, Website 9). While the body cells are connected to each other through cell to cell interactions, the presence of cytokine enables rapid progression of signals in regulated process at their nano to pico molar concentration (Lee *et al*, 2011).

1.3 Classification of cytokines:

Classification of cytokines depends mainly on either their origin or biological effects due to less available information regarding three dimensional conserved structures (Dinarello *et al*, 2000). On the functional basis, the cytokines may be either pro-inflammatory or anti inflammatory. Pro-inflammatory cytokines, like IL-1, IL-8, TNF, GMCSF, IFNγ mediate the process of inflammation by activating a cascade of genes. On the contrary, anti- inflammatory cytokines block or suppress the inflammation process. The cytokines, like TGF-β, IL-4, IL-10, IL-13 inhibit the production of IL-1, IL-8 and TNF (Dinarello *et al*, 2000). The cytokines produced by lymphocytes are called lymphokines, whereas those produced by monocytes or macrophages are called as monokines (Kouttab *et al*, 1984). Interleukins are a class of lymphokines, which are secreted by lymphocytes and govern proliferation function and cellular responses of lymphocytes (Akdis *et al*, 2011). One group of cytokines are chemokines, which are released by cells at the site of injury or infection and play a major role in inflammation by recruiting other immune cells to the affected region for repairing the damage. Based on their mode of action, chemokines may be homeostatic in nature and control the migration of cells in the body during tissue repairing, such as, CCL 12, CCL 19, CCL 21, CCL 25 or they may be inflammatory as CCL 3, CCL 5 (Le *et al*, 2004).

Receptor based classification distributes these molecules in three main subclasses (Lee *et al*, 2011):

1. Type I cytokine receptors share a common signaling subunit, γ chain as in IL-2, IL-4, IL-7, IL-9 and GMCSF.
2. Type II cytokine receptors composed of a signaling chain and a ligand binding chain eg. IFNα, IFNβ, IFNγ and IL-10.
3. Immunoglobin superfamily receptors have an extracellular immunoglobin domain which binds to MCSF, stem cell factors, IL-1, IL-18.

Cytokines include a diverse collection of colony stimulating growth factors such as MCSF, GMCSF, interleukins, interferon (Class I and II interferons). Clinical studies are being persued to test their benefits in diseases such as cancer, hepatitis C and HIV infection (Angel *et al*, 2001; Brown *et al*, 2005). Pleiotropic behavior, redundancy and multi-functionality are few important features for cytokines (Tayal *et al*, 2008). Most important role of lymphokines is to recruit immune cells including macrophages at the infection site and activate them to exert proper immune response. Colony stimulating factors (CSFs) stimulate growth and differentiation of many cell types of bone marrow. Similarly, Granulocyte macrophage colony stimulating factor (GMCSF) stimulates the growth and differentiation of all granulocytes, such as as eosinophil, neutrophils, basophils as well as macrophages (Barreda *et al*, 2004).

1.4 GMCSF (Granulocyte macrophage colony stimulating factor):

Human granulocyte macrophage colony stimulating factor (hGMCSF) is particularly responsible for proliferation and development of myeloid lineages. First human GMCSF cloning was reported using mouse GMCSF cDNA library derived from the mRNA libraries of HUT-102 and mitogen stimulated T lymphocyte. The gene for GMCSF was shown to be localized at the chromosomal region 5q23-q31. Human GMCSF protein is a 144 amino acid long peptide having molecular weight around 16 kDa (Cantrell *et al*, 1985). GMCSF is now a FDA approved cytokine for treatment of primary immunodeficiency of neutropenia, acute myeloid leukemia, myeloid reconstitution and bone marrow transplantation (Roy *et al*, 2009).

The role of GMCSF as a cancer vaccine is now being explored. Available reports showed mice vaccinated with autologous tumour cells expressing GMCSF were protected from subsequent tumour challenges (Shi *et al*, 1999). Genetically modified tumour vaccine has been reported to secrete GMCSF, which attracts phagocytic cells (dendritic cells) towards the tumour and finally these dendritic cells engulf the tumour

cells. Tumour cells express tumour antigens which are identified by T cell and thus T cells expansion and activation occur to mediate cell based immune response (Gupta *et al*, 2010).

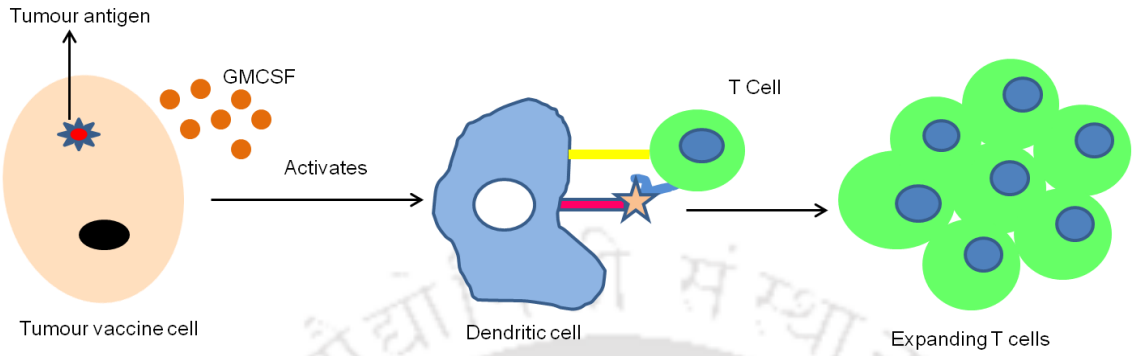

Fig 1.1. Mode of action of autologous tumour vaccine secreting GMCSF cytokine

High peritumoral level of GMCSF produced as transgenes, execute a much better anti-tumour response by attracting T lymphocytes, natural killer cells, neutrophils and macrophages to the tumour site without any systemic cytotoxicity (Shi *et al*, 1999). In addition to these, GMCSF helps in avoiding chronic inflammatory response and autoimmunity after chemo or any other therapy by clearing the load of apoptotic bodies by potentiating scavenger cells and APC to internalize apoptotic tumour cells (Galati *et al*, 2000).

1.5 IFNγ (Interferon gamma):

Another group of lymphokines are Interferons, which are identified on the basis of their antiviral activity. Among all these, IFNγ has drawn more attention in therapy. Human IFNγ gene is located at 12q24.1 (NM_000619). Complete coding region of human interferon is composed of 501 bp which are translated to 166 amino acids (Protein ID: AAH70256.1). It is a naturally occurring cytokine produced and secreted by the immune system cells which exerts tumoricidal and antimicrobial activity. IFNγ is also a FDA approved cytokine (Roy *et al*, 2009). It governs many immunoregulatory functions in different cell types. Figure 1.2 demonstrates briefly about the effector cells of interferon gamma:

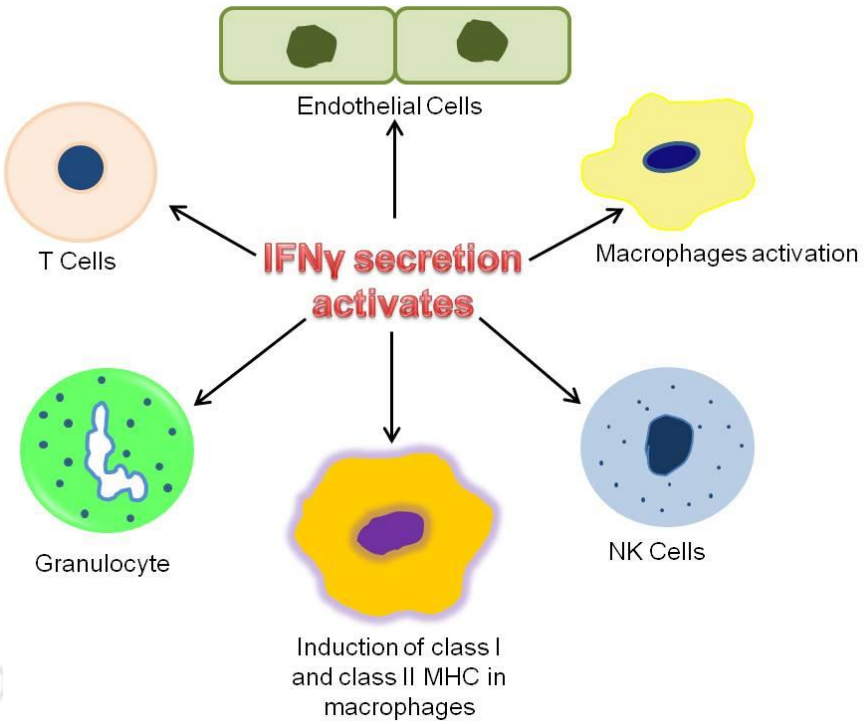

Fig 1.2. Mode of action of IFNγ

IFNγ exerts both defending and pathological effect. It is the principal macrophage activator (Schroder *et al*, 2003), which determines the fate of macrophages either in M1 cytotoxic form or in M2 alternative form. IFNγ generates reactive oxygen species (ROS), which in turn polarize macophages in M1 subtype. M1 subtype exerts cytotoxic and immune stimulatory responses against cancer (Sica *et al*, 2012).The profound immunomodulatory function of IFNγ has inspired its application in many diseases like, chronic granulomatous disease, autoimmune disease, rheumatic arthritis, multiple sclerosis, lupus nephritis and so many others (Schroder *et al*, 2003). However, therapeutic applications of IFNγ are limited due to its shorter life time and rapid clearance from body (Wills *et al*, 1990). Furthermore, its higher dose and repetitive uses may cause severe side effects Therefore, prolonged sustainability of IFNγ would be a viable option for exploiting maximum therapeutic benefits by its possible conjugation or stabilization with nanoparticles. Many cytokines including IFNγ have therapeutic importance, but still its rapid clearance from host body and repetitive administration limit its application for treatment. This problem can be overcome with the help of nanoparticles, which help in sustained release of cytokine, thus facilitates its effectiveness for a longer duration. There are few reports available regarding this, including that of IFNγ conjugated with BSA NPs (Segura *et al*, 2005).

1.6 PLGA (Poly lactide co glycolide):

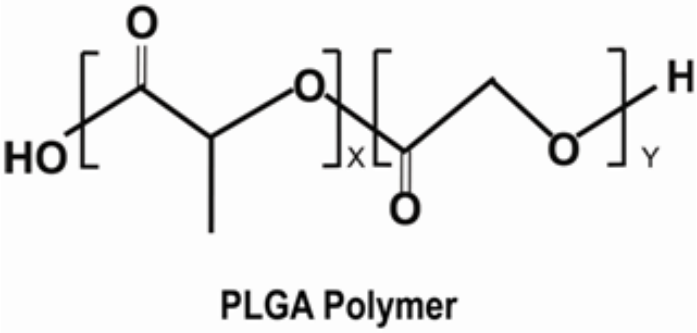

Fig 1.3. Repetitive subunit of PLGA polymer

Among all the delivery agents, PLGA (Poly lactide co glycolide) has emerged as most successful biodegradable nanoparticle with well described formulation procedures. The uptake of PLGA by different admistration routes such as, intravenously, oral, nasal, ocular, transdermal, make it more favourable as a delivery agent (Vila *et al*, 2002; Cegnar *et al*, 2004).

These FDA approved therapeutically important nanoparticles have revalorized the drug development process, as they can control the release as well as targeted delivery of anticancer agents (Dinarvand *et al*, 2011). After degradation, their metabolites lactic acid and glycolic acid enter into Kreb's cycle for complete degradation (Panyam *et al*, 2003; Vij *et al*, 2010). PLGA is already approved for drug delivery via parenteral administration by European Medicine Agency and FDA (Danhier *et al*, 2012).

Controlled release of GCSF (Choi *et al*, 2006), Endostar (a 20 kDa anti angiogenic peptide) and PE38KDL have been reported with the help of this polymer. The systemic administration of PLGA based drug leads to enhanced permeability. PLGA based nanoparticles are being actively used in inflammatory diseases like rheumatoid arthritis, inflammatory bowel disease and lung disease. Therapeutic proteins like superoxide dismutase, which is used in treatment of cerebral diseases and has *in vivo* half-life of 6 min only, could be effectively uptaken by neurons and passed through blood brain barrier with increased stability when encapsulated with PLGA. PLGA can be effectively incubated with other ligands as well, to increase their efficacy. Lactoferrin has a receptor on blood brain barrier; so conjugation of this glycoprotein with PLGA mediates its targeted delivery in brain. PLGA conjugation enhances the

efficacy of the system. Also curcumin conjugated with PLGA exerts more pronounced effect on cancer cells as compared to free curcumin (Mukerjee *et al*, 2009; Danhier *et al*, 2012). PLGA has been established as a multimodal polymeric system also, which could incorporate tailored antibodies with magnetic nanocrystals along with anticancer drugs. This ultrasensitive composite was shown to mediate sustained release of drug towards cancer site (Yang *et al*, 2007) (Figure 1.4). Surface modification of PLGA formulation provides a promising way to treat cancer (Kocbek *et al*, 2007; Cai *et al*, 2008).

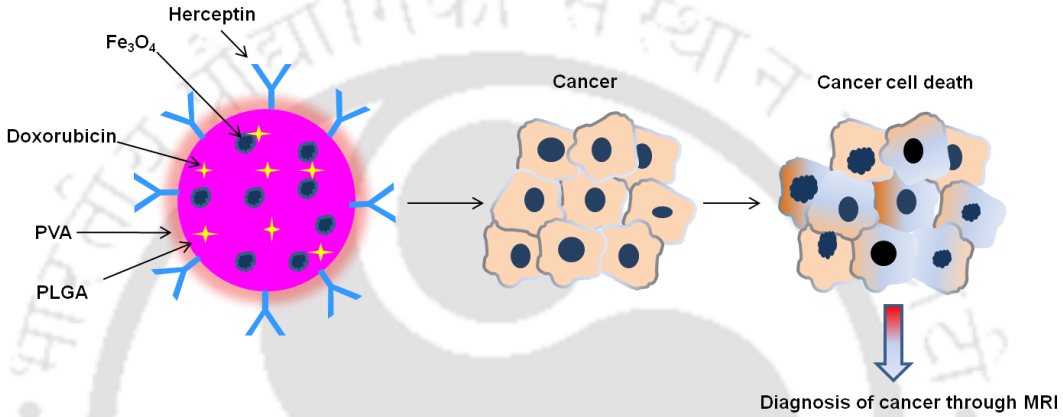

Fig 1.4. A multicomponent system for targeting cancer cells using PLGA

1.7 Silver Nanoparticles

Antimicrobial properties:

Silver is known for its antimicrobial properties against a wide range of micro organisms. The US Food and Drug Administration approved colloidal silver for wound treatment. In 1960s, research in antimicrobial efficacy of silver showed the use of 0.5% silver nitrate solution in the burn area by Moyer *et al* (1965) and 1% silver sulfadiazine (SSD) cream to treat burn wound infections by Fox *et al* (1968). Sondi *et al* (2004) first reported the antimicrobial activity of Ag NPs against *E. coli* as a model Gram negative bacterium. They found that Ag NPs accumulated in the membrane of treated cells thereby causing damage, was evident from the formation of pits on cell surface. Baker *et al* (2005) reported the antibacterial efficacy of Ag NPs against *E. coli* and related the surface area to volume ratio of NPs to their antibacterial activity. The smaller Ag NPs exhibited higher bactericidal activity owing to larger surface area to volume ratio. A very recent study by Falentin-Daudré *et al* (2012) showed formation of Ag NPs containing antimicrobial coating formed by layer-by-

layer (LbL) assembly, for imparting strong antibacterial activity against *E. coli* to stainless steel. In this regard, substantial research from our laboratory has also demonstrated antibacterial potential of Ag NPs either alone or in the form of composite. A three component antimicrobial iodinated chitosan-Ag NP composite was developed by Banerjee *et al* (2010), which exhibited antibacterial activity against *E. coli* at low concentration of its individual components i.e. chitosan, iodine and Ag NPs. In another study, Sahoo *et al* (2011) developed a nanocomposite comprised of p-hydroxyacetanilide (paracetamol) dimer and Ag NPs by reaction of $AgNO_3$ and paracetamol. The composite killed bacteria efficiently through ROS generation that led to oxidation of the dimer to N-acetyl-p-benzoquinone imine, which acted as a DNA gyrase inhibitor causing linearization of DNA leading to cell death.

Effect on Silver nanoparticles on Mammalian cells:

Ag NPs have been reprted to possess antiplatelet properties (Shrivastava *et al*, 2009). Studies are being pursued to explore the possible mechanisms of cytotoxicity and possible genotoxicity of Ag NPs in mammalian cells (AshaRani *et al*, 2008; 2009). In this regard, a study conducted by Hussain *et al* (2005) reported depletion in the level of glutathione, reduction in mitochondrial potential and increase in ROS level in BRL 3A rat liver cells exposed to Ag NPs, which suggested oxidative stress to be the possible mechanism of toxicity of Ag NPs. Similarly, Carlson *et al* (2008) also demonstrated Ag NPs-induced oxidative stress in alveolar macrophages and found toxicity of Ag NPs. Furthermore, Hsin *et al* (2008) demonstrated involvement of ROS and JNK dependent pathway in Ag NPs induced apoptosis in mouse fibroblast NIH3T3 cells. The *in vitro* toxicity study conducted by Arora *et al* (2008) suggested a safe range of use of 7–20 nm spherical Ag NPs in human fibrosarcoma (HT-1080) and human skin carcinoma (A431) cells. Besides, Franco-Molina *et al* (2010) reported antitumour activity of Ag NPs on MCF-7 human breast cancer cells. In our laboratory, Ag NPs alone or in combination with gene therapy have been demonstrated to induce apoptosis in mammalian cells (Gopinath *et al*, 2008; 2010).

1.8 Tumour progression phases in host:

Tumour formation in human body can be actively supervised and controlled by proper immune surveillance. Clinical studies have shown that our immune cells continuously

recognize and eliminate the tumour cells from the body. Basically, the progression of tumour happens in three main steps (Teng *et al*, 2008):

1. Elimination phase: In this phase body immune cells actively invade tumour cells.
2. Equilibrium phase: Tumour cells which are rescued from elimination phase establish themselve in equilibrium phase. Now immune cells can control the growth of transformed cells, but they can not eliminate tumour from body.
3. Escape phase: In this phase, transformed cells are able to rescue themselves from body immune responses and are free to divide.

Early diagnosis of these key features is vital for the detection of cancer. Upto the equilibrium phase, if immune cells can overcome with cancer cells, there will be a great breakthrough in cancer treatment. During the treatment of cancer, conventional therapy modules solely kill the cells, but non conventional approach of treatment opens up new avenues for combination of immune cells in therapy and enhance the effectuality of the whole system. If host immune cells directly respond to the infection or abnormality, the effect becomes more pronounced. But there are several reports available where host immune cells, like macrophages, can also play a bipolar role as tumour associated macrophages in cancer progression (Chen *et al*, 2004). Tumour associated macrophages, which are also known as M2 or alternative macrophages, produce polyamines, which induce proliferation and collagen production, thus helping in the progression of tumour, by the response of IL-4, IL-10, IL-13. The other form of macrophages is the classical/M1 type, which is the cytotoxic form of macrophages, generally activated in the presence of IFNγ or LPS and produce nitric oxide, TNF and other ROS intermediates, which mediate resistance towards intracellular pathogens, tissue destruction and antitumour resistance (Klimp *et al*, 2002; Classen *et al*, 2009; Mantovani *et al*, 2009). IFNγ also initiates dendritic cell, monocyte to macrophage conversion solely or in combination with some other cytokines, like GMCSF (Delneste *et al*, 2002; Martinez *et al*, 2006). Thus, it is clear that mononuclear phagocytic cells have an excellent tendency of plasticity towards the signaling molecule. Figure 1.5 presents the effect of external stimuli over the macrophages cells in a simple manner, which gives an idea about the coculture of these scavenger cells along with tumour cells in presence of different stimuli like GMCSF and IFNγ cytokines.

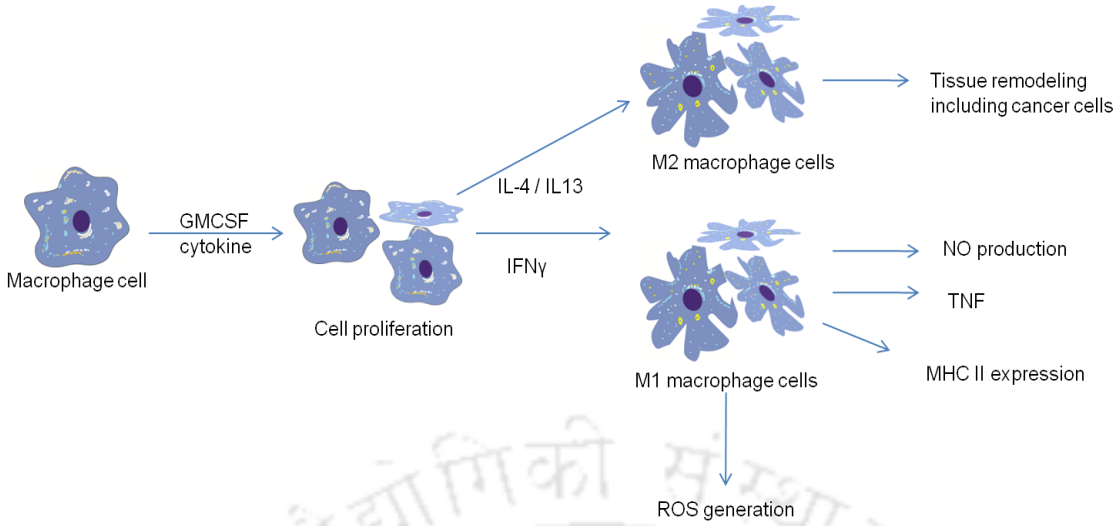

Fig 1.5. Interplay of GMCSF and IFNγ on macrophages cells

Reports regarding deregulation of cytokine levels showed a differential effect on human health (Mezzano *et al*, 2000; Kim *et al*, 2002). Overexpression system provides an excellent platform to study the signaling pathway as well as effect of drugs components in combination (Shi *et al*, 1999). An overexpressed system provides an oppurtunity to speculate the effect of drugs like doxorubicin, cisplatin and 5FU on cancer cells.

1.9 Chemotherapeutic drugs block cell cycle:

Chemotherapeutic drugs, such as, doxorubicin, cisplatin and 5FU block cell cycle progression by intercalating into DNA. Doxorubicin mainly blocks G2-M phases of cells (DiPaola *et al*, 2002) and cisplatin preferentially blocks S phase (Fishel *et al*, 2005), whereas, 5FU is involved in G1 or early S phase blockage (Takeda *et al*, 1999).

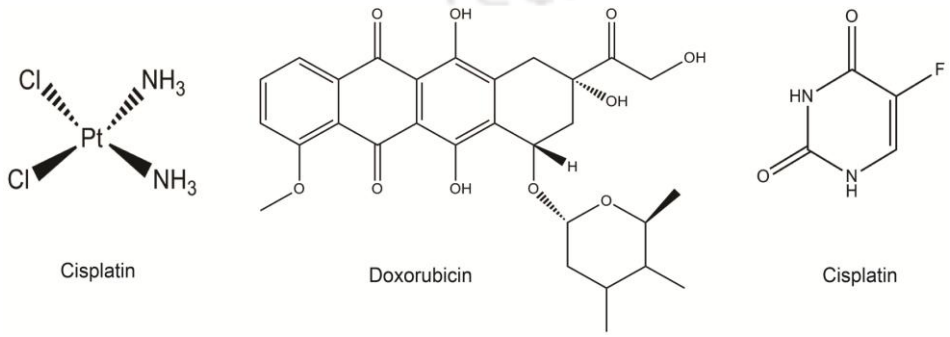

Fig 1.6. Chemical structure of some chemotherapeutic drugs

Among these drugs, 5FU, an antimetabolite drug is used to treat breast and ovarian cancers and solid tumours (Longley *et al*, 2003). It is converted into 5-fluorodeoxyuridine monophosphate (5-FdUMP) and 5-fluorouracil tri phosphate (5-FUTP). 5-FdUMP inhibits the catalytic activity of thymidylate synthase, thus disrupting DNA replication. 5-UTP is incorporated into RNA, thus impairing its function (Parker and Cheng, 1990; Longley *et al*, 2003).

Salient features:

From the literature review, the findings are as follows:

- Combination therapy with suitable therapeutic small molecules may augment the therapeutic efficacy.
- Proliferative effect of GMCSF is important for non-haematopoeitic cells
- Increased shelf life of IFNγ with suitable nanocarrier plays an important role in bio-therapeutic regime.
- Combined effect of recombinant cytokine GMCSF and IFNγ may augment therapeutic efficacy in a mixed cell population.
- Overexpression of recombinant cytokine in cancer cells may be useful to study their roles in presence of different chemotherapeutic drugs.

Thus, based on those key findings, the following strategies were devised to achieve the goal in this present thesis.

- Cloning of human GMCSF into bacterial expression vector for purification, characterization of recombinant protein and its proliferative activity study on various cell lines, also its *in silico* analysis.
- Cloning of IFNγ into bacterial expression vector for its purification, characterization and preparation of Ag NPs coated PLGA nanoparticles for its stablization.
- Establishment of coculture assay using macrophages along with breast cancer cells to examine the effect of purified GMCSF and IFNγ protein in mixed cell population. A quick flow cytometry based method to study mixed cell population in presence recombinant cytokines and doxorubicin.

- Generation of GMCSF overexpressing breast cancer and IFNγ overexpressing neuroblastoma stable cell lines to study their sensitization in presence of different chemotherapeutic drugs, such as 5FU, doxorubicin and cisplatin.

1.10 References

1. Akdis, M., Burgler, S., Crameri, R., Eiwegger, T., Fujita, H., Gomez, E., Klunker, S., Meyer, N., O'Mahony, L., Palomares, O., et al. (2011). Interleukins, from 1 to 37, and interferon-γ: receptors, functions, and roles in diseases. J. Allergy Clin. Immunol. *127*, 701–721.e1–70.
2. Andersen, D.C., and Krummen, L. (2002). Recombinant protein expression for therapeutic applications. Curr. Opin. Biotechnol. *13*, 117–123.
3. Angel, J.B. (2001). Improving immune function and controlling viral replication in HIV-1-infected patients with immune-based therapies. AIDS Read *11*, 209–221.
4. Arora, S., Jain, J., Rajwade, J.M., and Paknikar, K.M. (2008). Cellular responses induced by silver nanoparticles: In vitro studies. Toxicol. Lett. *179*, 93–100.
5. Asharani, P.V., Lian Wu, Y., Gong, Z., and Valiyaveettil, S. (2008). Toxicity of silver nanoparticles in zebrafish models. Nanotechnology *19*, 255102.
6. AshaRani, P.V., Low Kah Mun, G., Hande, M.P., and Valiyaveettil, S. (2009). Cytotoxicity and genotoxicity of silver nanoparticles in human cells. ACS Nano *3*, 279–290.
7. Baker, C., Pradhan, A., Pakstis, L., Pochan, D.J., and Shah, S.I. (2005). Synthesis and antibacterial properties of silver nanoparticles. J Nanosci Nanotechnol *5*, 244–249.
8. Banerjee, M., Mallick, S., Paul, A., Chattopadhyay, A., and Ghosh, S.S. (2010). Heightened reactive oxygen species generation in the antimicrobial activity of a three component iodinated chitosan-silver nanoparticle composite. Langmuir *26*, 5901–5908.
9. Barreda, D. (2004). Regulation of myeloid development and function by colony stimulating factors. Developmental & Comparative Immunology *28*, 509–554.
10. Brown, P.A., and Angel, J.B. (2005). Granulocyte-macrophage colony-stimulating factor as an immune-based therapy in HIV infection. J Immune Based Ther Vaccines *3*, 3.
11. Cai, C., Bakowsky, U., Rytting, E., Schaper, A.K., and Kissel, T. (2008). Charged nanoparticles as protein delivery systems: A feasibility study using lysozyme as model protein. European Journal of Pharmaceutics and

Biopharmaceutics *69*, 31–42.

12. Cantrell, M.A., Anderson, D., Cerretti, D.P., Price, V., McKereghan, K., Tushinski, R.J., Mochizuki, D.Y., Larsen, A., Grabstein, K., and Gillis, S. (1985). Cloning, sequence, and expression of a human granulocyte/macrophage colony-stimulating factor. Proc. Natl. Acad. Sci. U.S.A. *82*, 6250–6254.
13. Carlson, C., Hussain, S.M., Schrand, A.M., K. Braydich-Stolle, L., Hess, K.L., Jones, R.L., and Schlager, J.J. (2008). Unique Cellular Interaction of Silver Nanoparticles: Size-Dependent Generation of Reactive Oxygen Species. The Journal of Physical Chemistry B *112*, 13608–13619.
14. Cegnar, M., Premzl, A., Zavašnik-Bergant, V., Kristl, J., and Kos, J. (2004). Poly(lactide-co-glycolide) nanoparticles as a carrier system for delivering cysteine protease inhibitor cystatin into tumor cells. Experimental Cell Research *301*, 223–231.
15. Chen, J.J.W. (2004). Tumor-Associated Macrophages: The Double-Edged Sword in Cancer Progression. Journal of Clinical Oncology *23*, 953–964.
16. Chen, R. (2012). Bacterial expression systems for recombinant protein production: E. coli and beyond. Biotechnology Advances *30*, 1102–1107.
17. Choi, S.H., and Park, T.G. (2006). G-CSF loaded biodegradable PLGA nanoparticles prepared by a single oil-in-water emulsion method. Int J Pharm *311*, 223–228.
18. Classen, A., Lloberas, J., and Celada, A. (2009). Macrophage Activation: Classical Vs. Alternative. In Macrophages and Dendritic Cells, N.E. Reiner, ed. (Totowa, NJ: Humana Press), pp. 29–43.
19. Danhier, F., Ansorena, E., Silva, J.M., Coco, R., Le Breton, A., and Préat, V. (2012). PLGA-based nanoparticles: An overview of biomedical applications. Journal of Controlled Release *161*, 505–522.
20. Delneste, Y. (2002). Interferon-gamma switches monocyte differentiation from dendritic cells to macrophages. Blood *101*, 143–150.
21. Dinarello, Charles A. (2000). Proinflammatory cytokines. Chest *118*, 503–508.
22. Dinarvand, R., Sepehri, N., Manoochehri, S., Rouhani, H., and Atyabi, F. (2011). Polylactide-co-glycolide nanoparticles for controlled delivery of anticancer agents. Int J Nanomedicine *6*, 877–895.
23. DiPaola, R.S. (2002). To arrest or not to G(2)-M Cell-cycle arrest :

commentary re: A. K. Tyagi et al., Silibinin strongly synergizes human prostate carcinoma DU145 cells to doxorubicin-induced growth inhibition, G(2)-M arrest, and apoptosis. Clin. cancer res., 8: 3512-3519, 2002. Clin. Cancer Res. *8*, 3311–3314.

24. Falentin-Daudré, C., Faure, E., Svaldo-Lanero, T., Farina, F., Jérôme, C., Van De Weerdt, C., Martial, J., Duwez, A.-S., and Detrembleur, C. (2012). Antibacterial polyelectrolyte micelles for coating stainless steel. Langmuir *28*, 7233–7241.
25. Fishel, M.L., Newell, D.R., Griffin, R.J., Davison, R., Wang, L.-Z., Curtin, N.J., Zuhowski, E.G., Kasza, K., Egorin, M.J., Moschel, R.C., et al. (2005). Effect of cell cycle inhibition on Cisplatin-induced cytotoxicity. J. Pharmacol. Exp. Ther. *312*, 206–213.
26. Fox, C.L., Jr (1968). Silver sulfadiazine--a new topical therapy for Pseudomonas in burns. Therapy of Pseudomonas infection in burns. Arch Surg *96*, 184–188.
27. Franco-Molina, M.A., Mendoza-Gamboa, E., Sierra-Rivera, C.A., Gómez-Flores, R.A., Zapata-Benavides, P., Castillo-Tello, P., Alcocer-González, J.M., Miranda-Hernández, D.F., Tamez-Guerra, R.S., and Rodríguez-Padilla, C. (2010). Antitumor activity of colloidal silver on MCF-7 human breast cancer cells. J. Exp. Clin. Cancer Res. *29*, 148.
28. Galati, G., Rovere, P., Citterio, G., Bondanza, A., Scagliette, U., Bucci, E., Heltai, S., Fascio, U., Rugarli, C., and Manfredi, A.A. (2000). In vivo administration of GM-CSF promotes the clearance of apoptotic cells: effects on monocytes and polymorphonuclear leukocytes. J. Leukoc. Biol. *67*, 174–182.
29. Gopinath, P., Gogoi, S.K., Chattopadhyay, A., and Ghosh, S.S. (2008). Implications of silver nanoparticle induced cell apoptosis for *in vitro* gene therapy. Nanotechnology *19*, 075104.
30. Gopinath, P., Gogoi, S.K., Sanpui, P., Paul, A., Chattopadhyay, A., and Ghosh, S.S. (2010). Signaling gene cascade in silver nanoparticle induced apoptosis. Colloids Surf B Biointerfaces *77*, 240–245.
31. Gupta, R., and Emens, L.A. (2010). GM-CSF-secreting vaccines for solid tumors: moving forward. Discov Med *10*, 52–60.
32. Hsin, Y.-H., Chen, C.-F., Huang, S., Shih, T.-S., Lai, P.-S., and Chueh, P.J. (2008). The apoptotic effect of nanosilver is mediated by a ROS- and JNK-

dependent mechanism involving the mitochondrial pathway in NIH3T3 cells. Toxicology Letters *179*, 130–139.

33. Hussain, S.M., Hess, K.L., Gearhart, J.M., Geiss, K.T., and Schlager, J.J. (2005). In vitro toxicity of nanoparticles in BRL 3A rat liver cells. Toxicol In Vitro *19*, 975–983.
34. Kim, M.R., Manoukian, R., Yeh, R., Silbiger, S.M., Danilenko, D.M., Scully, S., Sun, J., DeRose, M.L., Stolina, M., Chang, D., et al. (2002). Transgenic overexpression of human IL-17E results in eosinophilia, B-lymphocyte hyperplasia, and altered antibody production. Blood *100*, 2330–2340.
35. Klimp, A.H., de Vries, E.G.E., Scherphof, G.L., and Daemen, T. (2002). A potential role of macrophage activation in the treatment of cancer. Crit. Rev. Oncol. Hematol. *44*, 143–161.
36. Kocbek, P., Obermajer, N., Cegnar, M., Kos, J., and Kristl, J. (2007). Targeting cancer cells using PLGA nanoparticles surface modified with monoclonal antibody. Journal of Controlled Release *120*, 18–26.
37. Komarova, N.L., and Boland, C.R. (2013). Cancer: Calculated treatment. Nature *499*, 291–292.
38. Kouttab, N.M., Mehta, S., Morgan, J., Tannir, N., Sahasrabuddhe, C., and Maizel, A.L. (1984). Lymphokines and monokines as regulators of human lymphoproliferation. Clin. Chem. *30*, 1539–1545.
39. Kreitman, R.J. (2003). Recombinant toxins for the treatment of cancer. Curr. Opin. Mol. Ther. *5*, 44–51.
40. Le, Y., Zhou, Y., Iribarren, P., and Wang, J. (2004). Chemokines and chemokine receptors: their manifold roles in homeostasis and disease. Cell. Mol. Immunol. *1*, 95–104.
41. Lee, S., and Margolin, K. (2011). Cytokines in Cancer Immunotherapy. Cancers *3*, 3856–3893.
42. Longley, D.B., Harkin, D.P., and Johnston, P.G. (2003). 5-fluorouracil: mechanisms of action and clinical strategies. Nat. Rev. Cancer *3*, 330–338.
43. Mantovani, A., and Locati, M. (2009). Orchestration of macrophage polarization. Blood *114*, 3135–3136.
44. Martinez, F.O., Gordon, S., Locati, M., and Mantovani, A. (2006). Transcriptional profiling of the human monocyte-to-macrophage differentiation and polarization: new molecules and patterns of gene expression. J. Immunol. *177*, 7303–7311.

45. Mezzano, S.A., Droguett, M.A., Burgos, M.E., Ardiles, L.G., Aros, C.A., Caorsi, I., and Egido, J. (2000). Overexpression of chemokines, fibrogenic cytokines, and myofibroblasts in human membranous nephropathy. Kidney International *57*, 147–158.
46. Miles, D., von Minckwitz, G., and Seidman, A.D. (2002). Combination versus sequential single-agent therapy in metastatic breast cancer. Oncologist *7 Suppl 6*, 13–19.
47. Moyer, C.A., Brentano, L., Gravens, D.L., Margraf, H.W., and Monafo, W.W., Jr (1965). Treatment of large human burns with 0.5 per cent silver nitrate solution. Arch Surg *90*, 812–867.
48. Mukerjee, A., and Vishwanatha, J.K. (2009). Formulation, characterization and evaluation of curcumin-loaded PLGA nanospheres for cancer therapy. Anticancer Res. *29*, 3867–3875.
49. Panyam, J., and Labhasetwar, V. (2003). Biodegradable nanoparticles for drug and gene delivery to cells and tissue. Adv. Drug Deliv. Rev. *55*, 329–347.
50. Pappachan, A., Savithri, H.S., and Murthy, M.R.N. (2008). Structural and functional studies on a mesophilic stationary phase survival protein (Sur E) from Salmonella typhimurium. FEBS J. *275*, 5855–5864.
51. Parker, W.B., and Cheng, Y.C. (1990). Metabolism and mechanism of action of 5-fluorouracil. Pharmacol. Ther. *48*, 381–395.
52. Pastan, I., and FitzGerald, D. (1991). Recombinant toxins for cancer treatment. Science *254*, 1173–1177.
53. Pastan, I., Beers, R., and Bera, T.K. (2003) Recombinant Immunotoxins in the Treatment of Cancer. In Antibody Engineering, (New Jersey: Humana Press), pp. 503–518.
54. Roy-Ghanta, S., and Orange, J.S. (2009). Use of Cytokine Therapy in Primary Immunodeficiency. Clinical Reviews in Allergy & Immunology *38*, 39–53.
55. Sahoo, A.K., Sk, M.P., Ghosh, S.S., and Chattopadhyay, A. (2011). Plasmid DNA linearization in the antibacterial action of a new fluorescent Ag nanoparticle-paracetamol dimer composite. Nanoscale *3*, 4226–4233.
56. Sakai, N., Umeda, T., Suzuki, H., Ishimatsu, Y., and Shikita, M. (1987). Macrophage colony-stimulating factor purified from normal human urine. Amino-terminal sequence and amino acid composition. FEBS Lett. *222*, 341–344.
57. Schroder, K. (2003). Interferon- : an overview of signals, mechanisms and

functions. Journal of Leukocyte Biology *75*, 163–189.

58. Segura, S., Espuelas, S., Renedo, M.J., and Irache, J.M. (2005). Potential of albumin nanoparticles as carriers for interferon gamma. Drug Dev Ind Pharm *31*, 271–280.
59. Shi, F.S., Weber, S., Gan, J., Rakhmilevich, A.L., and Mahvi, D.M. (1999). Granulocyte-macrophage colony-stimulating factor (GM-CSF) secreted by cDNA-transfected tumor cells induces a more potent antitumor response than exogenous GM-CSF. Cancer Gene Ther. *6*, 81–88.
60. Shrivastava, S., Bera, T., Singh, S.K., Singh, G., Ramachandrarao, P., and Dash, D. (2009). Characterization of antiplatelet properties of silver nanoparticles. ACS Nano *3*, 1357–1364.
61. Sica, A., and Mantovani, A. (2012). Macrophage plasticity and polarization: in vivo veritas. Journal of Clinical Investigation *122*, 787–795.
62. Sondi, I., and Salopek-Sondi, B. (2004). Silver nanoparticles as antimicrobial agent: a case study on E. coli as a model for Gram-negative bacteria. J Colloid Interface Sci *275*, 177–182.
63. Takeda, H., Haisa, M., Naomoto, Y., Kawashima, R., Satomoto, K., Yamatuji, T., and Tanaka, N. (1999). Effect of 5-fluorouracil on cell cycle regulatory proteins in human colon cancer cell line. Jpn. J. Cancer Res. *90*, 677–684.
64. Tayal, V., and Kalra, B.S. (2008). Cytokines and anti-cytokines as therapeutics — An update. European Journal of Pharmacology *579*, 1–12.
65. Teng, M.W.L., Swann, J.B., Koebel, C.M., Schreiber, R.D., and Smyth, M.J. (2008). Immune-mediated dormancy: an equilibrium with cancer. Journal of Leukocyte Biology *84*, 988–993.
66. Toren, A., Segal, G., Ron, E.Z., and Rosenberg, E. (2002). Structure--function studies of the recombinant protein bioemulsifier AlnA. Environ. Microbiol. *4*, 257–261.
67. Vázquez, E., Ferrer-Miralles, N., Mangues, R., Corchero, J.L., Schwartz, S., Jr, and Villaverde, A. (2009). Modular protein engineering in emerging cancer therapies. Curr. Pharm. Des. *15*, 893–916.
68. Vij, N., Min, T., Marasigan, R., Belcher, C.N., Mazur, S., Ding, H., Yong, K.-T., and Roy, I. (2010). Development of PEGylated PLGA nanoparticle for controlled and sustained drug delivery in cystic fibrosis. Journal of Nanobiotechnology *8*, 22.
69. Vila, A., Sánchez, A., Tobío, M., Calvo, P., and Alonso, M.J. (2002). Design

of biodegradable particles for protein delivery. Journal of Controlled Release *78*, 15–24.

70. Wacker, M., Linton, D., Hitchen, P.G., Nita-Lazar, M., Haslam, S.M., North, S.J., Panico, M., Morris, H.R., Dell, A., Wren, B.W., et al. (2002). N-linked glycosylation in Campylobacter jejuni and its functional transfer into E. coli. Science *298*, 1790–1793.
71. Website 1: http://www.drugbank.ca/drugs/DB00030)
72. Website 2: http://fpc.state.gov/6176.htm
73. Website 3: http://www.copewithcytokines.de/cope.cgi?key=recombinant%20cytokines
74. Website 4: http://www.who.int/mediacentre/factsheets/fs297/en/
75. Website 5: http://www.cdc.gov/nchs/fastats/lcod.htm
76. Website 6: http://www.cancer.gov/cancertopics/factsheet/Therapy/adjuvant-breast
77. Website 7: http://www.york.ac.uk/news-and-events/news/2013/research/yorkshire-cancer-research/.
78. Website 8: http://www.ascopost.com/ViewNews.aspx?nid=4188.
79. Website 9: http:// www.niaid.nih.gov/topics/immunecells/Pages/cytokines.aspx.
80. Whiles, J.A., Deems, R., Vold, R.R., and Dennis, E.A. (2002). Bicelles in structure-function studies of membrane-associated proteins. Bioorg. Chem. *30*, 431–442.
81. Wills, R.J. (1990). Clinical Pharmacokinetics of Interferons: Clinical Pharmacokinetics *19*, 390–399.
82. Yang, J., Lee, C.-H., Park, J., Seo, S., Lim, E.-K., Song, Y.J., Suh, J.-S., Yoon, H.-G., Huh, Y.-M., and Haam, S. (2007). Antibody conjugated magnetic PLGA nanoparticles for diagnosis and treatment of breast cancer. Journal of Materials Chemistry *17*, 2695.
83. Gualandi-Signorini, A.M., and Giorgi, G. (2001). Insulin formulations--a review. Eur Rev Med Pharmacol Sci *5*, 73–83.
84. Von Fange, T., McDiarmid, T., Mackler, L., and Zolotor, A. (2008). Clinical inquiries: can recombinant growth hormone effectively treat idiopathic short stature? J Fam Pract *57*, 611–612.
85. Manco-Johnson, M.J. (2010). Advances in the care and treatment of children with hemophilia. Adv Pediatr *57*, 287–294.

CHAPTER 2

Molecular cloning, purification and functional implications of recombinant GST tagged hGMCSF cytokine

CHAPTER 2

2.1 Introduction

Granulocyte macrophage colony stimulating factor (GMCSF also known as CSF2) is now best studied cytokine as major regulator for governing the function of granulocytes and macrophages lineages and their maturation throughout the developmental phases. GMCSF is a cytokine, which works as linkers in between innate and adaptive immune system and regulate survival (Belardelli *et al*, 2002), proliferation, differentiation and activation of haematopoietic lineages (Gasson *et al*, 1986). Human Granulocyte Macrophage colony stimulating factor is responsible for proliferation and development of myeloid lineages. It is involved in the clearance of apoptotic loads and thus, prevents chronic inflammation and autoimmune effects (Galati *et al*, 2000). FDA has approved its use in treatment of neutropenia, primary immunodeficiency of AML, myeloid reconstitution and also now it has being actively incorporated in stem cell and bone marrow transplantation therapy for the establishment of myeloid cells (Roy *et al*, 2010). Human GMCSF is soluble glycoprotein (144 amino acid) found to be expressed by T lymphocytes, macrophages, endothelial cells and fibroblast in the response to any inflammatory signal (Cantrell *et al*, 1985). It consists of four α helices that comprise 42% of its structure. Four cysteine residues form two disulfide bonds necessary to retain the biological activity of GMCSF protein (Walter *et al*, 1992; Barreda *et al*, 2004). Although the naturally occurring form of GMCSF is glycosylated, the non-glycosylated form of recombinant GMCSF protein expressed in *E.coli* have been reported to show high biological activity *in vitro* (Kaushansky *et al*, 1987; Moonen *et al*, 1987; Cebon *et al*, 1990). Recombinant human GMCSF protein is also available commercially such as Molgramostim produced from *E.coli* and Sargramostim produced from yeast marketed under trade name of Leukine (Schwanke *et al*, 2009). Recombinant GMCSF protein is also expressed in bacterial host in insoluble form because heterologous gene expression in bacteria leads to the formation of inclusion bodies which remarkably reduce the biological importance and remain no more cost effective (Ventura *et al*, 2006). Several reports are available to resolve the solubility problem of cytokines expressed in bacteria (Petrov *et al*, 2010). One such solution is to add a suitable N-terminal tag with the protein (Hammarström *et al*, 2002; Ghosh *et al*, 2004) and then solubilize it from inclusion bodies with bile reagent, which is

primarily used to emulsify fat. Intracellular localization of GST tagged protein inside the bacterial host is not known, but it could possibly sort the synthesized protein into the periplasmic space, and thus, helps in dissolving protein from inclusion bodies in mild conditions (Speers *et al*, 2007).

In this present chapter, the GMCSF gene was cloned from total RNA obtained from ACHN renal carcinoma cells, without its prior induction. The GMCSF gene was cloned into the pGEX4T2 bacterial expression vector to generate the GST fused GMCSF. The expressed recombinant protein was recovered from inclusion bodies easily by modifying the methods of Schwanke RC *et al.* The protein characterization was carried out using sophisticated analytical tools. Three dimensional structure of GST-GMCSF and its binding domain with GMCSF receptor were predicted by *in silico* modelling and protein-protein docking studies. Further, the proliferative action of GST-GMCSF protein on different cell types was found to be remarkably dose dependent. To our knowledge this is the first report for demonstration of effect of GST tagged GMCSF cytokine in cell proliferation. A schematic diagram has depicted the cloning, purification and activity assay of the recombinant cytokine (Scheme 2.1).

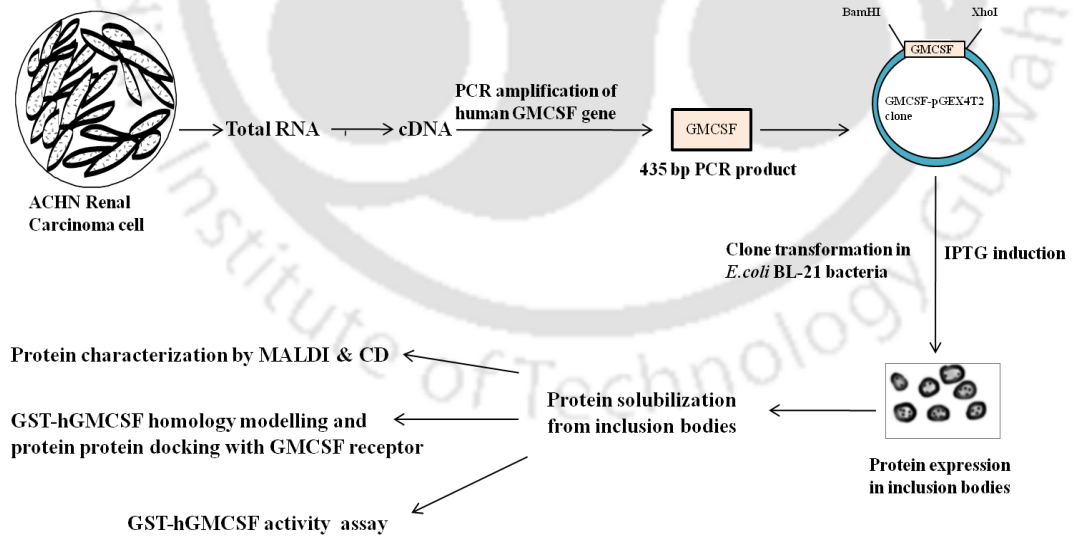

Scheme 2.1. An overview of cloning and functional details of human GMCSF

2.2 Materials and Methods

2.2.1 Cell Culture:

Cell lines were obtained from National Centre for Cell Science, India. The cells were periodically cultured in DMEM media supplemented with 10% FBS, 20 U/mL penicillin and 50 mg/mL streptomycin in 5% CO_2 humidity at 37°C in a humidified incubator. Media was periodically changed after 3 days and the optimum cell density (80-90% confluency) was maintained by culturing the cells. First of all, the old media was removed and then the cells were washed with sterile phosphate buffer saline (PBS). Then, trypsin/EDTA solution was added and the cells were kept at 37°C for 2-3 minutes. Further, the complete media was added to the cells and centrifuged at 500 g for 10 minutes. The supernatant was discarded and the cell pellet was dissolved in 1 mL of fresh media and further seeded in culture plate, according to the cell density requirement.

2.2.2 Isolation of RNA from mammalian cell lines:

Total RNA was isolated from ACHN (renal carcinoma cells) for cloning of GMCSF. All plastic wares were treated by 0.1 % DEPC to make them RNase free for 2 h at 37°C, followed by removal of DEPC by autoclaving at 121°C, 15 psi for 20 min. Total cellular RNA was extracted by TRI reagent (Sigma). About 1 mL of TRI reagent was used to isolate RNA from a confluent 35 mm culture plate and RNA was isolated as per the manufacturer's protocol. After addition of TRI reagent over the monolayer of cells, the cell lysate was passed several times through a syringe to form a homogenous lysate followed by 5 min incubation at room temperature for complete dissociation of nucleoprotein complexes. Then, 200 µl of chloroform was added for 1 mL of TRI Reagent. At this step, sample was shaked vigorously for 1 min and allowed to stand at room temperature for 10 minutes. Resulting mixture was centrifuged at 12,000 g for 15 min at 4°C. The aqueous phase having RNA was transferred to a fresh eppendorf tube followed by addition of 500 µl of isopropanol per mL of TRI Reagent to precipitate RNA. After 10 min incubation at room temperature, the sample was centrifuged at 12,000 g for 10 min at 4°C. Supernatant was removed and the RNA pellet was washed with 1 mL of 75% chilled ethanol and

centrifuged again at 12,000 g for 10 min at 4°C. At this step, RNA pellet in ethanol was also stored at -80 °C for long-term storage. However, the RNA pellet was air-dried and dissolved in sterile DEPC and stored at -20°C. Before further use RNA concentration was estimated at spectrophotometer for cDNA synthesis.

2.2.3 Reverse transcription for cDNA synthesis:

1 µg of total RNA was used for cDNA synthesis by H Minus reverse transcriptase (RT) (Fermentas) and oligo dT primer. Following protocol was followed for 20 µL of reaction mixture:

RNA	1 µg
Oligo dT (100 picomole/µL)	1 µL
Nuclease free water	upto 10 µL

This mixture was incubated at 65°C for 5 min to break RNA secondary structures with immediately chilling on ice. After the denaturation step, the residual components were added in reaction mix as follows:

5X reaction buffer	4 µL
dNTP mix (10 mM each)	2 µL (1 mM each)
H Minus reverse transcriptase (200 U/µL)	1 µL
Nuclease free water	3 µL

Reverse transcription reaction was carried out at 37°C for 1 h with final heating step at 70°C for 10 min followed by chilling on ice. Now this RT product was used as cDNA for downstream PCR amplification steps.

2.2.4 Quantification of DNA and RNA:

Nucleic acid quantification was done by spectrophotometry. The samples were diluted in Milli Q water and OD was measured at 260 nm and at 280 nm. The OD value 1 at 260 nm represents 40 µg/mL of RNA and 50 µg/mL of double stranded DNA. Concentrations of RNA in samples were calculated from the optical densities by considering dilution factors.

2.2.5 Polymerase Chain Reaction:

Primers were designed by NCBI blast to amplify the cDNA of GMCSF gene. Gene specific forward primer (5'ATGTGGCTGCAGAGCCTGCTG3') and reverse primer (5'TCACTCCTGGACTGGCTCCCA3') were designed for PCR amplification and cloning of GMCSF amplified cDNA in pGEMT Easy vector; NCBI Accession Number NM-000758.29. PCR reaction was conducted by Taq DNA polymerase with following constituents:

10 X buffer	2.0 µL
(10 mM Tris Cl pH 9.0), 1.5 mM $MgCl_2$, 50 mM KCl, 0.1% gelatin	
10 mM dNTP mix	1.0 µL
Taq DNA polymerase (4 U/µL)	0.5 µL
Forward Primer (20 picomoles/µL)	1.0 µL
Reverse Primer (20 picomoles/µL)	1.0 µL
Nuclease free water	upto 20 µL

PCR amplification involves initial denaturation of plasmid DNA (10 ng) for 5 min at 94°C followed by 30 cycles of annealing step (94°C for 1 min, 1 min at 56°C and 1 min at 72°C) and finally extension at 72°C for 10 minutes.

2.2.6 Agarose gel electrophoresis:

All DNA samples were examined by agarose gel electrophoresis (1% agarose containing 0.5 µg of ethidium bromide) in 1X TAE buffer at 100 volts. DNA bands

were analysed from UV transilluminator and imaged by Gel documentation system (Gel Logic System 1500, Kodak).

2.2.7 Gel Elution:

The amplified PCR products and digested plasmids were eluted from agarose gel by using QIAquick gel extraction kit. For gel elution, required fragments were excised and stored at -20°C followed by manufacturer's protocol for elution. The desired DNA was stored at -20 °C for further use.

2.2.8 Plasmid DNA Isolation (Mini-Prep Method):

Plasmid DNA was isolated from 3.5 mL of overnight cultures in LB media, by alkaline lysis method (Sambrook *et al*, 1989). Single *E.coli* colony was inoculated in LB broth for 14-18 h containing specific antibiotic for selective growth of desired plasmid at 37°C with continuous shaking at 180 rpm. The bacterial cells were harvested from culture by centrifugation and pellet was resuspended in 100 µL of solution I. The cells were lysed by adding 200 µL of freshly prepared lysis solution II (refer to Appendix, Table 1). All the contents were mixed thoroughly by gently inverting the tube. After 2-3 min incubation at ice, bacterial cell debris and genomic DNA were precipitated by adding 150 µL of ice cold solution III (refer to Appendix, Table 1) followed by 5 min incubation on ice. Afterwards debris was removed by centrifugation at 12000 g for 10 min at 4°C and supernatant was transferred to a fresh tube. Protein contamination was removed by adding equal volume of phenol/chloroform and isoamyl alcohol (25:24:1). Mixture was gently inverted thrice and centrifuged at 12,000 g for 10 min at 4°C for phase separation. The aqueous phase was taken out in a fresh tube and 2 volume of ethanol was added to precipitate the plasmid DNA. At this step, sample can be stored at -20°C for months or after 15 min incubation at RT, plasmid DNA was precipitated by centrifugation at 12,000 g for 10 min at 4°C. Plasmid DNA pellet was washed with 70% ethanol and dried in Speed vac for evaporation of ethanol content and resuspended in the nuclease-free water. Sample was analysed by agarose gel electrophoresis before further use.

2.2.9 Preparation of the Competent Cells:

Competent cells are the bacteria which can uptake extrachromosomal DNA or

plasmid easily. Competency in *E. coli* cells were gained by one step competent cell preparation method by TSS (Chung *et al*, 1989). A single colony was inoculated in 5 mL LB broth and incubated overnight at 37°C under continuous shaking. Primary culture was inoculated in 1:1000 ratio in 50 mL of LB media and grown till 0.4-0.5 OD_{590}. The culture was kept on ice for 10 min and centrifuged at 2500 g for 10 min at 4 °C. The pellet was resuspended uniformly in 2.0 ml of ice-cold sterile TSS solution and stored at -80°C as 200 µL aliquots in separate eppendorf tubes for further use.

2.2.10 Transformation in bacterial cells:

Plasmids were transformed in competent *E.coli* DH5α cells by heat shock method (Sambrook *et al*, 1989). Ligation mixtures (10-20 µL) was mixed with 200 µL of competent cells and placed on ice for 45 min under sterile condition. The cells were given heat shock at 42°C for 90 seconds in water bath and immediately kept on ice for chilling. Afterwards, 800 µL of fresh LB media (37°C) was added and the cells were incubated at 37°C upto two generation dividing time (around 45 min for *E.coli* DH5α) with continuous shaking. Bacterial cells were pellet down by centrifugation at 2500 g for 10 min at 4°C and resuspended in 100 µL of fresh LB media. Resuspended cells were plated on LB agar plates containing the appropriate antibiotic and incubated at 37°C for 14-18 h. Subsequently, the colonies were picked for screening either by colony PCR or by restriction digestion of plasmid containing insert.

2.2.11 Colony PCR for screening recombinant clones:

Transformed cells carrying recombinant plasmid containing desired insert was screened out by colony PCR analysis. Single colony was picked and marked very carefully to take few bacterial cells only in PCR mixture as sample DNA, marking of colony helped in future identification of the clone. All PCR reaction conditions were same except the initial heating period which was extended upto 10 min to break bacterial cell wall. PCR products were analyzed by agarose gel electrophoresis. Colonies having desired insert were inoculated further in 5 mL LB tube for plasmid isolation and further analysis by restriction digestion.

2.2.12 Digestion by Restriction Enzymes:

Plasmids or the PCR amplified DNA fragments were digested by restriction

endonucleases. Upto 1 µg of DNA was incubated with 1 U of restriction endonuclease either for overnight digestion or upto 3-5 h with at 37°C. Digested sample was loaded on an agarose gel and the desired fragment was taken out by cutting the band for gel elution purpose (QIAquick Gel Extraction Kit) to avoid any contamination of unwanted DNA in ligation.

2.2.13 Ligation reaction:

For ligation purpose, linearized vector and the insert fragment were mixed in 1:3 molar ratio, respectively and incubated with IX ligation buffer and 2 units of T4 DNA ligase enzyme as suggested by manufacturer's protocol (Promega). Sample was incubated at 4°C for 12-16 h and terminated by incubating at 65°C for 10 minutes.

2.2.14 Cloning of PCR amplified DNA fragments in T/A vector system:

PCR amplified, gel eluted (QIAquick Gel Extraction Kit) DNA fragments were proceeded for TA cloning, (pGEMT Easy, Promega). Ligation mixture was prepared as per manufacturer's protocol:

pGEMT Easy Vector	50 ng
Insert DNA	25 ng
2X rapid ligation buffer	5 µL
T4 DNA Ligase	1 µL
Nuclease free water	upto 10 µL

The reaction mix was overnight incubated at 4°C and the ligated mix was transformed in *E. coli* DH5α cells. Transformed cells were spreaded over LB agar plate containing X-gal/IPTG for blue white selection and overnight incubated at 37°C. After overnight growth, white colonies were picked and checked by colony PCR. Positive clones were processed for plasmid isolation and restriction digested with *Eco RI* (For insert release in pGEMT Easy vector) and analyzed with agarose gel electrophoresis. Recombinant clones having proper insert were grown in LB media for making their glycerol stocks (15% glycerol) for storage purpose at -80°C.

2.2.15 Bacterial cell culture:

All bacterial stocks (*E.coli*) and clones were stored at -80°C (15% glycerol in Milli Q water). For work purpose all strains were cultured and maintained in LB medium.

2.2.16 Sequencing of DNA fragments cloned in pGEMT Easy Vector:

Recombinant pGEMT clones having desired gene were subjected for sequencing before further subcloning in expression vectors. Sequencing was done by dideoxy method using M13 universal primers. Sequencing was performed by Axygen, India.

2.2.17 Subcloning of GMCSF in pGEX4T2 Expression vector:

The GMCSF gene was transferred from pGEMT-GMCSF construct into pGEX4T2 expression vector (Amersham) using forward (5'GTGGATCCATGTGGCTGCAGAGCCT '3) and reverse primers (5'GACTCGAGTCACTCCTGGACTGGCTC 3') just after N- terminal GST tag between *Bam HI* and *Xho I* site. For this purpose, GMCSF gene was amplified by PCR from pGEMT-GMCSF construct, the amplified band was examined by agarose gel electrophoresis, desired fragment was eluted out from gel and further preceded for *Bam HI* and *Xho I* double digestion. Plasmid DNA was also treated with same restriction enzymes followed by gel elution of linearized plasmid and DNA fragment. Ligation reaction was carried out by using T4 DNA ligase enzyme and the ligated product was transformed into suitable expression host.

2.2.18 Expression of GMCSF in *E.coli* BL21 DE3 strain:

The pGEX4T2-GMCSF plasmid was transformed into *E.coli* BL21 DE3 (Novagen) expression host. A single colony was inoculated in 3 mL LB medium with 100 µg/mL ampicillin and incubated at 37°C for 12 h to generate the starter culture. An inoculum of (1:200) dilution was added to large scale of 500 mL LB with ampicillin media. Afterwards, 1 mM IPTG was added and the culture was allowed to grow for another 12 h for induction of the recombinant protein. Finally, the cells were harvested at 15,000 g for 10 min and stored at -20°C for further steps.

2.2.19 Purification:

A. Solubilisation of inclusion bodies

Although bacterial expression for any recombinant protein is an easy and convenient way to attain in substantial amount, but sometimes heterologous gene expression in bacterial host leads to the formation of insoluble aggregates of inclusion bodies due to incomplete folding. Herein, the GST-GMCSF protein also appeared as inclusion bodies. Hence, the following steps were performed to solubilise the recombinant protein from inclusion bodies. At first, frozen cell paste was dissolved in solution I containing 10 mM phosphate buffer saline (PBS), 1 mM PMSF, 1 mM EDTA, 1% Triton X-100 and passed through a French press operating at 20 kpsi. The cell suspension was pelleted at 15,000 g for 30 min at 4°C. The cell pellet was further suspended in solution II (50 mM TrisCl, 5 mM EDTA and 2% Triton X-100) (1:30 w/v) with continuous stirring for 2 h at room temperature. The suspension was again pelleted by centrifugation at 15,000 g. The pellet was then resuspended in solution III (50 mM TrisCl containing 1% Na deoxycholate, 0.5 mM EDTA) with continuous stirring for 4 h and GST-GMCSF protein was dissolved at this step. Thus GST-GMCSF protein was isolated from inclusion bodies and the purity was checked in 12% SDS PAGE gel.

B. Refolding and purification

Sodium deoxycholate suspension having soluble GST-GMCSF was separated out from bacterial debris by centrifugation at 15,000 g for 10 min at 4 °C. The supernatant was taken out separately and dialysed with 10 mM Tris-Cl buffer (pH 8.0) and subsequently passed through the glutathione agarose beads for GST tagged protein purification by affinity chromatography (Sigma). The recombinant GST-GMCSF protein was eluted with 10 mM reduced glutathione. The purified GST-GMCSF protein was checked by Laemmli method of SDS PAGE analysis (Laemmli *et al*, 1970). The electrophoresis was carried out by 5 % stacking and 12 % separating gels (thickness 0.75 mm) at constant current of 20 mA and 30 mA for stacking and separating gel respectively, in a MiniVE vertical electrophoresis system (G.E Healthcare).

2.2.20 Homology Modelling of GST-GMCSF protein:

For analysing the three dimensional structure of GST GMCSF protein *in silico*, firstly amino acid sequence of GST (Glutathione S-transferase of *Schistosoma japonicum*) was tagged with GMCSF amino acid by C terminal addition of GST with N terminal of GMCSF. Following sequence has been submitted for homology modelling, sequence of GST has been mentioned in black colour while GMCSF in red colour:

MSPILGYWKIKGLVQPTIRLLLEYLEEKYEEHLYERDEGDKVVRNKKFELGLE
FPNLPYYIDGDVKLTQSMAIIRYIADKHNMLGGCPKERAEISMLEGAVLDIRY
GVSRIAYSKDFETLKVDFLSKLPEMLKMFEDRLCHKTYLNGDHVTHPDFMLD
ALDVVLYMDPMCLDAFPKLVCFKKRIEAIPQIDKYLKSSKYIAVVPLQGVVA
TFGGGDHPPKMWLQSLLLLGTVACSISAPARSPSPSTQPVVEHVNAIQEARRL
LNLSRDTAAEMNETVEVISEMFDLQEPTCLQTRLELYKQGLRGSLTKLKGPLT
MMASHYKQHCPPTPETSCATQIITFESFKENLKDFLLVIP FDCWEPVQE Stop

Homology modelling was performed using I-TASSER online web server (http://zhanglab.ccmb.med.umich.edu/I-TASSER/). I-Tasser builds 3D models of the protein based on multiple-threading alignments by LOMETS and iterative TASSER assembly simulations. Based on the aforesaid, five high quality protein models were generated. The quality of the protein models were validated through the Saves server (http://nihserver.mbi.ucla.edu/SAVES/). The best model was selected for further analysis. Interactions between the modelled GST-GMCSF protein with GMCSF receptor subunits (PDBID: 3CXE), GST alone with GMCSF receptor and modelled GMCSF alone with the receptor were obtained using protein-protein docking server ClusPro (Kozakov *et al*, 2010). The interactions were compared with that of the crystallized structure of GMCSF (3CXE: PDB ID).

2.2.21 Western Blot Analysis:

Western blot using anti-GMCSF antibody confirmed the presence of recombinant GMCSF protein. Purified GST-GMCSF was run in SDS-PAGE and then transferred on PVDF membrane. Protein transfer was checked by ponceau S staining of the membrane. The membrane was blocked overnight with blocking reagent containing 5% skim milk in 10 mM PBS with 0.1% Tween 20. Then the membrane was incubated with human GMCSF specific monoclonal antibody (Rat anti GMCSF 1^0Ab,

BD Biosciences) for 3 h. Afterwards, it was washed with PBST (10 mM PBS with 0.1% Tween 20) and further incubated with anti-rat HRP conjugated secondary antibody (Calbiochem) for 2 h. Membrane was again thoroughly washed with PBST and the brown colour was developed by H_2O_2 mediated catalytic activity of Horse radish peroxidase enzyme using DAB (3,3'diaminobenzidine, Amresco) as a substrate. Similarly, the presence of GST tag was confirmed using mouse anti-GST antibody (Bangalore Genei, India).

2.2.22 MALDI TOF TOF analysis:

MALDI MS/MS analysis has been carried out with 4700 Proteomics analyzer with TOF TOF Optics^{TM} (Applied Biosystems) under diode pumped Nd:YAG laser at 355 nm. Data has been acquired by 300 shots per spectrum in MS positive reflector mode with automated acquisition. MS spectrum was further subjected to MS/MS mode by semi-automatic method. Ions generated by MS mode were again induced by a positive ion mode in collision induced dissociation cell (CID) with the employment of 1 KeV positive collision energy. Protein sample was prepared by *in situ* gel digestion of SDS PAGE separated protein. Gel destaining was done in 50 mM ammonium bicarbonate buffer in 50% acetonitrile (ACN). Destained gel was completely dehydrated in 100% ACN. The protein bands were excised and further preceded for trypsin digestion within the gel in 50 mM ammonium bicarbonate buffer, pH 7.8, at 37°C for overnight (Jimenez *et al*, 1998; Havlis *et al*, 2003). After digestion the residual peptides were taken out by the addition of peptide extraction solution (0.1% trifluoroacetic acid in 50% acetonitrile) in the gel and the fractions were pooled. For MALDI-MS analysis the dried sample was dissolved in 30% ACN containing 0.1% TFA. Trypsinized GST-GMCSF protein (20 pmol) was analyzed with CHCA matrix (α cyano-4-hydroxycinnamic acid). Equal volume of CHCA matrix (10 mg/mL) was added with trypsinized protein and loaded on analyzer plate.

2.2.23 Circular dichroism analysis:

Far-UV Circular dichroism spectra of recombinant GST-GMCSF protein were

measured by Jasco J-815 CD spectrophotometer. Purified GST-GMCSF protein was dialyzed against 100 mM Tris-Cl buffer pH 8.0, and then filtered through 0.22 µm unit to get clear protein solution. Spectra were recorded using 1mm cuvette at 20°C, with 1.00 nm bandwidth and 50 nm/min scan speed against the blank 100 mM Tris-Cl buffer. Three independent scans were recorded at 190-240 nm wavelength range to obtain the resultant spectra.

2.2.24 Cell proliferation Assay:

The biological activity for recombinant GST-GMCSF was examined on THP1 (human leukaemia), Raw 264.7 (mouse macrophage), MCF7 (human breast cancer) and U87MG (human neuroblastoma) cells. Cells were seeded in 96 well plates with DMEM media supplemented with 10% FCS. After 12 h, the media was removed and the cells were washed with PBS. Then recombinant GST-GMCSF was added with serum free DMEM media to the cells. THP-1 leukemia suspension cells were directly seeded in serum free media supplemented with GST-GMCSF protein. Recombinant GST-GMCSF was added in different concentration to the cells and the cells were incubated at 37 °C for 24 h in CO_2 incubator. Cell viability was checked by spectrophotometric analysis of XTT (2, 3-bis (2 methoxy-4 nitro-5-sulfophenyl)-2H-tetrazolium-5-carboxanilide), which gets converted into orange colour formazan by actively respiring cells and the colour is measured at 450 nm. A control experiment was performed with purified GST to nullify any effect of GST on cells.

2.3 Results and Discussion

2.3.1 Cloning of GMCSF cDNA:

A 435 bp CDS (NM_000758.2) of human GMCSF gene was amplified using gene specific primers as mentioned in method section. The full length gene was cloned into the pGEMT Easy vector (Fig. 2.1) and subsequently subcloned into the pGEX4T2 bacterial expression vector to obtain recombinant pGEX4T2-GMCSF plasmid that expressed N terminal GST tagged GMCSF (Fig. 2.2).

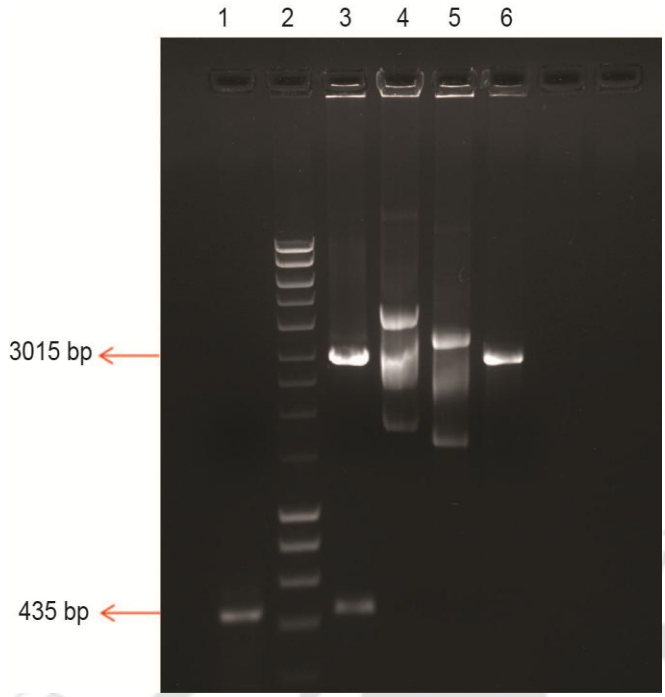

Fig 2.1. Cloning of GMCSF in pGEMT Easy vector. Lane 1: PCR product, Lane 2: Marker, Lane 3: *EcoR1* digested pGEMT GMCSF construct, Lane 4: Uncut pGEMT backbone, Lane5: Uncut pGEMT GMCSF construct, Lane 6: *Eco RI* digested pGEMT backbone.

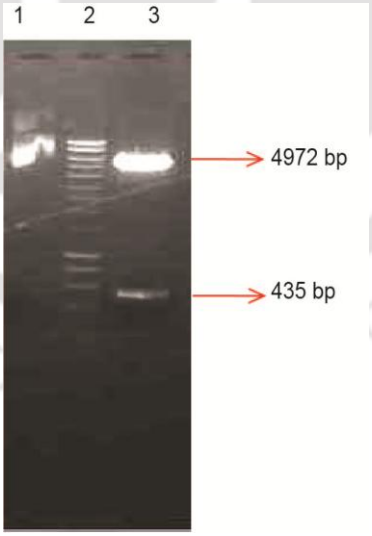

Fig 2.2. Subcloning of GMCSF in pGEX4T2 bacterial expression vector. Lane 1: Uncut plasmid, Lane 2: Marker, Lane 3: pGEX4T2 GMCSF after *Bam HI* and *Xho I* digestion.

2.3.2 Expression and Purification of GMCSF:

The recombinant protein was induced in *E.coli* BL21 DE3 (Novagen) expression bacteria by 1 mM IPTG at 28 °C for 12 h. The 42 kDa GST-GMCSF protein was found to be present in insoluble fraction of *E.coli* expression host BL21 (Fig. 2.3). The protein was solubilized (discussed in detail in method section) dialysed against 10 mM Tris Cl and then passed through a column containing glutathione beads, which has strong binding affinity for GST. Column bound GST-GMCSF protein was eluted with 10 mM reduced glutathione (Fig. 2.4).

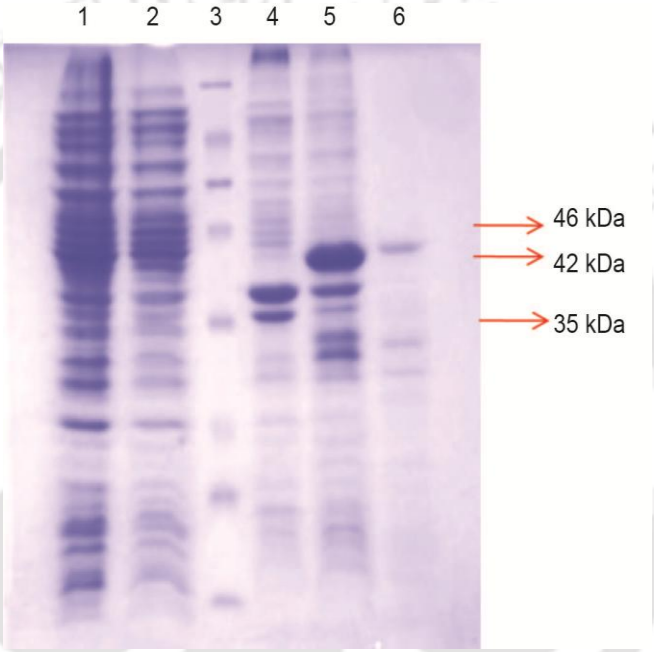

Fig 2.3. Expression of recombinant GST-GMCSF protein. Lane 1: pGEX4T2 supernatant, Lane 2: GST-GMCSF supernatant, Lane 3: Marker, Lane 4: pGEX4T2 Debris, Lane 5: GST GMCSF expression in debris, Lane 6: GST-GMCSF dissolved protein.

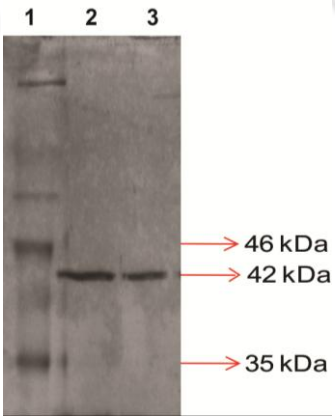

Fig 2.4. Showing purified recombinant GST-GMCSF protein, Lane 1: Marker, Lane 2 and 3: GST GMCSF protein.

2.3.3 Analysis of GST-GMCSF by Western Blot:

Western blot using anti GST antibody depicted a 42 kDa band of GST-GMCSF in lane 1 and a 26 kDa band of GST in lane 2 of Fig 2.5. Furthermore, Western blot with anti-GMCSF antibody confirmed the 42 kDa GST GMCSF protein band in lane 2 of Fig 2.6.

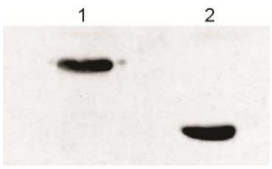

Fig 2.5. Anti GST western analysis of GST GMCSF protein. Lane 1- GST GMCSF protein, Lane 2- GST protein.

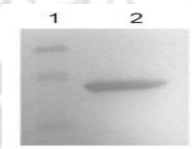

Fig 2.6. GMCSF gene specific western analysis of GST GMCSF protein. Lane 1- Protein Marker, Lane 2- GST GMCSF protein.

2.3.4 Ananlysis of MALDI TOF TOF:

Subsequently, the GST-GMCSF peptide sequence was also confirmed by MALDI-TOF/TOF analysis. Peptides generated by trypsin digestion were preceded for MALDI-TOF/TOF (Fig 2.7). The results matched with identical 19 aa of human GMCSF in MASCOT data base (Table 2.1) by 13% sequence coverage of query with a score value of 179.

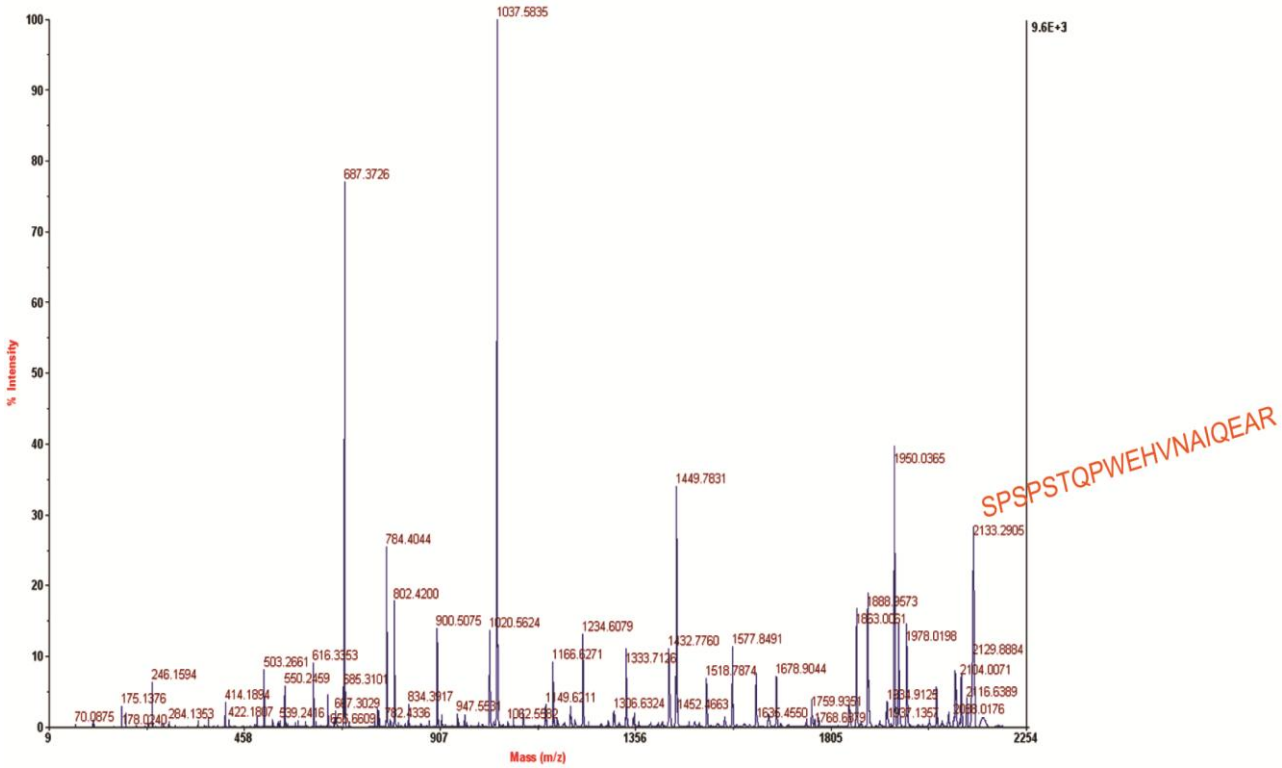

Fig 2.7. MALDI Spectra of GST-GMCSF protein after trypsin digestion.

Table 2.1 Sequence similarity of GST-GMCSF with Human CSF2 in MASCOT Database

m/z	Sequence	Protein	Method
2133.29	SPSPSTQPW EHVNAIQEAR	CSF2	M (179)

2.3.5 Analysis of Circular dichroism:

CD analysis of GST-GMCSF protein was performed using model, make Jasco. The CD spectra showed around α helix (15.6 %), β sheet (43.9 %) and the rest with 40.5% random coils (Fig. 2.8). The spectrum was analyzed by Yang's reference algorithm after baseline subtraction.

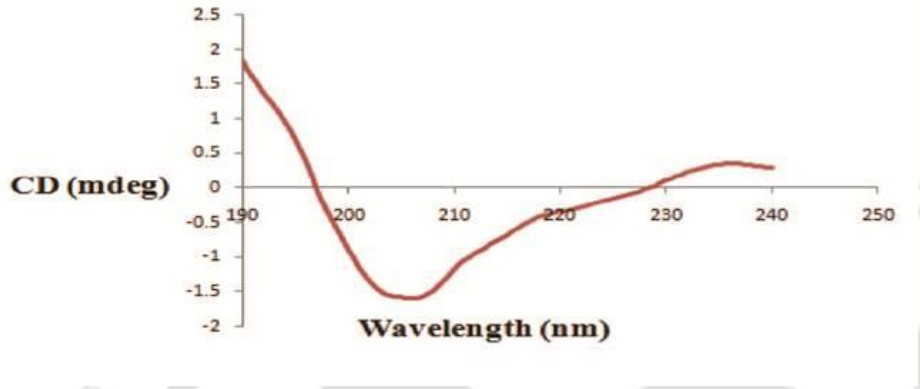

Fig 2.8. Circular Dichroism analysis of GST-GMCSF protein

2.3.6 Homology Modelling of GST-GMCSF and docking of GST-GMCSF protein with GMCSF receptor:

Three dimensional structure of GST-GMCSF protein was predicted by I-TASSER server (Fig. 2.9). PDBsum analysis of the secondary structure of the GST-GMCSF protein model showed 48 % α helix and no β sheets. The modelled structure of GST conjugation with GMCSF showed negligible structural differences from that of already crystallised structure of GST (1UA5: PDB ID) as well as with GMCSF (1CXE: PDB ID). Thus, we may assume that our predicted model did not make any difference in the wild type structure and thus may not hinder with its functionality. Hansen *et al.* (Hansen *et al*, 2008) reported the crystallized structure of GMCSF with its receptor. According to their report helix 6 of the crystallized GMCSF protein is responsible for recognizing the receptor α-subunit and helix 4 is important for interacting with the receptor β-subunit. This study showed that the residues in receptor reported to interact with GMCSF in the crystallized structure is also involved

in recognition of the GMCSF-GST conjugated model protein. Thus it can be conclusively said that Val104, Val105, Tyr 39 of the receptor subunit in both crystallized and modelled protein are the residues most important for GMCSF-receptor recognition. However it was observed that the residues in GMCSF recognizing the receptor were not interacting in the case of GST-GMCSF conjugated model protein. Two loop regions between helix 1 and helix 2; helix 4 and helix 5 were observed to be important in recognizing the receptor β-subunit (Figure 2.10). CD data obtained also showed negligible percentage of helices, and thus it may be assumed that GST conjugation with the N-terminal residues of GMCSF did not affect GMCSF interaction with the receptor subunits and the loop regions were more important for receptor β-subunit recognition. Moreover it was also observed that GST conjugation with GMCSF (modelled protein), results in greater number of residues of receptor α-subunit in the modelled protein to interact with the helix 1 (H1), helix 5 (H5) and C-terminal loop region of the modelled GMCSF (Figure 2.11). However in the crystallized structure (3CXE) only helix 5 interacts with the receptor. Thus the helix 1, helix 5 and C-terminal loop of GMCSF were interacting with that of the receptor α-subunit. GST conjugation also results in stronger interaction between the receptor α subunit and GMCSF. It was observed that residues important in interacting with the receptor β-subunit in the crystallized structure of GMCSF with its receptor interacted with the GST in the GST-GMCSF conjugated protein model (Fig. 2.12). The proliferation data supported the aforementioned observation as it suggests activity of the receptor with the purified GST-GMCSF conjugated model, thus it can be emphasized here that the reported residues are not mutually exclusively involved in GMCSF-receptor recognition. Moreover, GST alone when docked with GMCSF receptor did not interact with the interface of the GMCSF receptor α and β-subunits, which are the actual binding site of GMCSF with its receptor in the crystallized structure (Fig. 2.13). This stresses on the fact that GST alone is not involved in the activation of the GMCSF receptor. Furthermore, GMCSF modelled protein when docked with the GMCSF receptor showed interaction with the similar residues as in the crystallized GMCSF-receptor complex (Fig. 2.14). Thus the modelling data showed that the GST conjugation with GMCSF involved its loop region to activate GMCSF receptor.

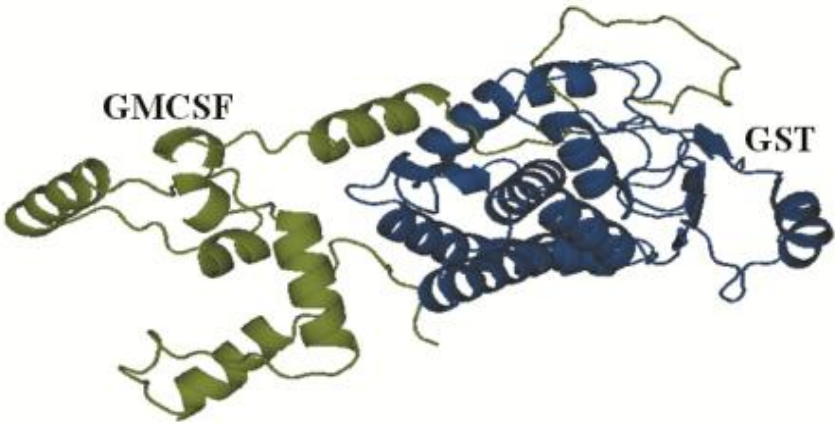

Fig 2.9. Homology model of GST GMCSF protein

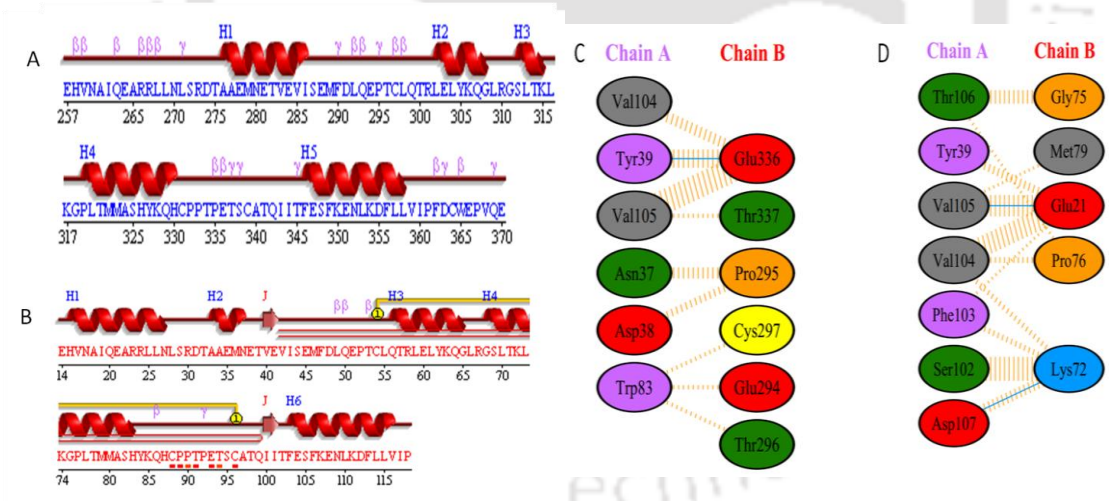

Fig 2.10 A. Secondary structure of GMCSF in modelled protein **B.** Secondary structure of crystallized GMCSF. Residue number is different in both cases **C.** Comparison of protein–protein interaction between modelled GMCSF (chain B) with that of GMCSF β-subunit (chain A) **D.** Crystallized structure of GMCSF with that of its receptor β subunit (3CXE).

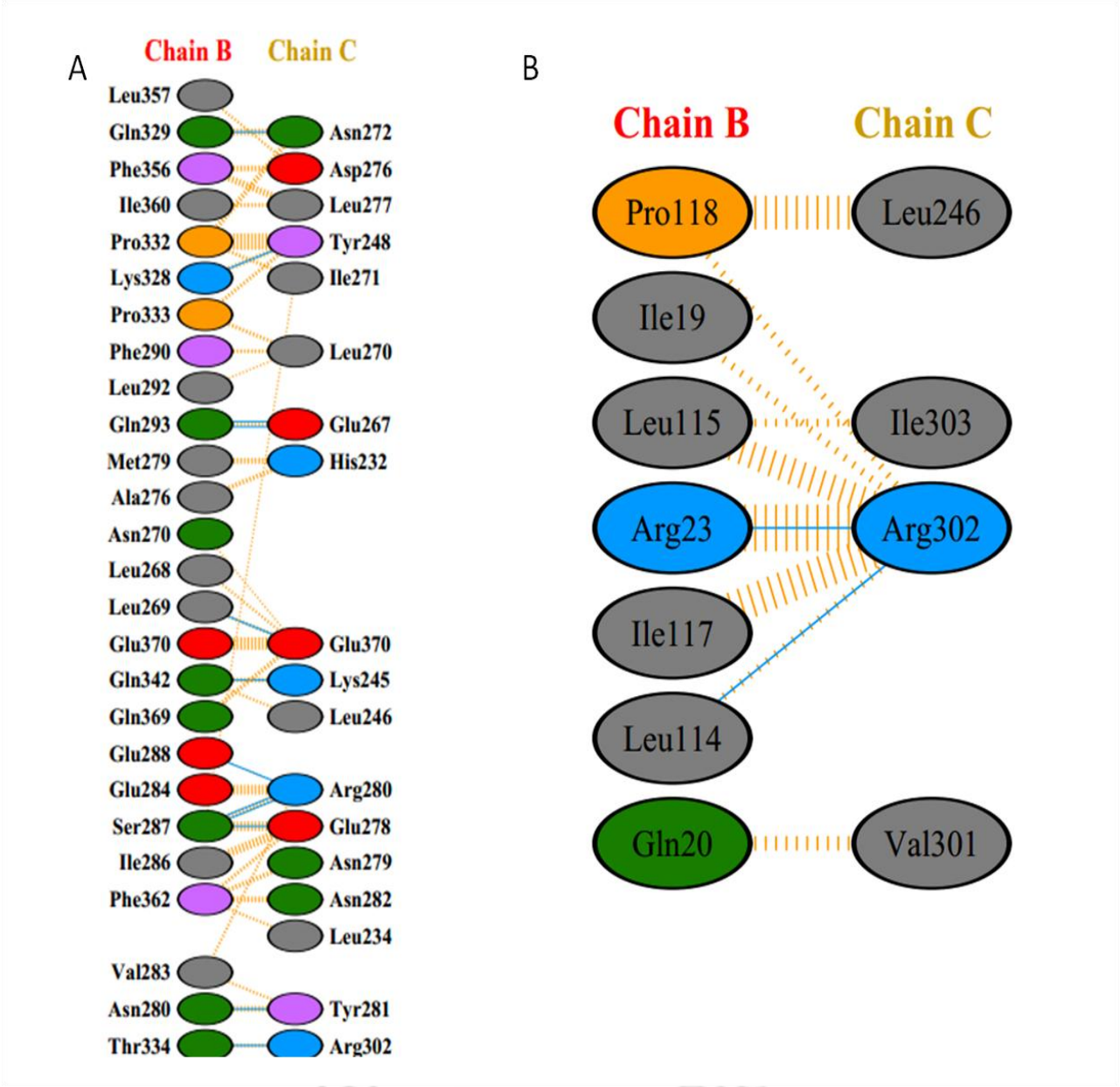

Fig 2.11 A. Amino acid residue interaction of modelled GMCSF (chain B) with receptor α subunit (chain C) **B.** Amino acid residue interaction of crystallized GMCSF (chain B) with receptor α subunit (chain C).

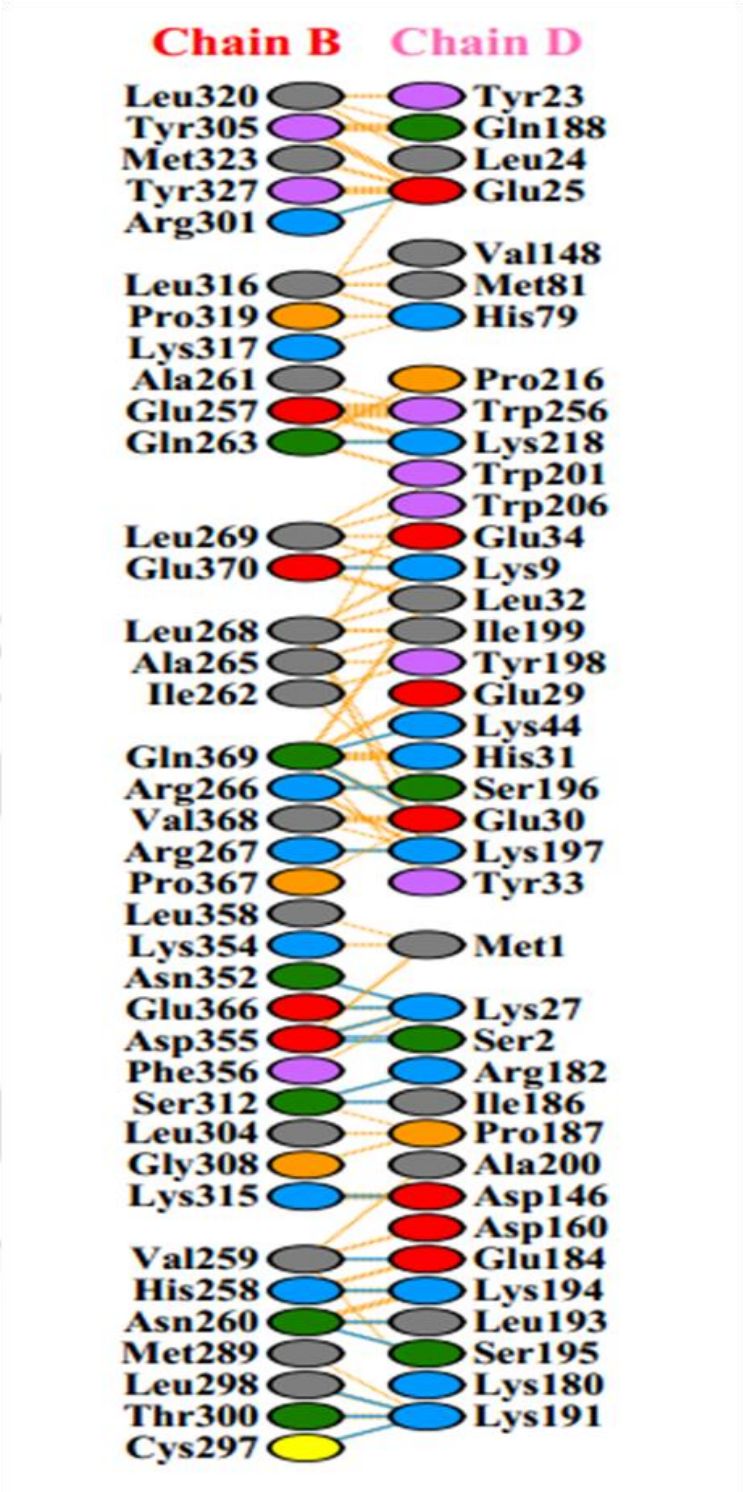

Fig 2.12. GST-GMCSF interface interaction

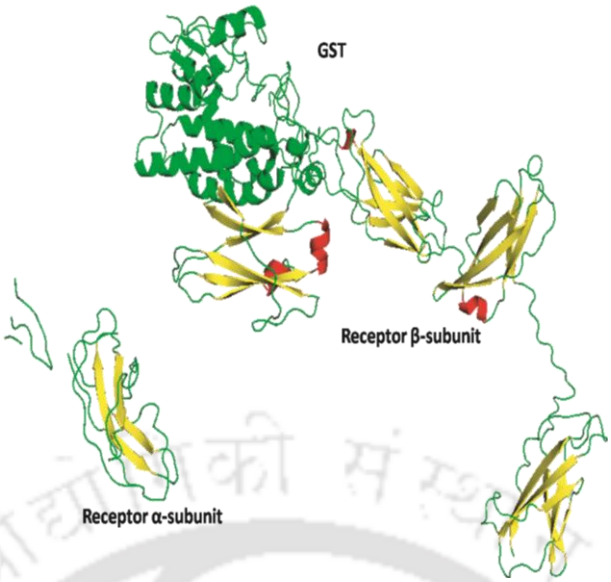

Fig 2.13. Protein–protein docked structure showing GST interaction with GMCSF receptor. GST only interacts with GMCSF β subunit.

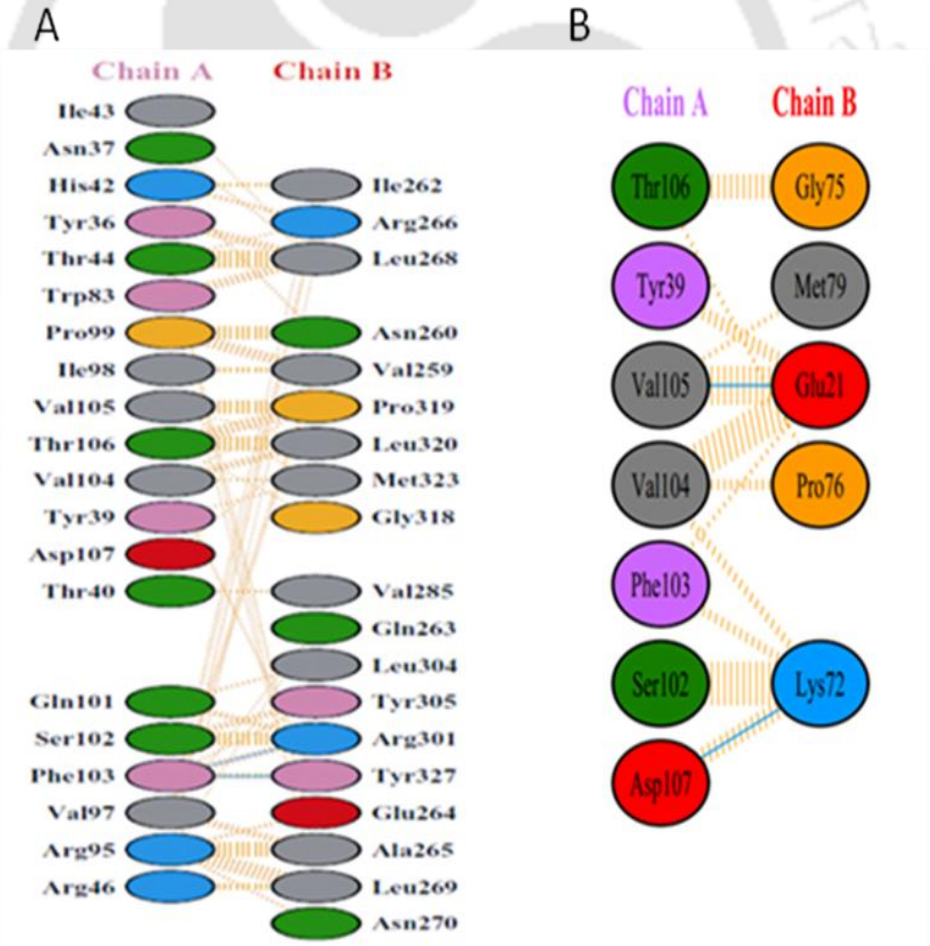

Fig 2.14. Interaction of **(A)** Modelled GMCSF with receptor **(B)** crystallized GMCSF with receptor.

2.3.7 Activity assay of GST-GMCSF:

We have tested cell proliferative activity of GST-GMCSF on haematopoietic THP-1 cell line and three non-haematopoietic cell lines, such as, MCF-7, Raw 264.7 and U87MG. The GST-GMCSF exerted its effect in a dose dependent manner and the optimum protein concentration for executing maximum proliferative response varied for different cell lines. More than two fold increase in cell proliferation was observed after 24 h of GST-GMCSF addition on THP-1, Raw 264.7 and MCF-7 cells as compared to untreated control, whereas U87MG showed 1.4 fold increased in proliferation (Fig. 2.15). GST-GMCSF stimulated the proliferation of different cell lines in a dose dependent manner at varies protein concentration and the required amount of protein for proliferating Raw 264.7 macrophages cells and THP-1 cells was less. These cells were proliferating upto 1.5 fold in 20 ng/mL protein concentration only while there was no significant effect observed over U87MG cells and MCF-7 cells, at this protein concentration. Different cells exhibited maximum proliferation at a particular dose of GST-GMCSF as compared to the untreated cells. Cell viability was checked by XTT assay after 24 hrs of GST-GMCSF addition and the percentage cell viability was calculated comparing the untreated cells.

% viability= (Treated cells absorbance / untreated cells control absorbance) × 100

All the experimental data were represented as Mean ± standard deviation (SD) of three independent experiments. Statistical significance was checked by two way analysis of variance (ANOVA). The significance of data was considered for $P < 0.05$.

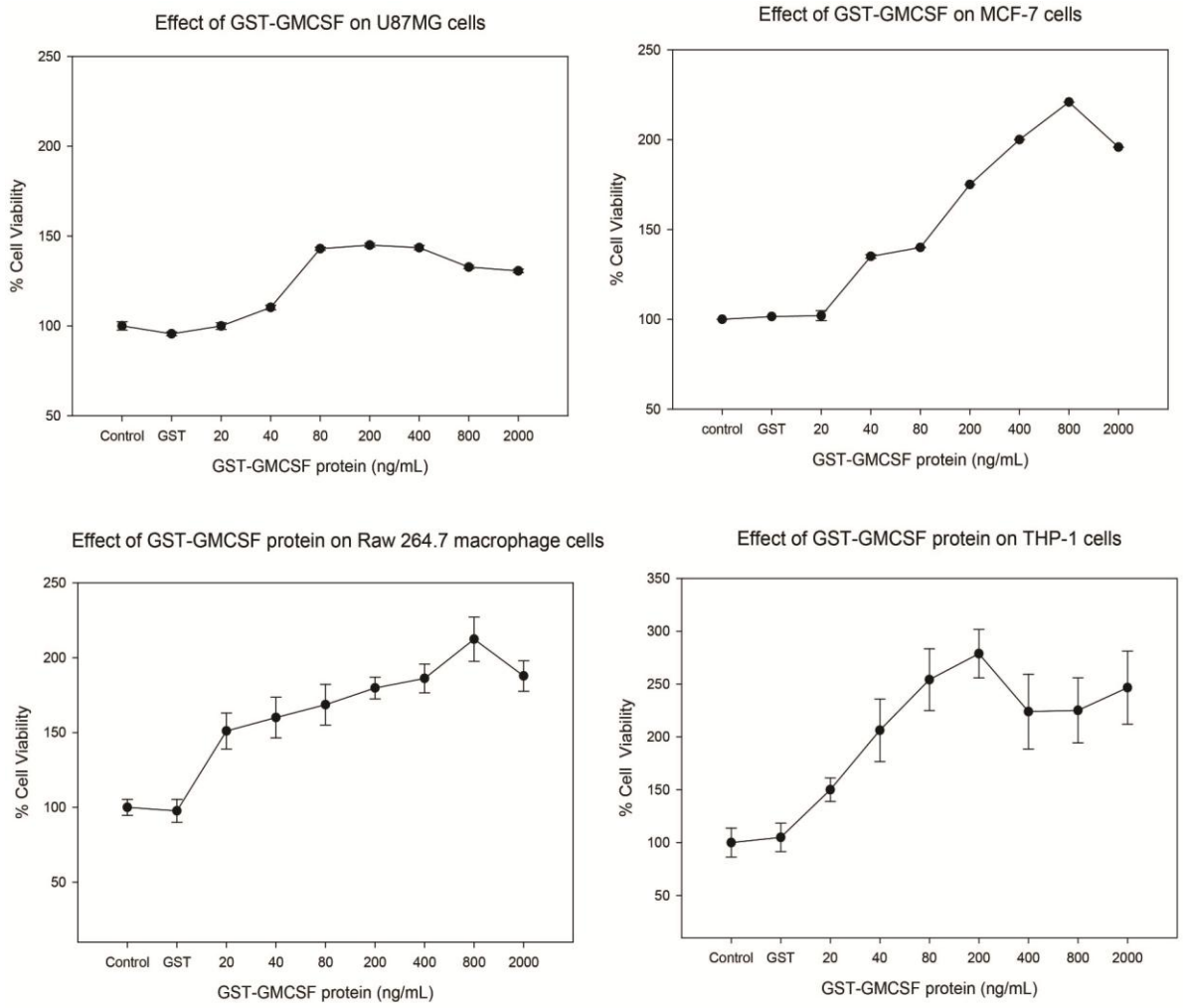

Fig 2.15. Effect of GST-GMCSF on cell viability

Table 2.2. Optimum protein conc. of GST-GMCSF for maximum proliferation in different cell lines

Serial No.	Cell lines	Optimum protein Conc. of GST-GMCSF (ng/mL)	Fold proliferation (with respect to untreated control)
1.	THP-1 human leukemia	200	2.7
2.	Raw 264.7 mouse Macrophages	800	2.2
3.	MCF-7 human breast cancer	800	2.2
4.	U87 MG	80	1.4

2.4 Conclusion

In this chapter 2, a novel cytokine GMCSF from unstimulated human renal carcinoma ACHN cells was cloned. An easy method to solubilize GST-GMCSF from inclusion bodies was developed. The GST tag was very useful for one step purification of the recombinant protein. The recombinant GST-GMCSF was thoroughly characterized using analytical tools. The CD data revealed a major portion of β sheets along with less α-helix. The recombinant protein showed cell proliferative activity. It has been reported by Hansen *et al* that helicity is responsible for binding to GMCSF receptor; however, the modelling and docking results (GST-GMCSF docked with GMCSF receptor) implicated that a hydrophobic loop might be responsible for binding with the GMCSF receptor, and thus the protein activity was retained. Furthermore, the GST tag provided functional stability to the recombinant GST-GMCSF. Experimental data suggested that the recombinant GMCSF could induce proliferation of various types of cells. This possibly is the first report to show the effect of a GST tagged GMCSF activity in cell proliferation. This recombinant cytokine could be further explored as an adjuvant in viral gene therapy (Ghosh *et al*, 2006; Yata *et al*, 2012). This recombinant GMCSF is not only useful to ameliorate growth of macrophages near ablated tumour sites, but may facilitate the growth and recovery of normal cells after prolonged treatment with chemotherapeutic drugs during cancer therapy.

2.5 References

1. Barreda, D.R., Hanington, P.C., and Belosevic, M. (2004). Regulation of myeloid development and function by colony stimulating factors. Dev. Comp. Immunol. *28*, 509–554.
2. Belardelli, F., and Ferrantini, M. (2002). Cytokines as a link between innate and adaptive antitumor immunity. Trends Immunol. *23*, 201–208.
3. Cantrell, M.A., Anderson, D., Cerretti, D.P., Price, V., McKereghan, K., Tushinski, R.J., Mochizuki, D.Y., Larsen, A., Grabstein, K., and Gillis, S. (1985). Cloning, sequence, and expression of a human granulocyte/macrophage colony-stimulating factor. Proc. Natl. Acad. Sci. U.S.A. *82*, 6250–6254.
4. Cebon, J., Nicola, N., Ward, M., Gardner, I., Dempsey, P., Layton, J., Dührsen, U., Burgess, A.W., Nice, E., and Morstyn, G. (1990). Granulocyte-macrophage colony stimulating factor from human lymphocytes. The effect of glycosylation on receptor binding and biological activity. J. Biol. Chem. *265*, 4483–4491.
5. Chung, C.T., Niemela, S.L., and Miller, R.H. (1989). One-step preparation of competent Escherichia coli: transformation and storage of bacterial cells in the same solution. Proc. Natl. Acad. Sci. U.S.A. *86*, 2172–2175.
6. Galati, G., Rovere, P., Citterio, G., Bondanza, A., Scagliette, U., Bucci, E., Heltai, S., Fascio, U., Rugarli, C., and Manfredi, A.A. (2000). In vivo administration of GM-CSF promotes the clearance of apoptotic cells: effects on monocytes and polymorphonuclear leukocytes. J. Leukoc. Biol. *67*, 174–182.
7. Gasson, J.C., Kaufman, S.E., Weisbart, R.H., Tomonaga, M., and Golde, D.W. (1986). High-affinity binding of granulocyte-macrophage colony-stimulating factor to normal and leukemic human myeloid cells. Proc. Natl. Acad. Sci. U.S.A. *83*, 669–673.
8. Ghosh, S., Rasheedi, S., Rahim, S.S., Banerjee, S., Choudhary, R.K., Chakhaiyar, P., Ehtesham, N.Z., Mukhopadhyay, S., and Hasnain, S.E. (2004). Method for enhancing solubility of the expressed recombinant proteins in Escherichia coli. BioTechniques *37*, 418, 420, 422–423.
9. Ghosh, S.S., Gopinath, P., and Ramesh, A. (2006). Adenoviral vectors: a promising tool for gene therapy. Appl. Biochem. Biotechnol. *133*, 9–29.

10. Hammarström, M., Hellgren, N., van Den Berg, S., Berglund, H., and Härd, T. (2002). Rapid screening for improved solubility of small human proteins produced as fusion proteins in Escherichia coli. Protein Sci. *11*, 313–321.
11. Hansen, G., Hercus, T.R., McClure, B.J., Stomski, F.C., Dottore, M., Powell, J., Ramshaw, H., Woodcock, J.M., Xu, Y., Guthridge, M., et al. (2008). The structure of the GM-CSF receptor complex reveals a distinct mode of cytokine receptor activation. Cell *134*, 496–507.
12. Havlis, J., Thomas, H., Sebela, M., and Shevchenko, A. (2003). Fast-response proteomics by accelerated in-gel digestion of proteins. Anal. Chem. *75*, 1300–1306.
13. Jimenez, C. R., Huang, L., Qiu, Y., and Burlingame, A. L. (1998).Current Protocols in Protein Science, 16, 4.1-16.4.5.
14. Kaushansky, K., O'Hara, P.J., Hart, C.E., Forstrom, J.W., and Hagen, F.S. (1987). Role of carbohydrate in the function of human granulocyte-macrophage colony-stimulating factor. Biochemistry *26*, 4861–4867.
15. Kozakov, D., Hall, D.R., Beglov, D., Brenke, R., Comeau, S.R., Shen, Y., Li, K., Zheng, J., Vakili, P., Paschalidis, I.C., et al. (2010). Achieving reliability and high accuracy in automated protein docking: ClusPro, PIPER, SDU, and stability analysis in CAPRI rounds 13-19. Proteins *78*, 3124–3130.
16. Laemmli, U.K. (1970). Cleavage of structural proteins during the assembly of the head of bacteriophage T4. Nature *227*, 680–685.
17. Moonen, P., Mermod, J.J., Ernst, J.F., Hirschi, M., and DeLamarter, J.F. (1987). Increased biological activity of deglycosylated recombinant human granulocyte/macrophage colony-stimulating factor produced by yeast or animal cells. Proc. Natl. Acad. Sci. U.S.A. *84*, 4428–4431.
18. Petrov, S., Nacheva, G., and Ivanov, I. (2010). Purification and refolding of recombinant human interferon-gamma in urea-ammonium chloride solution. Protein Expr. Purif. *73*, 70–73.
19. Roy-Ghanta, S., and Orange, J.S. (2010). Use of cytokine therapy in primary immunodeficiency. Clin Rev Allergy Immunol *38*, 39–53.
20. Sambrook, J., Fritsch, EF., Maniatis, T. (1989) Molecular Cloning: A Laboratory Manual. 3rd ed, Cold Spring Harbor, New York: Cold Spring Harbor Laboratory Press.
21. Schwanke, R.C., Renard, G., Chies, J.M., Campos, M.M., Batista, E.L., Jr, Santos, D.S., and Basso, L.A. (2009). Molecular cloning, expression in

Escherichia coli and production of bioactive homogeneous recombinant human granulocyte and macrophage colony stimulating factor. Int. J. Biol. Macromol. *45*, 97–102.

22. Speers, A.E., and Wu, C.C. (2007). Proteomics of integral membrane proteins--theory and application. Chem. Rev. *107*, 3687–3714.
23. Ventura, S., and Villaverde, A. (2006). Protein quality in bacterial inclusion bodies. Trends Biotechnol. *24*, 179–185.
24. Walter, M.R., Cook, W.J., Ealick, S.E., Nagabhushan, T.L., Trotta, P.P., and Bugg, C.E. (1992). Three-dimensional structure of recombinant human granulocyte-macrophage colony-stimulating factor. J. Mol. Biol. *224*, 1075–1085.
25. Yata, V.K., Gopinath, P., and Ghosh, S.S. (2012). Emerging implications of nonmammalian cytosine deaminases on cancer therapeutics. Appl. Biochem. Biotechnol. *167*, 2103–2116.

CHAPTER 3

Silver nanoparticle loaded PLGA composite nanoparticles for improving therapeutic efficacy of recombinant IFNγ by targeting cell surface

CHAPTER 3

3.1 Introduction

In last few decades, an ample growth has occurred in the field of cancer therapy, due to advent of new molecular entities and unearthing of crucial cell signalling pathways, which provide new opportunities in both therapeutic and basic research frontiers. However, suitable drug molecule(s) or novel therapeutic methods that imply to replace the conventional chemo /radio therapy have not been translated to therapeutic level, at least not in clinical practice so far. Preferential delivery of therapeutic agents at the tumour sites while avoiding their undesired accumulation at the other sites i.e. "spatial drug delivery" is a matter of pivotal importance to curb the amount and subsequent side effects of drugs are now under consideration (Danhier *et al* 2010; Bae *et al*, 2011; Lammers *et al*, 2012). In this scenario, nanoparticle mediated drug delivery offers promising opportunities, as it exhibits high efficacy due to its favourable size and tunable physicochemical properties. Moreover, conjugation of specific ligand(s) on the surface of the NPs provides significant level of selectivity by active targeting (Peer *et al*, 2007; Cho *et al*, 2008; Farokhzad *et al*, 2009; Dinarvand *et al*, 2012). However, the major difficulty faced by any chemotherapeutic drug to access tumour site is mainly due to intricate cellular organization of surrounding cells. In such case, NPs mediated drug delivery increases blood circulation half-life and bioavailability of the drugs within a therapeutic frame and consequently, avoid immediate dose and frequency escalation, thus mediating a controlled release of drug (Segura *et al*, 2005; Vij *et al*, 2010).

Furthermore, it would be beneficial to apply recombinant therapeutic agents of human origin, which may reduce the likelihood of host antagonistic responses. In this context, protein therapeutics has gained an edge over other options as their rate of industrial translation is high. For example, recombinant insulin isolated from *E.coli* has replaced the whole market from animal source (Vajo *et al*, 2001) and the recombinant IFNα-2a is now used in cancer therapy and treatment of autoimmune diseases (Minasian *et al*, 1993). Another such molecule is IFNγ, a naturally occurring cytokine, which is produced and secreted by the immune system cells e.g., white blood cells and natural killer cells. IFNγ interacts with its cell surface receptors and induce signal transduction through JAK-STAT pathway (Lange *et al*, 2011), which

subsequently elicits multiple responses, such as, prevention of viral replication, cell growth inhibition and cell differentiation (Kano *et al*, 1997; Samuel *et al*, 2001; Billiau *et al*, 2009; Lange *et al*, 2011). IFNγ is an FDA approved cytokine (Roy *et al*, 2010), which is involved in activation of T cells and macrophage, exerts tumoricidal and antimicrobial activity, having a huge impact on host defence system (Girdlestone *et al*, 1996). Moreover, recent studies portray the important role of IFNγ in cancer immunesurveillance (Ikeda *et al*, 2002; Dunn *et al*, 2004; Brandacher *et al*, 2006).

However, therapeutic applications of IFNγ is limited due to its shorter life time and rapid clearance from body, and furthermore, its higher dose and repetitive uses cause severe side effects (Dong *et al*, 2005; Segura *et al*, 2005). Therefore, prolonged sustainability of IFNγ in blood would be a viable option for exploiting maximum therapeutic efficacy by its possible integration with nanoparticles. Recent studies from several laboratories including ours, demonstrated that Ag NPs has great potential as antibacterial as well as anti-cell proliferative agent. Essentially, Ag NPs lead to apoptosis in mammalian cells (Gopinath *et al*, 2008; Gopinath *et al*, 2010; Sahoo *et al*, 2011).

Keeping this in view, we have cloned, expressed and purified GST fused IFNγ protein. It is to be mentioned here that GST tag minimises the steps of protein purification, provides stability and facilitates single step purification of the recombinant protein (Smyth *et al*, 2003; Ghosh *et al*, 2004). Recombinant IFNγ protein was being expressed in inclusion bodies (Petrov *et al*, 2010), which was further purified and delivered to cancer cells by freshly synthesized Ag NPs coated poly lactic-co-glycolic acid (PLGA) composite NPs. The PLGA is known as a biodegradable polymer comprising of monomers of lactic and glycolic acids (Murakami *et al*, 1999; Dinarvand *et al*, 2011; Danhier *et al*, 2012). We explored the complementary effects of the composite NPs, where the recombinant IFNγ was shown to block cell cycle and the Ag NPs had induced apoptosis by cell surface receptor mediated targeting with the recombinant IFNγ as ligand. This combination therapy is a novel approach, where the additive effects of the recombinant IFNγ and Ag NPs at their low concentrations, may provide a new platform to enhance therapeutic efficacy of IFNγ stabilized composite nanoparticles. Scheme 3.1 provides a brief overview of the current work encompassing cloning, purification, functional aspects of recombinant protein and delivery with Ag NPs for therapeutic application.

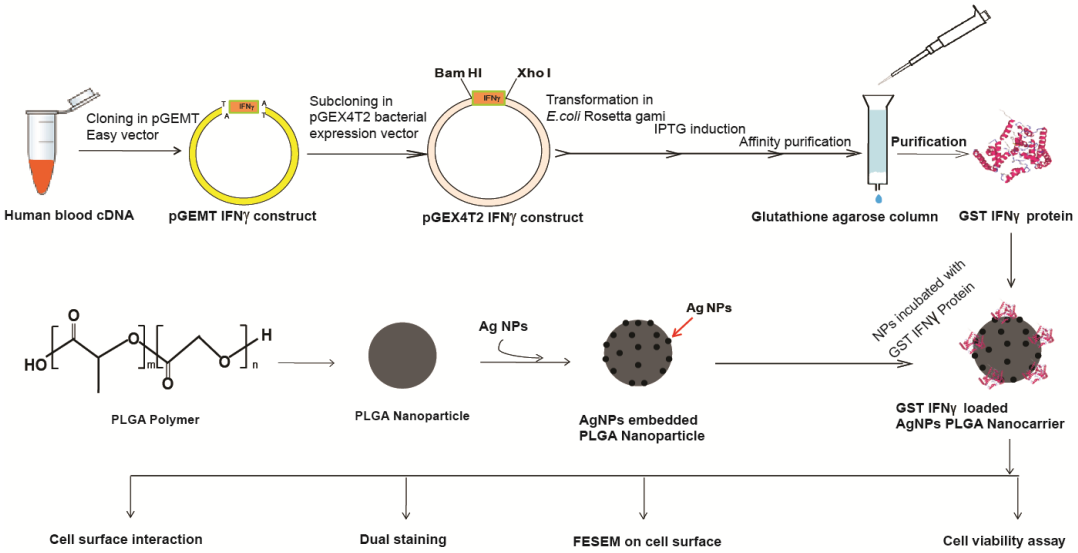

Scheme 3.1. Schematic representation of development and functional aspects of composite nanoparticles (GST IFNγ -Ag PLGA NPs)**.**

3.3 Materials and Methods

3.2.1 Cell Culture:

Cell lines for work were obtained from NCCS Pune, India. The cells were periodically subcultured in DMEM media supplemented with 10% FBS, 20 U/mL penicillin and 50 mg/mL streptomycin in 5% CO_2 humidity at 37 °C.

3.2.2 Cloning of Human IFNγ:

IFNγ gene was cloned from human blood cDNA. Gene specific forward primer (5'ATGTGGCTGCAGAGCCTGCTG3') and reverse primer (5'TCACTCCTGGACTGGCTCCCA3') were designed for PCR and cloning of IFNγ in pGEMT Easy vector was done. Subsequently IFNγ gene was subcloned into N terminal GST tag pGEX4T2 expression vector (Amersham) using primers with *Bam HI* and *Xho I* in flanking sites (Forward primer: 5' GCGGATCCATGAAATATACAAGTTAT 3'; Reverse primer: 5' GACTCGAGTTACTGGGATGCTCTTC 3'). IFNγ gene is located at chromosome 5q23-q31 (NM_000619.2).

3.2.3 Expression of IFNγ in *E.coli* Rosetta gami strain:

The pGEX4T2 IFNγ construct was transformed into *E.coli* Rosetta gami expression host. A starter mini culture was developed by inoculating a single colony in LB medium supplemented with 100 µg/mL ampicillin for 14 h at 37°C. This culture was further used as inoculum (1:250 dilutions) for scale up in 500 mL LB media with ampicillin. At 0.4-0.6 OD_{590}, IPTG was added to the growing culture for expression of Lac operon regulated recombinant protein and allowed to grow for another 12 h for induction of recombinant GST tagged IFNγ protein. Finally the grown culture was centrifuged at 12,000 g for 15 min to harvest the bacterial pellet and stored at -20°C for further applications.

3.2.4 Solubilisation, refolding and purification of GST IFNγ from inclusion bodies:

The GST IFNγ overexpressing bacterial cells were suspended in ice chilled lysis buffer (50 mM Tris pH 8.0 with 1% of sarkosyl, 1 mM PMSF, 1 mM EDTA) and sonicated at 20 kpsi for 10 min for cell lysis (Tao *et al*, 2010; Park *et al*, 2011). The presence of GST IFNγ protein was confirmed by 12% SDS-PAGE analysis of the cell lysate. After cell lysis, 20 mM CHAPS and 2% Triton X 100 were added to the lysed cell solution and kept for continuous stirring for 30 min to form micelle of sarkosyl. This step opens up the covering of sarkosyl from GST IFNγ and makes the protein free. CHAPS and Triton X 100 are neutral detergent molecules, which help in the micelle formation of sarkosyl itself and thus the solubilised protein becomes free of its cationic surrounding made by sarkosyl. Further this solution was separated from the debris through centrifugation followed by dialysis in PBS (pH 7.4). This protein mixture was passed through the glutathione agarose 4B matrix (Sigma). The recombinant GST IFNγ protein was eluted with 10 mM reduced glutathione in PBS and checked by 12 % SDS PAGE analysis followed by silver staining (Kerényi *et al*, 1973).

3.2.5 Protein estimation by Bradford assay:

The protein sample which was present in PBS was estimated by Bradford assay (Sigma). As per the manufacturer protocol, 200 µL of protein sample was mixed with 200 µL Bradford Reagent and kept at room temperature for 15 min. After incubation,

200 µL of the reaction mixture of each sample was transferred to the 96 well plate and the optical density was measured at 595 nm by ELISA reader (Bradford *et al*, 1976).

3.2.6 Western Blot analysis:

Purified GST IFNγ was confirmed by anti-GST Western blot. Mouse anti-GST (Sigma) and mouse anti-human IFNγ antibodies were used as primary antibodies (BD Pharmingen, USA). Horse radish peroxidase conjugated goat anti-mouse polyclonal IgG was used as secondary antibody (BD Pharmingen, USA). Blot was developed using chemiluminescence (Super Signal West Dura, Thermo Scientific) and imaged using gel documentation system (Gel logic 1500, Kodak).

3.2.7 MALDI analysis:

Purified GST IFNγ protein was characterized with MALDI TOF TOF (4800 Plus Applied Biosystem) before loading on nanoparticles. Recombinant protein was eluted by in gel trypsin digestion (Sigma Kit) for 12 h and spotted at α cyano 4 hydroxy cinnamic acid matrix of MALDI plate. The samples were analyzed by MALDI TOF (Yergey *et al*, 2002; Havlis *et al*, 2003).

3.2.8 Measurement of ROS generated by IFNγ on Raw 264.7 cells:

To determine the activity of GST IFNγ purified protein in ROS generation, we added 5 µM Dichloro fluorescein (DCFDA, Sigma) on Raw 264.7 mouse macrophages after 24 h treatment with recombinant GST IFNγ protein. The samples were analysed by flow cytometer (FacsCalibur, BD Biosciences, NJ) at an excitation wavelength of 488 nm and emission wavelength of 530. The fluorescence data were recorded with the CellQuest program (BD Biosciences) for 15,000 cells in each sample.

3.2.9 Synthesis of PLGA and composite (Ag PLGA NPs) NPs:

The PLGA NPs were synthesized by using emulsification solvent evaporation method (Murakami *et al*, 1999; Dinarvand *et al*, 2011; Danhier *et al*, 2012). In brief, 10 mg of PLGA was dissolved in 1.5 mL of chloroform. Then, the PLGA solution was added dropwise into 2 mL of 0.5% of PVA (5 mg/mL) solution under continuous sonication at 40 kpsi for 10 minutes. During sonication the temperature of the reaction was maintained at 90°C which facilitated the removal of organic solvent. The NPs were

collected by centrifugation at 6,000 rpm for 5 minutes. The collected NPs were extensively washed with water for the complete removal of organic solvent which is toxic to the mammalian cells and finally dissolved in deionized water. For the preparation of fluorescent NPs, 10 µL of fluorescein (1 mg/mL) was added into the PVA solution before addition of PLGA. For the synthesis of composite NPs of Ag NPs and PLGA NPs, first, silver nano particles were synthesised with the reaction of 200 µL of 10 mM Ag NO_3 and 1 mL of sodium borohydride (10 mM) into 2 mL of 0.5% of PVA (5 mg/mL) where PVA acted as stabilizing agent of the Ag NPs. Then, this pre formed PVA stabilized Ag NPs were used as emulsifying agent for the synthesis of composite NPs (Ag PLGA NPs) by maintaining the same reaction conditions as described above.

3.2.10 Hydrodynamic diameter and zeta potential measurement:

Hydrodynamic diameter and zeta potential of PLGA and composite NPs (Ag PLGA NPs) were analysed by Malvern Zeta Sizer Nano ZS in PBS buffer. The same experiment was also performed after incubation with GST IFNγ protein.

3.2.11 Surface Morphology study:

Surface morphology of NPs was studied with Field Emission Scanning electron microscopy (FESEM) and transmission electron microscopy (TEM). For FESEM analysis, 20 µL of the sample was drop casted on the glass slide which was rapped with aluminium foil and sputter-coated with gold film using a sputter coater (SC7620"Mini", Polaron Sputter Coater, Quorum Technologies, New haven, England) and analysed by FESEM. For the TEM analysis, 7 µL of the sample was added on the carbon coated copper grid, dried and analysed under TEM (TEM; JEM 2100; Jeol, Peabody, MA) which was operating at an accelerating voltage of 200 keV.

3.2.12 Determination of IFNγ protein binding efficiency with NPs:

Binding of GST IFNγ protein with the PLGA and composite NPs was confirmed by fluorescence spectroscopy study. For that, different amount of protein (5-40 ng) were incubated with the fixed amount of NPs (1 µg) for 1 h at 37°C, followed by centrifugation (6,000 rpm, 5 min) to remove the unbound protein. The fluorescence intensity of the FITC was gradually decreased at 520 nm (when excited at 480 nm) for

both the NPs such as PLGA and composite NPs with increasing concentration of the protein. The protein binding was also validated by UV-vis spectroscopy study. For that, both the NPs i.e. PLGA and composite NPs (20 µg) were incubated with different amounts of the recombinant IFNγ (500-3000 ng) for 1 h at 37°C, followed by centrifugation at 6,000 rpm for 2 minutes. The NPs were collected by discarding the supernatant and measured the absorbance at 280 nm to find out the amount of protein immobilized on the surface of the NPs.

3.2.13 Protein Release Assay:

To study the protein release, 5 µg of GST-IFNγ was incubated with 200 µg of Ag PLGA NPs at 37°C for 72 h in PBS (pH 7.4). The samples were taken out periodically and centrifuged to pellet down the nanoparticles. The supernatant was collected and the absorbance was measured at 280 nm by UV-Vis spectroscopy, which corresponds to the amount of released protein.

3.2.14 Fourier Transform Infrared Spectroscopy Analysis:

To perform FTIR analysis, the samples were first lyophilized to remove the water. Then the dried samples were mixed with KBr to make the pellets and analysed by Perkin-Elmer Spectrum in the range of 4000 - 400 cm^{-1}.

3.2.15 Fluorescence Microscopy Study:

To perform the microscopy imaging, cells were grown in a 6-well plate (1×10^5 cells/ well) for 12 h. The cells were treated with the PLGA NPs, composite NPs (Ag PLGA NPs) and GST IFNγ protein immobilized NPs for 3 h. After that, the cells were thoroughly washed with PBS to remove the residual NPs and observed by epi fluorescence microscopy (20 X, Nikon ECLIPSE, TS100, Tokyo). As FITC was incorporated with the NPs, treated cells showed green emission with the excitation with blue light as compared to the control cells.

3.2.16 Protease protection assay:

For protease protection assay, 500 ng of free GST IFNγ as well as the GST IFNγ loaded Ag PLGA NPs (20 µg) was incubated with Protease (Qiagen) at 37°C for 30 minutes. After that, samples were analyzed using 12% SDS PAGE analysis.

3.2.17 Acridine Orange/ Ethidium Bromide (AO/EtBr) double staining:

For the double staining, 5×10^3 HeLa cells and 3×10^3 MCF-7 cells were seeded in 96 wells plate and grown overnight. Cells were treated with PLGA, composite NPs (GST IFNγ -Ag PLGA NPs), GST IFNγ protein and protein immobilized NPs for 24 h. Then mixture of acridine orange (20 µg/mL) and ethidium bromide (20 µg/mL) was applied to cells for 5 minutes. The cells were washed with PBS to remove the free dye and observed under epi fluorescence microscope at 20X (Nikon ECLIPSE, TS100, Tokyo).

3.2.18 Cell Viability assay:

The cell viability assay was performed after treatment with the NPs and the protein immobilized NPs by MTT (3-(4,5- dimethylthiazol-2-yl)-2,5-diphenyltetrazolium bromide). 5×10^3 HeLa cells and 3×10^3 MCF-7 cells were seeded in 96 wells plate and grown overnight. Then, varying amounts of PLGA, composite NPs (Ag PLGA NPs), GST protein, GST IFNγ protein and protein immobilized Ag PLGA NPs were added separately to the cells. MTT assay was performed after 48 h. The colorless MTT (3-(4, 5-Dimethylthiazol-2-yl)-2,5-diphenyltetrazolium bromide) was converted into blue color formazan by dehydrogenases of respiring mitochondria in viable cells. Water insoluble formazan was solubilized by adding DMSO, and the color product measured (absorbance at 550 nM) was directly correlated with the number of viable cells with background substraction at 650 nM (Mosmann *et al,* 1983).

3.2.19 Cell Cycle analysis:

Cell cycle analysis was performed by FACS, for which cells were grown in a 6 well plate (1×10^5 cells/ well) for 12 h followed by the treatment with the GST IFNγ protein, composite NPs (Ag PLGA NPs) and GST IFNγ protein immobilized NPs for 48 h. The cells were trypsinized and collected by centrifugation at 650 rcf, 6 min at 4°C. The cells were then fixed with 70% ethanol at -20°C for 1 h. The 100 µg/mL RNase was added into that fixed cells and incubated for 30 min at 37°C. Next, 40 µg/mL propidium iodide (PI) was added with 0.01% Triton X-100 into the cells and samples were analysed by Florescence Activated Cells Sorter (FacsCalibur, BD Biosciences, NJ). The fluorescence data were recorded with the Cell Quest program

(BD Biosciences) for 10,000 cells in each sample.

3.2.20 Caspase 3 Assay:

HeLa cells were seeded at 1×10^5 cells/ well and treated with IC_{50} of the Ag PLGA NPs in serum media, (1.36 µg/mL) for 18 h. Then cells were trypsinized and fixed with 0.1% of formaldehyde in PBS for 15 min at room temperature (25°C). Further, cells were pellet down by centrifugation at 300 g and incubated with 1 mL of membrane permealization solution (0.5% of Tween 20 in PBS) for another 15 min in dark followed by washing with double volume of PBS. Finally cells were treated with PE conjugated Rabbit Anti –Active-Caspase-3 (Catalog No. 550821, BD Biosciences) for 30 min in dark. Finally, the samples were analysed in FACS.

3.3 Results and Discussions

3.3.1 Cloning of human IFNγ:

A 501 bp IFNγ gene was PCR amplified from human blood cDNA and initially cloned into the pGEMT Easy cloning vector. The clone was confirmed by *Eco RI* restriction digestion (Fig. 3.1A) and further subcloned into pGEX4T2 bacterial expression vector to generate recombinant pGEX4T2-IFNγ plasmid (Fig. 3.1B). The clone was further confirmed by restriction digestion with *Xho I* and *Bam HI* enzymes followed by sequencing.

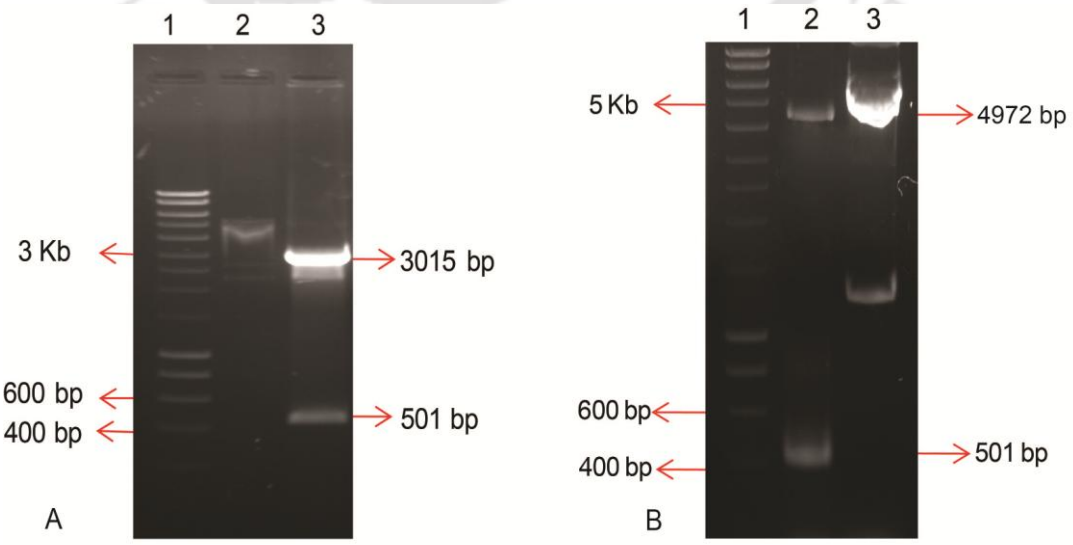

Fig 3.1. Agarose gel electrophoresis of pGEX4T2-IFNγ plasmid **(A)** Lane 1: Hyper ladder (NEB) , Lane 2: Undigested plasmid, Lane 3: *Eco RI* digested pGEMT IFNγ

construct **(B)** Lane 1: Hyper ladder (NEB), Lane 2: pGEX4T2 IFNγ plasmid digested with *Bam HI* and *Xho I* showing 4972 bp vector backbone 501 bp IFNγ insert, Lane3: Undigested plasmid.

3.3.2 Expression and characterization of GST IFNγ:

The construct was transformed into *E.coli* Rosetta gami and the recombinant IFNγ expression was induced with IPTG (Fig. 3.2A). However, the recombinant protein mainly appeared in inclusion bodies (Lane 5, Fig. 3.2A), which was solubilised using 1% sarkosyl, 20 mM CHAPS and 2% Triton X-100. The recombinant IFNγ was purified to a single band of 44 kDa using glutathione agarose affinity chromatography (Lane 1, Fig. 3.2B).

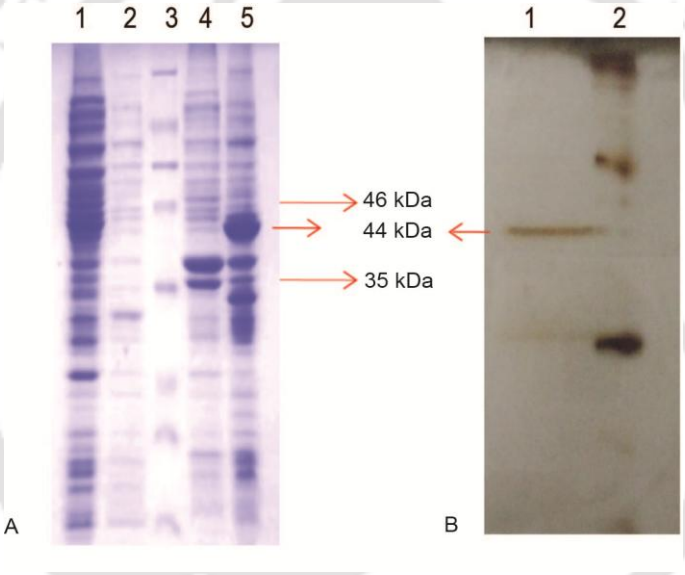

Fig 3.2. (A) SDS-PAGE of *E.coli* Rosseta gami cell lysates. Lane 1: supernatant of pGEX4T2 transformed IPTG induced cell lysates, Lane 2: cell pellet of pGEX4T2 backbone transformed IPTG induced cells, Lane 3: protein marker, Lane 4: supernatant of pGEX4T2-IFNγ transformed cell lysate after IPTG induction, Lane 5: inclusion bodies of pGEX4T2-IFNγ transformed cells after IPTG induction **(B)** SDS-PAGE of purified GST IFNγ using GST glutathione affinity chromatography, Lane 1: protein marker and Lane 2: purified GST IFNγ protein.

3.3.3 Western blot analysis of GST IFNγ:

Western blotting also showed a single band of 44 kDa for GST tagged IFNγ either with anti-GST antibody (Fig. 3.3A) or with anti-IFNγ antibody (Fig. 3.3B), separately.

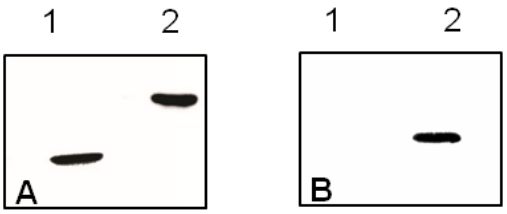

Fig 3.3. (A) Lane 1: GST band of 26 kDa by anti GST western blotting, Lane 2: 44 kDa band of GST IFNγ by anti GST western analysis **(B)** Lane 1: empty lane for GST protein by anti IFNγ western blotting, Lane 2: Band of GMCSF protein by anti GMCSF western analysis.

3.3.4 MALDI analysis of recombinant IFNγ:

Furthermore, MALDI-TOF analysis of trypsin digested recombinant IFNγ protein depicted significant similarity with human IFNγ protein by Mascot search in NCBI BLAST showing 39% of sequence coverage with a score value of 86 (Fig. 3.4). Table 3.1 is showing matched sequence with human IFNγ.

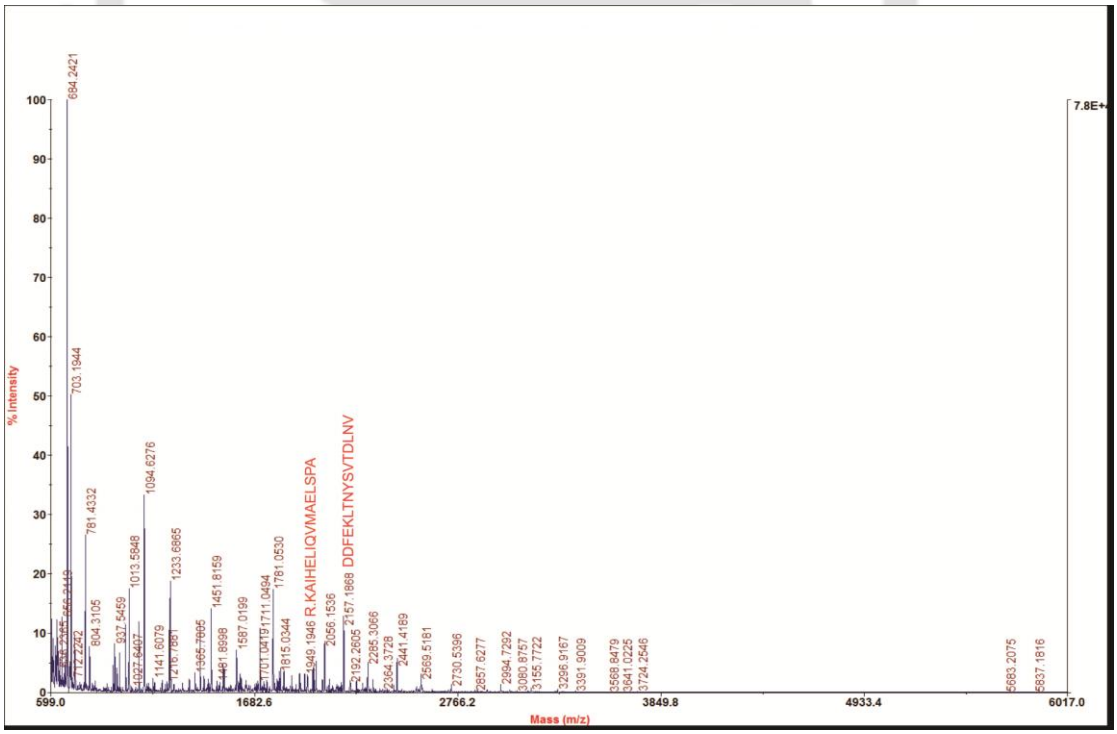

Fig 3.4. Spectra of IFNγ by MALDI TOF analysis.

Table 3.1. Showing matched query sequence with human Interferon gamma protein

m/z	Sequence	Protein	Method
2157.1868	SPSPSTQPW EHVNAIQEAR	IFNγ	M (86)
1949.2034	R.KAIHELIQVMAELSPA	IFNγ	M (86)

3.3.5 Activity study of the recombinant IFNγ:

Macrophage cells are known to produce high amount of reactive oxygen species (ROS) in response to IFNγ (Amatore *et al*, 2010). Thus, measurement of ROS in macrophage cells, after treatment with the IFNγ is a well-established bioassay for functional activity of IFNγ (Eruslanov *et al*, 2010). We have treated mouse macrophage cells (Raw 264.7) with purified recombinant GST IFNγ protein for 24 h, and measured ROS by FACS analysis (Yang *et al*, 2007), using 2, 7-dichlorofluoresceindiacetate (DCFDA) staining method. The non-fluorescent DCFDA freely diffuses into the cells through the plasma membrane, and converts to green fluorescent DCFH due to intracellular oxidation by ROS. Thus, the amount of fluorescence intensity of DCFH produced is directly correlated with the amount of ROS production inside treated cells. The FACS results demonstrated that cells treated with recombinant IFNγ protein generated ROS, which was evident from a prominent shift of fluorescence intensity in the FL-1H channel corresponding to the green emission as compared to the untreated cells (Fig. 3.5). These results revealed that recombinant IFNγ purified obtained from bacterial expression host could retain functional activity.

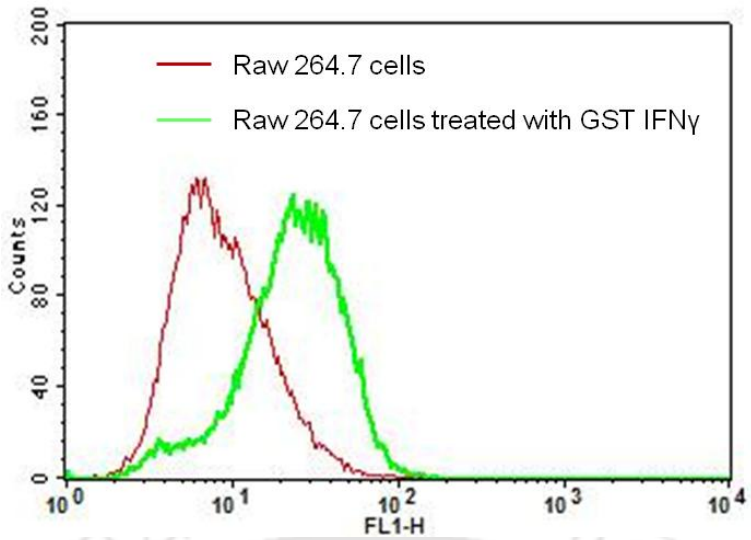

Fig 3.5. FACS analysis of recombinant IFNγ mediated reactive oxygen species (ROS) generation in macrophage (Raw 264.7) cells. The FL1-H corresponds to the green emission of the DCFDA.

3.3.6 Antiproliferative effect of IFNγ:

The anti-cell proliferative activity of the recombinant IFNγ was further tested on MCF-7 and HeLa cells using MTT assay. The results showed maximum of 20-25% cell death in a wide concentration range (10-400 ng/mL) of the recombinant protein. The MTT assay for activity of GST and PLGA were also examined, which showed no significant effect of GST and PLGA on cell viability (Fig. 3.6).

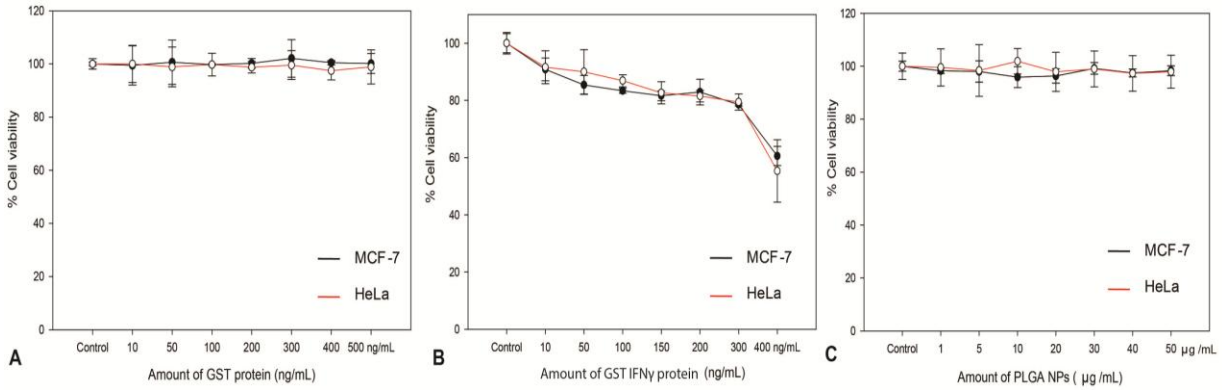

Fig 3.6. MTT assay showing effect of **A.** GST protein on HeLa and MCF-7 cell lines **B.** GST IFNγ protein on HeLa and MCF-7 cell lines **C.** PLGA NPs on HeLa and MCF-7 cells.

3.3.7 Nanoparticle synthesis, characterization and binding confirmation with GST IFNγ protein:

The composite nanoparticles (Ag PLGA NPs) were synthesised in two steps, first Ag NPs were synthesised by reaction of sodium borohydride and Ag NO_3 in presence of PVA, which acted as a stabilizing agent for Ag NPs. The formation of Ag NPs was confirmed by its characteristics surface plasmon peak at 415 nm in UV-Vis spectroscopy (Fig. 3.7). The Ag NPs-PVA composite was used to stabilize the PLGA NPs by using emulsification solvent evaporation method. Usually, PVA a biodegradable polymer is used as an emulsifying agent during the synthesis of PLGA NPs. However, in the present case, the preformed Ag NPs- PVA composite was used for the same. Thus, we were able to deposit Ag NPs on the surface of the PLGA NPs. In addition, we have incorporated FITC during synthesis of the NPs to make these NPs fluorescent. The PLGA NPs were also synthesized without Ag NPs to perform the control experiments. The formation of NPs was confirmed by TEM analysis (Fig. 3.8). The FESEM and TEM images of PLGA (Fig. 3.8 A and 3.8B) and the composite Ag PLGA NPs (Fig. 3.8C and 3.8D) showed that both NPs were spherical in shape and average particle sizes were 259.28 ± 34.31 nm and 266.40 ± 29.08 nm respectively. Interestingly; the Ag NPs were clearly visible to be embedded in the PLGA NPs in case of the composite NPs. The FESEM analysis of PLGA and composite NPs showed average particles size around 238.23 ± 60.1 nm and 246.45 ± 48.57, respectively which are in close compliance with the TEM results. The average Ag NP size was found to be 7.04 ± 3.2 nm. The selected area electron diffraction (SAED) analysis of the same sample showed corresponding Scherrer ring patters confirming the presence of the metallic silver (Fig. 3.8E). In addition, TEM image showed that the composite NPs didn't agglomerate or lose its structural integrity as the diameter and shape of the NPs remained almost similar after immobilization of the recombinant protein (Fig. 3.8F).

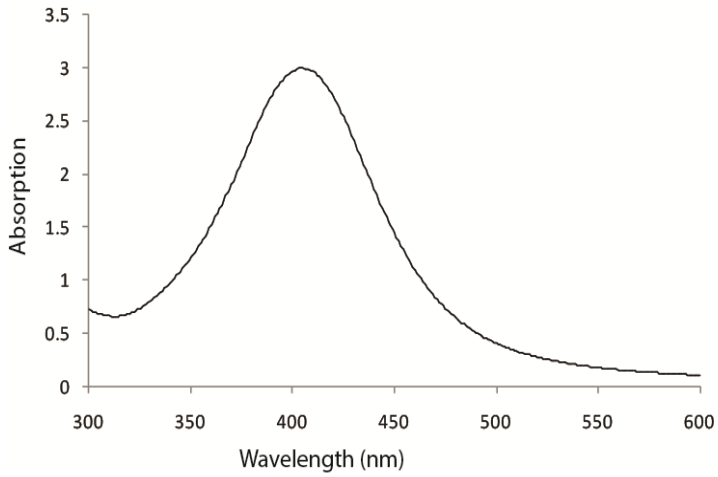

Fig 3.7. UV-Vis spectra of the Ag NPs

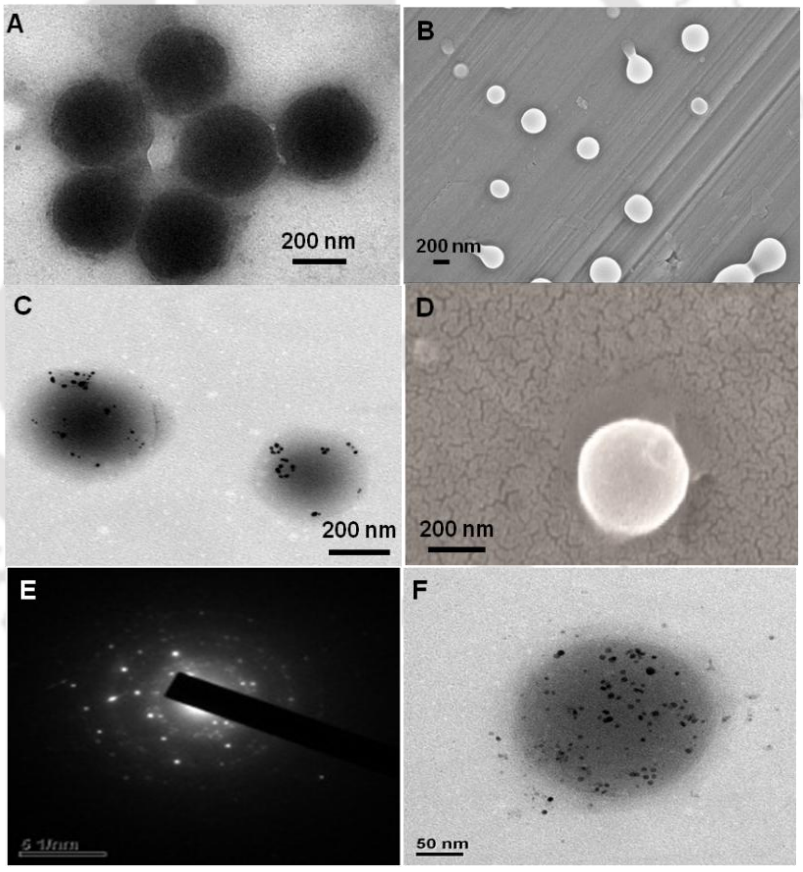

Fig 3.8. (A and B) showing TEM and FESEM image of PLGA NPs **(C and D)** TEM and FESEM image of Ag PLGA NPs **(E)** Selected area electron diffraction (SAED) analysis of Ag PLGA NPs and **(F)** TEM image of GST IFNγ incubated Ag PLGA NP.

3.3.8 Dynamic Light scattering and Zeta potential estimation:

We performed the DLS analysis to determine the hydrodynamic diameter of the composite NPs. The average hydrodynamic diameter was 356 nm which increases upto 375 nm after incubation with the recombinant IFNγ protein. Hydrodynamic diameter of PLGA NPs also increased from 275 nm to 350 nm, after its incubation with GST IFNγ protein (Fig. 3.9). The zeta potential value of the Ag PLGA NPs were decreased to -3.83 mV from -26 mV and -3.53 from -21.8 for PLGA NPs (Fig. 3.10). This effect was possibly due to interaction with the protein. It should be mentioned here that the recombinant GST IFNγ protein has PI value of 8.76 (based on ExPASy PI Calculator) and thus, it is positively charged at physiological pH (i.e. 7.4). On the other hand, the zeta potential of the NPs showed that synthesized NPs was negatively charged; thereby creating a plausibility of electrostatic interaction between the duos.

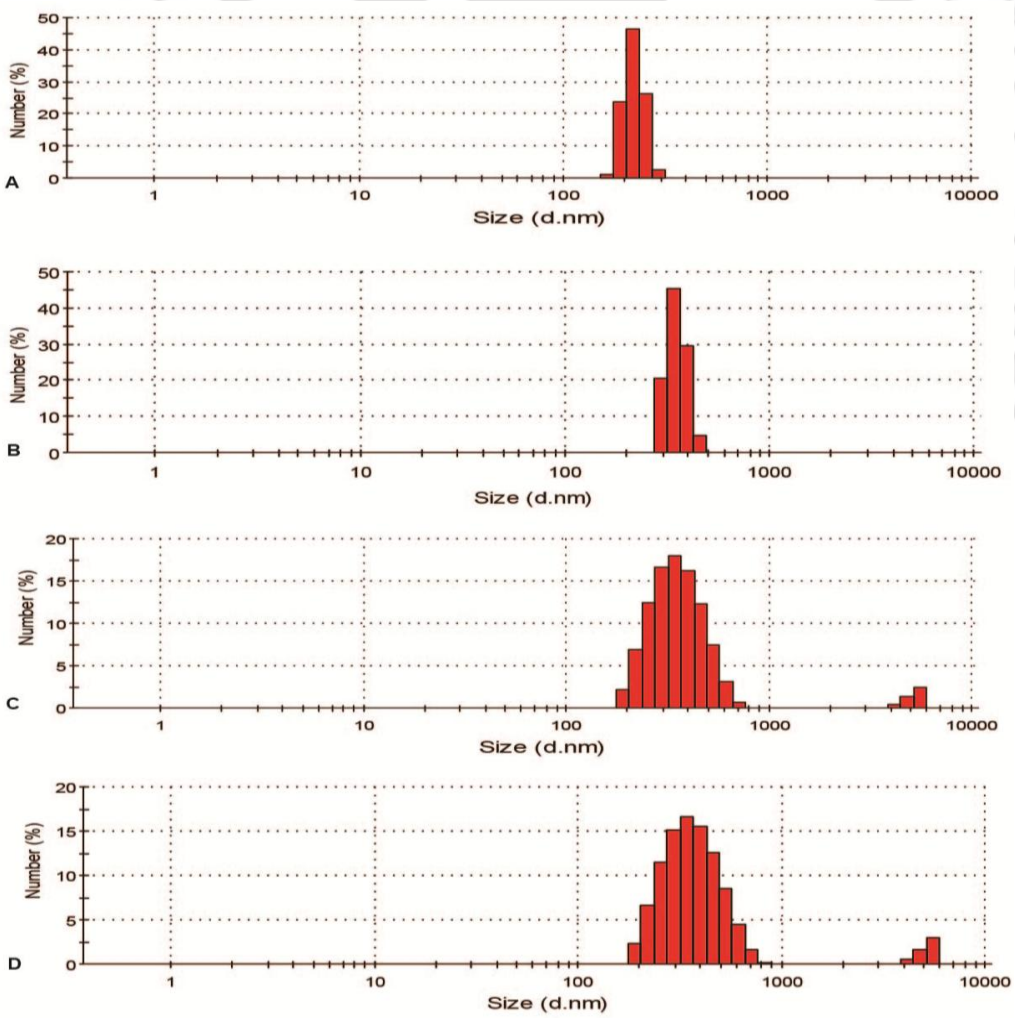

Fig 3.9. Hydrodynamic diameter study of **(A)** PLGA NPs **(B)** PLGA NPs with IFNγ **(C)** Ag PLGA NPs only **(D)** Ag PLGA NPs with IFNγ.

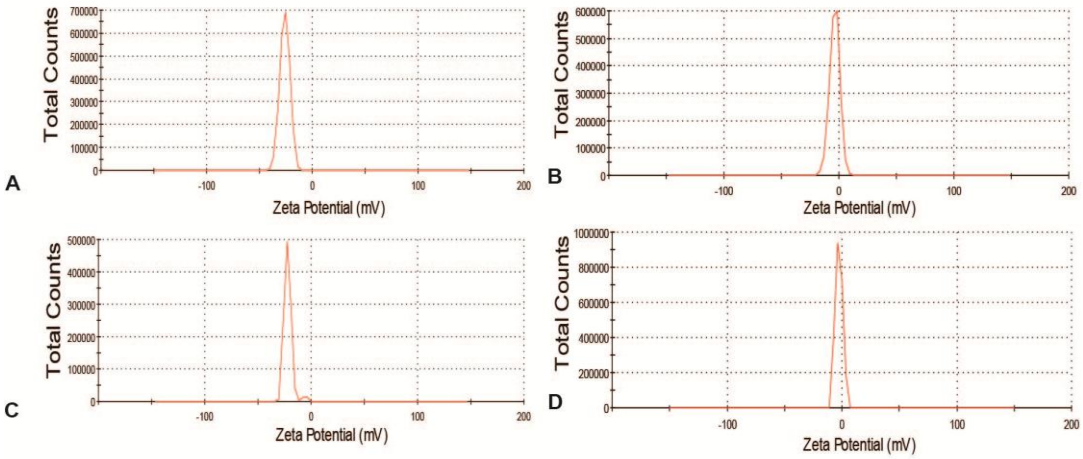

Fig 3.10. (A) and **(C)** showing zeta potential of Ag PLGA nanocomposite and PLGA particles respectively **(B)** and **(D)** are surface charge after GST IFNγ protein incubation with composite Ag PLGA NPs and PLGA NPs respectively.

To immobilize the purified GST IFNγ protein on the surface of the PLGA and composite NPs, different amounts of recombinant IFNγ were incubated with the fixed amount of NPs for 1 h at 37°C, followed by centrifugation to remove the unbound protein. The protein bound NPs collected by centrifugation revealed that the fluorescence intensity of the NPs gradually decreased with the addition of protein up to 25-30 ng protein/µg of NPs after which it became saturated (Fig. 3.11).

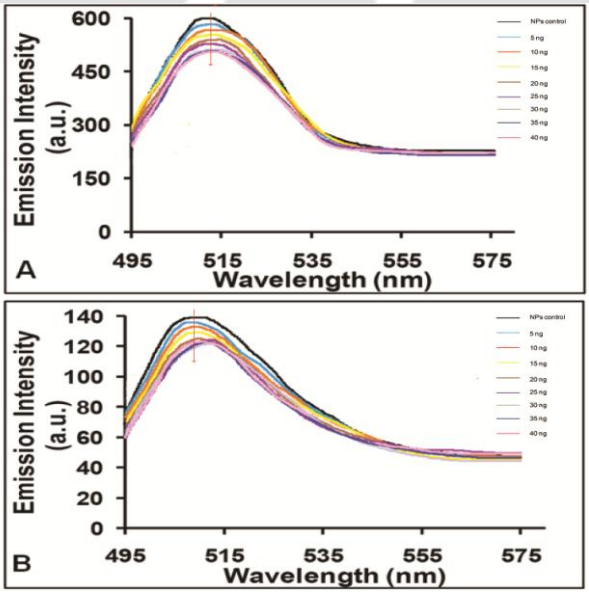

Fig 3.11. Fluorescence emission study of FITC loaded **(A)** PLGA NPs **(B)** Ag PLGA NPs with addition of GST IFNγ protein.

3.3.9 Optimum protein binding study:

The protein immobilized NPs were further probed for the quantitative estimation by UV-vis spectroscopy. Absorption at 280 nm that corresponds to the amount of bound protein revealed that maximum 25 ng protein was bound with 1 µg of PLGA NPs as well as composite Ag PLGA NPs (Fig. 3.12A and 3.12B respectively).

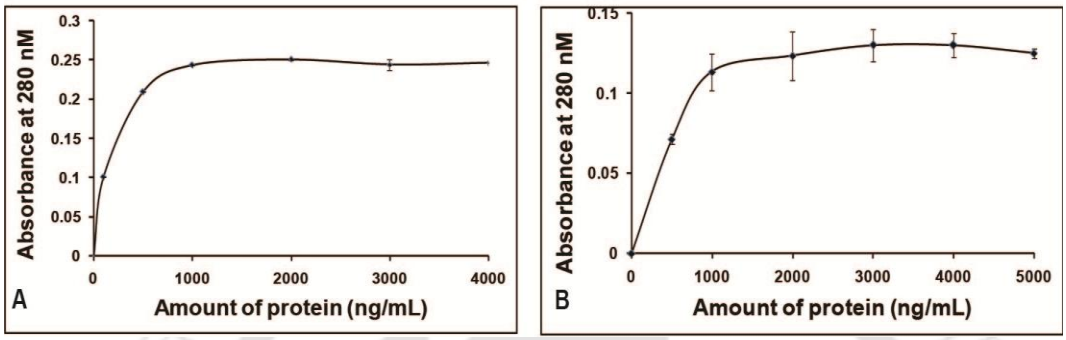

Fig 3.12. UV-Vis study of the binding of GST IFNγ protein with **(A)** PLGA only **(B)** composite NPs (Ag PLGA NPs). The values are represented as mean ± SD of three individual experiments.

3.3.10 FTIR analysis:

The interaction was also supported by FTIR analysis. The FTIR spectra of the composite NPs alone and after its interaction with the recombinant protein showed that the most of the peaks were unaltered. However, the peaks at 1760 cm^{-1} and 1162 cm^{-1} corresponding to C=O and C-O stretching vibrations were more prominent in case of only composite NPs (Khemani *et al*, 2012). One additional peak appeared for protein immobilized NPs at 1651 cm^{-1} corresponding to amide bond I (HNC=O) bond stretching, indicating the presence of protein on the surface of the NPs (Fig. 3.13).

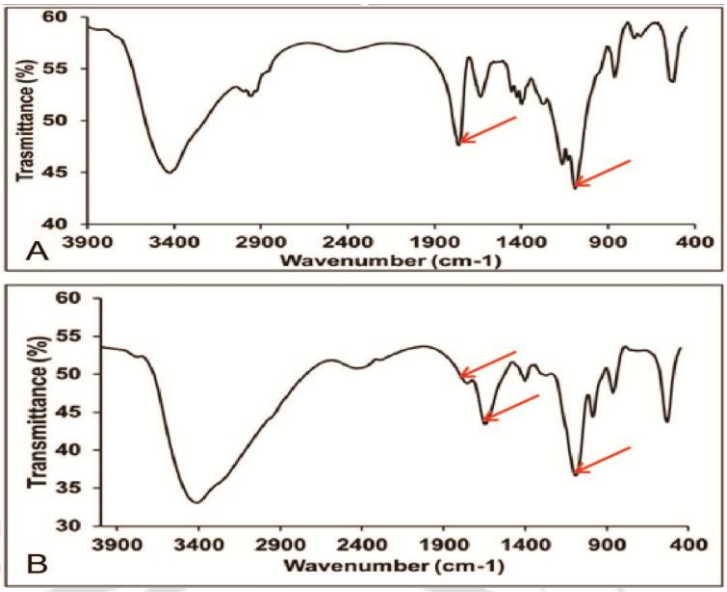

Fig 3.13. FTIR spectra of the **(A)** composite NPs and **(B)** recombinant GST IFNγ immobilized GST IFNγ Ag PLGA composite NPs.

3.3.11 Protein release profile:

Protein release data showed that maximum 34% release of GST IFNγ from NPs in 72 h at physiological pH, while the rest was bound with the nanoparticles (Fig. 3.14). The sustained release of the protein in physiological condition could reduce the frequency of its doses.

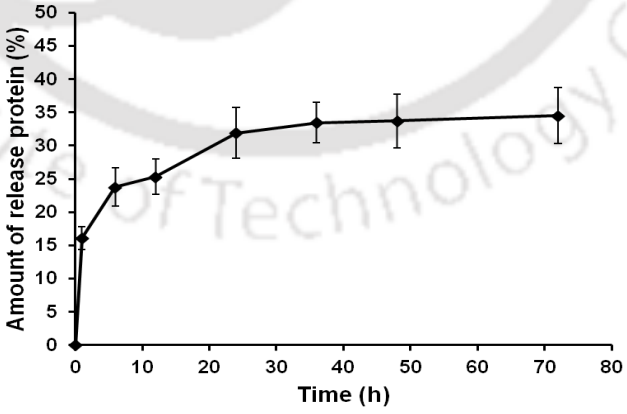

Fig 3.14. GST IFNγ protein release profile from Ag PLGA NPs.

3.3.12 Protease protection assay:

More importantly, we have performed the protease protection assay in which Ag PLGA NPs was incubated with GST IFNγ protein. Result showed that GST IFNγ protein loaded Ag PLGA NPs was more stable than free protein (Fig. 3.15).

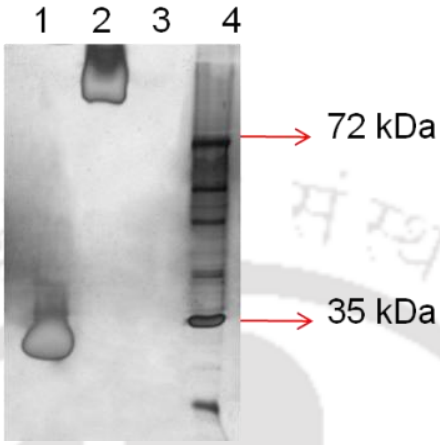

Fig 3.15. SDS PAGE analysis for protease protection assay. Lane 1: GST IFNγ protein digested with protease, Lane 2: GST IFNγ Ag PLGA NPs nanocomposite digested with protease, Lane 3: Nanocomposite digested with protease, Lane 4: Protein Marker.

3.3.13 Microscopy based cell surface interaction study:

To study the interaction of protein immobilized NPs with the cells, HeLa and MCF-7 cells were incubated with FITC loaded GST IFNγ PLGA NPs for 1 h, followed by PBS washing and analysed with the fluorescence microscope as well as FACS. Fluorescence microscopy images showed green fluorescence emission at the surface of the treated cells when excited with blue light (Fig. 3.16B and 3.16D) while there was no green fluorescence observed in FITC loaded PLGA NPs treated control cells (Fig. 3.16A and 3.16B). This effect could be due to binding of IFNγ with its surface receptor which allowed the nanoparticles to attach on cell surface which gives green colour. Under similar conditions, DAPI, a well-known nuclear dye stained nuclei blue. Interestingly, the merged images showed both green and blue fluorescence for GST IFNγ Ag PLGA NPs treated cells (Fig. 3.17B and 3.17D) whereas the NPs treated cells showed only blue fluorescence due to DAPI staining (Fig. 3.17A and 3.17B). Thus, the microscopy images illustrated the evidence of IFNγ mediated NPs interaction with cell surface.

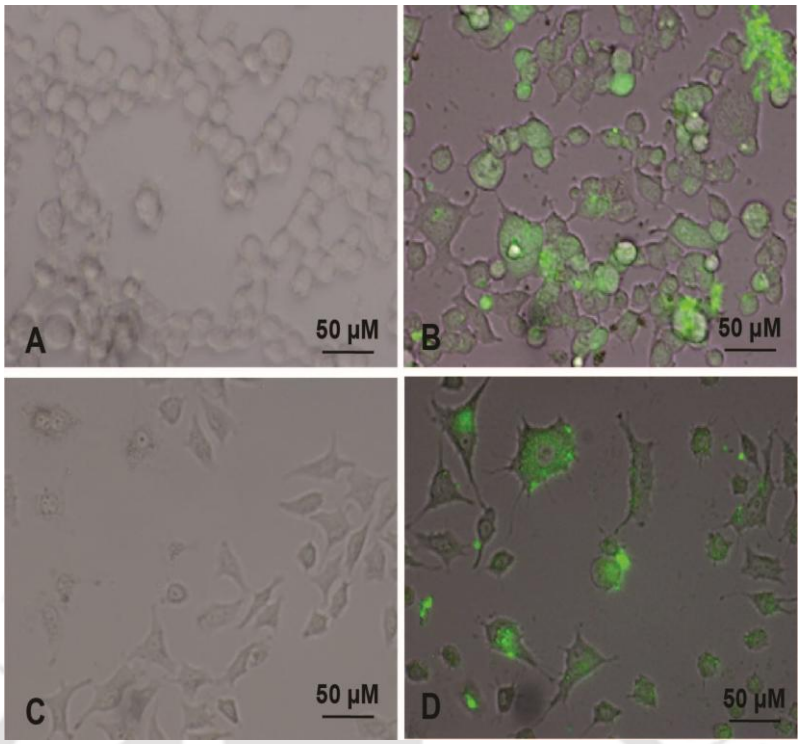

Fig 3.16. Fluorescent microscopy images of **(A, B)** HeLa control and GST IFNγ loaded Ag PLGA composite nanoparticles treated cells respectively **(C, D)** MCF-7 control and GST IFNγ loaded Ag PLGA composite nanoparticles treated cells, respectively.

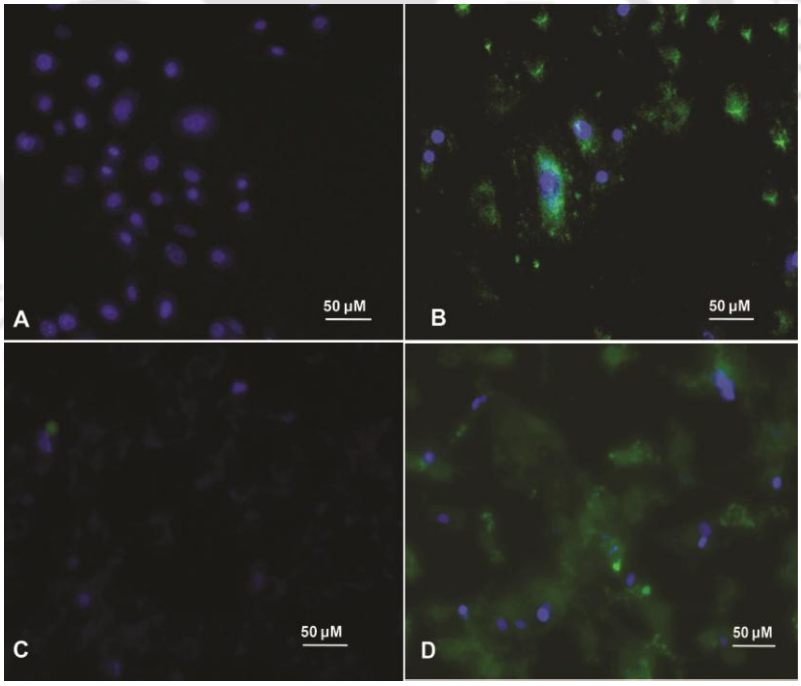

Fig 3.17. DAPI stained images of **(A, B)** HeLa cells treated with Ag PLGA NPs and GST IFNγ loaded Ag PLGA composite treated cells **(C, D)** Ag PLGA NPs treated MCF-7 control cells and GST IFNγ Ag PLGA composite treated MCF-7 cells respectively.

3.3.14 FACS based GST IFNγ PLGA NPs binding study:

The finding was substantiated by FACS analysis of the cells treated with FITC loaded GST IFNγ PLGA NPs. FACS results revealed a prominent shift of fluorescence intensity in the FL-1H channel corresponding to the green emission of FITC loaded NPs attached on cell surface, which was not seen in the control cells treated with nanoparticles only (Fig. 3.18). This is possibly due to binding of IFNγ with its cell surface receptor leading to the change in fluorescence intensity as observed during FACS analysis (Schroder *et al*, 2004).

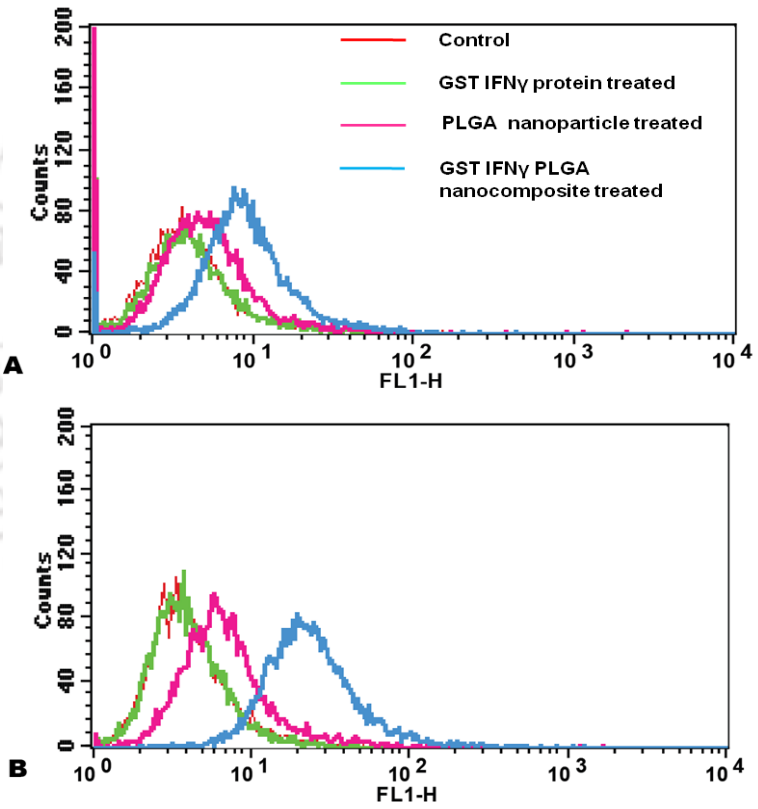

Fig 3.18. GST IFNγ Ag PLGA cell surface binding study with FACS on **(A)** HeLa and **(B)** MCF-7 cells.

3.3.15 Cell viability analysis of GST IFNγ loaded Ag PLGA composite treated cells:

The impact of individual PLGA NPs and Ag PLGA NPs on HeLa and MCF-7 cells was studied before combining them in to the composite nanoparticles. The cells

treated with various amounts of PLGA NPs and the Ag PLGA NPs were estimated for viability estimation by MTT assay. Our results showed that PLGA NPs did not produce cell mortality (Fig. 3.6C); however cell viability gradually decreased with increasing concentration of Ag PLGA NPs for both the cell lines. The IC_{50} of the Ag PLGA NPs, where the 50% cells were killed, was found to be 1.5 µg/mL and 1.25 µg/mL for the HeLa and MCF-7 cells, respectively (Fig. 3.19A). Finally, MTT assay was performed to assess the cell viability in presence of the protein immobilized composite NPs (Ag PLGA NPs). The protein was immobilized on the NPs at 30°C for 1 h followed by centrifugation to remove the free protein (25µg protein/ mg Ag PLGA nanoparticles) and the cells were treated with the protein immobilized NPs to check the combined effect. Cell viability data showed that protein immobilized NPs had killed the cancer cells more effectively than Ag PLGA NPs or GST IFNγ protein alone.

At IC_{50} the GST IFNγ Ag PLGA composite GST IFNγ loaded PLGA nanoparticles nanoparticles comprise 0.95 µg/mL of Ag PLGA NPs and 25 ng/mL of IFNγ protein for both cell lines (Fig. 3.19B). The amount of silver required here to attain the IC_{50} was much less than the amount required for Ag PLGA NPs alone.

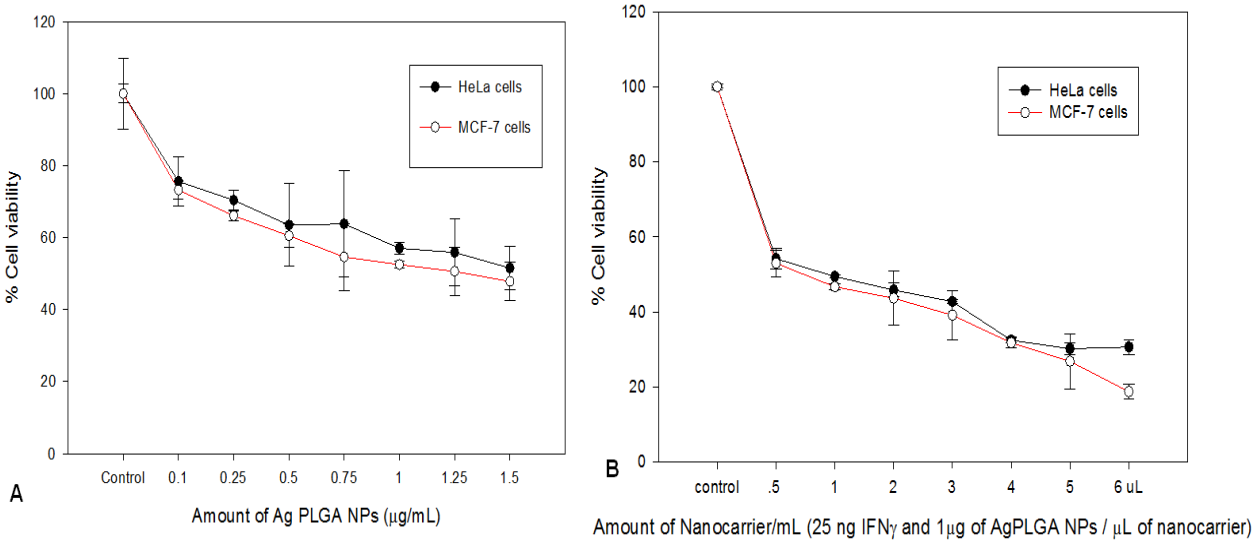

Fig 3.19. Cell viability analysis of **(A)** Ag PLGA NPs treated cells **(B)** GST IFNγ Ag PLGA NPs treated cells. The values are represented as mean ± SD of three individual experiments with $p < 0.005$.

3.3.16 Cell Cycle analysis:

Understand mode of cell death by IFNγ and Ag PLGA NPs composite NPs, the HeLa cells were treated with IC_{20} of Ag PLGA NPs composite NPs and with GST IFNγ protein (25 ng/mL) .Cell cycle analysis using flow cytometry revealed cell cycle arrest mainly in G1 phase after treatment with 25 ng/mL of recombinant IFNγ, whereas the other phases were unaffected (Fig. 3.20B). The low cell death could be due to the short half-life of IFNγ. Thus, it was clear from our results that although the recombinant IFNγ could block cell cycle, but was not able to kill cancer cells effectively in a short time period. Therefore, we further immobilized the recombinant IFNγ on the surface of Ag NPs coated PLGA NPs. This was being performed with the hope that the attachment of the recombinant IFNγ with the polymer nanoparticles (NPs) would not only impart stability, but also increase its anti-cancer effect due to Ag NPs. However, the Ag NPs, a known anti-proliferative agent is required at high concentration to kill cancer cells. But the combination of GST IFNγ protein and Ag PLGA composite effectively target cancer cells by dual mode of action as IFNγ blocked G1 phase of cell cycle and Ag PLGA composite caused apoptosis in the cells (Fig. 3.20D). Treatment with recombinant IFNγ alone did not show any sub G0 population, whereas a significant (15 %) sub G0 population was observed due to apoptosis after composite NPs treatment at IC_{20} value which further increased in combination therapy with GST IFNγ Ag PLGA NPs (Fig. 3.20 E). Moreover, the composite NPs could be targeted easily on the cells with the help of the interaction between IFNγ and its cell surface receptors. Hence, this combination therapy module could potentiate anti-proliferative effect of the recombinant IFNγ in presence of low amount of Ag NPs.

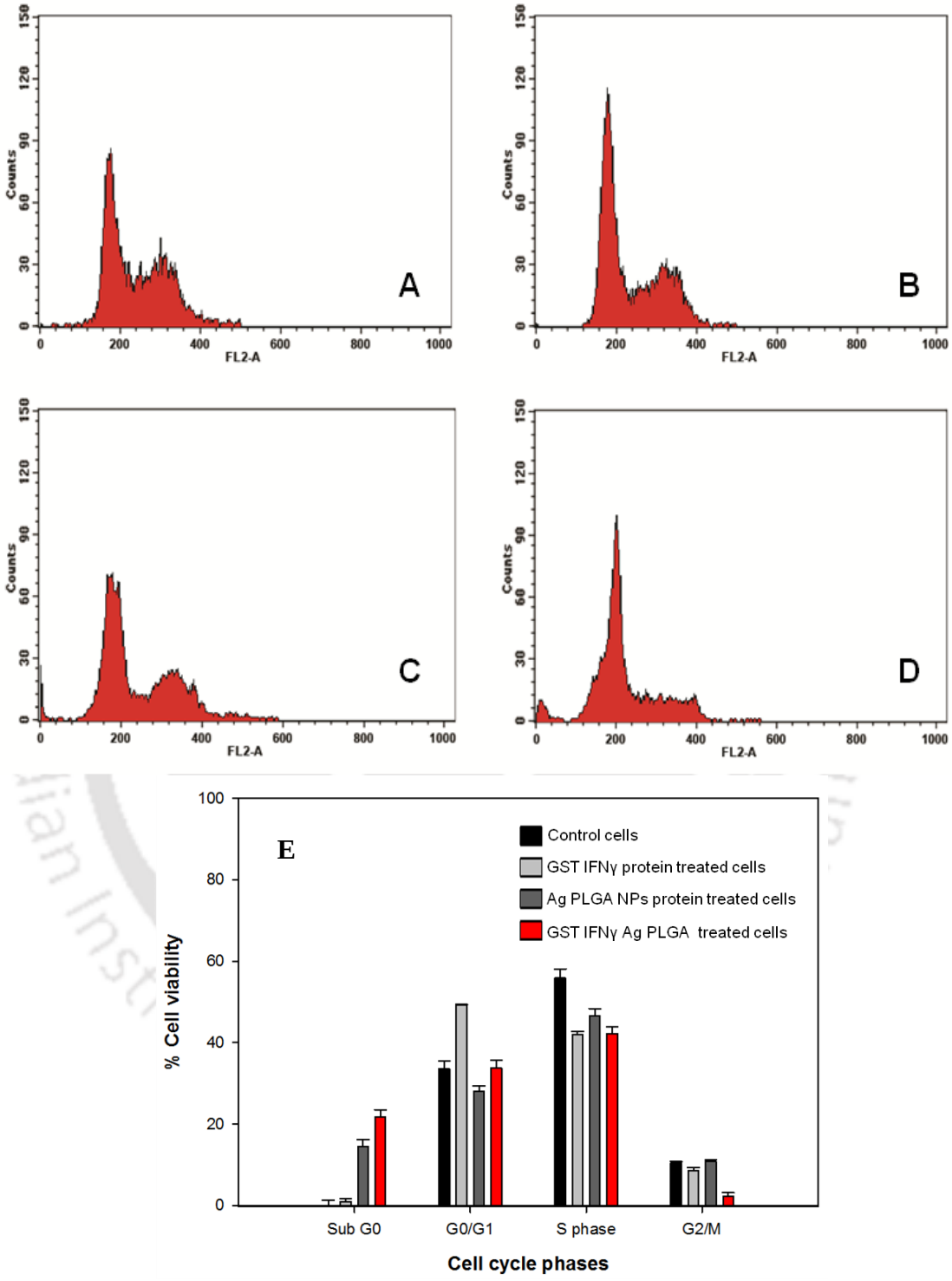

Fig 3.20. Cell cycle analysis of HeLa cells **(A)** Untreated HeLa cells **(B)** GST IFNγ treated cells **(C)** Ag PLGA IFNγ treated cells **(D)** GST IFNγ Ag PLGA treated cells **(E)** Bar diagram showing percentage of cells after treatment. The values are represented as mean ± SD of three individual experiments with $p < 0.005$.

3.3.17 AO/EtBr Double staining:

The composite nanoparticle treated cells were stained with acridine orange (AO)/ethidium bromide (EtBr) and observed them under fluorescence microscope. The live cells allowed permeation of AO which stained nuclei green, whereas the dead cells emitted red fluorescence due to uptake of EtBr. Thus dual staining facilitated an easier view of dead and live cell populations. The cell treated with the IC_{50} dose of protein immobilized NPs (Fig. 3.21B and 3.21D) showed more red cells as compared to the control untreated cells. Moreover, careful observation depicted chromatin condensation and fragmentation in case of NPs treated cells, which is the distinctive feature of apoptotic cell death.

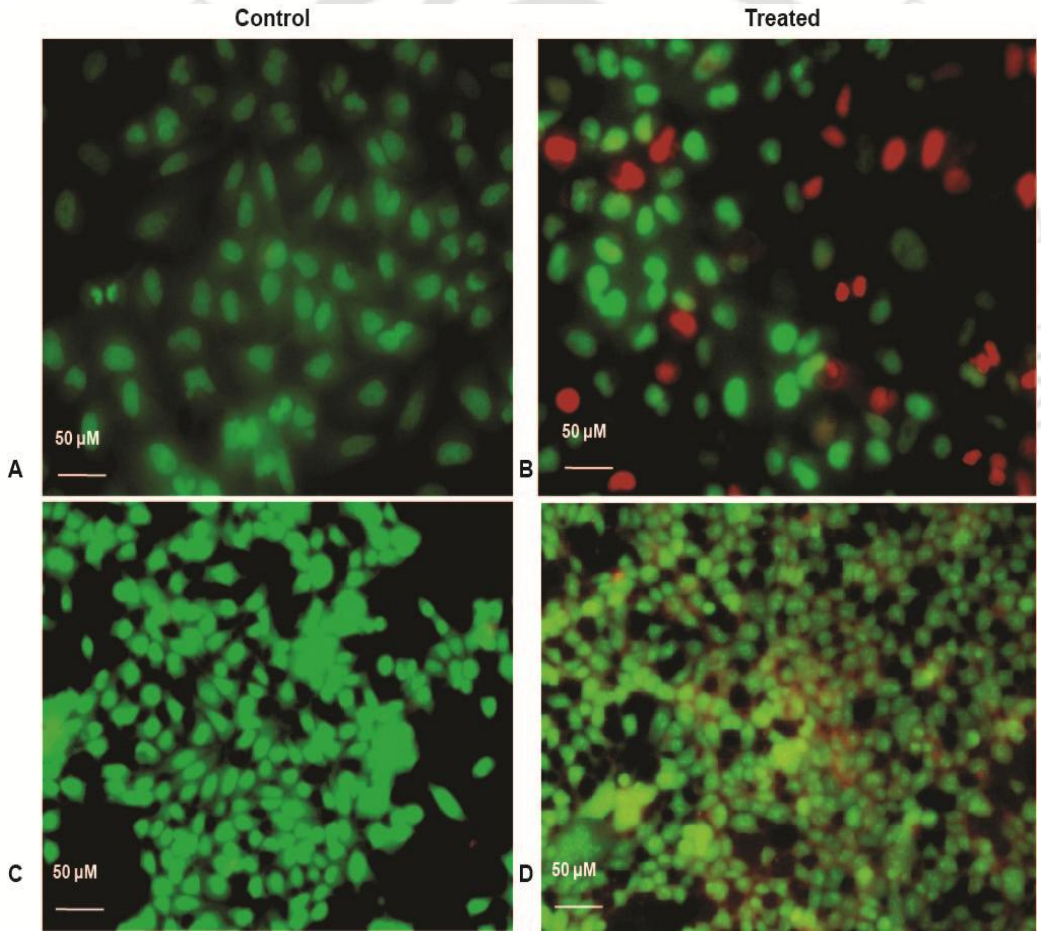

Fig 3.21. (A) AO/EtBr dual staining of control HeLa cells **(B)** HeLa cells treated with GST IFNγ PLGA nanoparticles **(C)** Control MCF-7 cells **(D)** MCF-7 cells treated with GST IFNγ PLGA nanoparticles.

3.3.18 FESEM analysis for Ag PLGA NPs treated cells:

FESEM analysis revealed indentation and irregular membrane structure of the composite NPs treated cells as compared to the untreated populations. This was in agreement with initiation of apoptosis, which ultimately formed apoptotic bodies (Fig. 3.22).

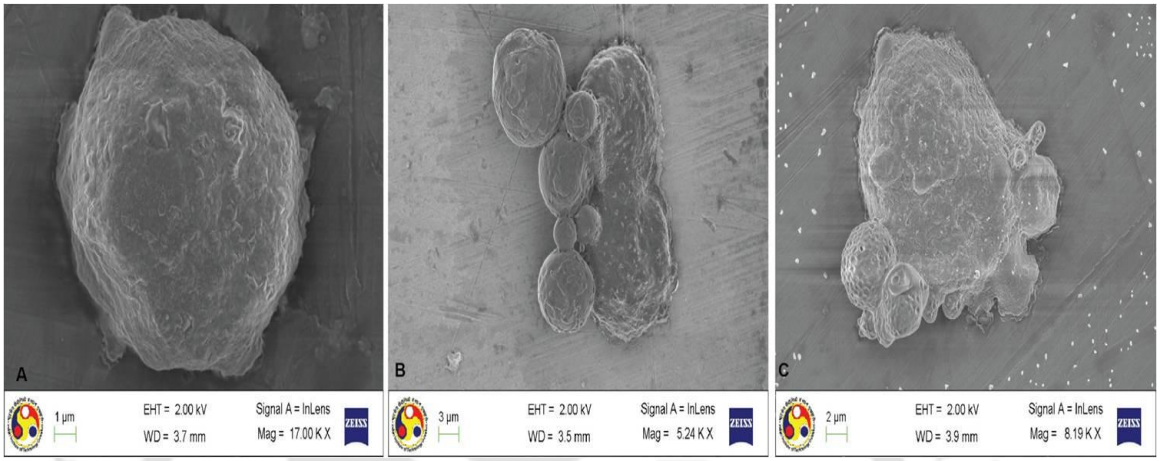

Fig 3.22 FESEM analysis of **(A)** Untreated HeLa cells **(B and C)** HeLa cells treated with GST IFNγ Ag PLGA composite nanoparticles.

3.3.19 Caspase 3 Assay:

Further, to confirm the apoptotic mode of cell death, caspase-3 assay was performed in HeLa cells. Caspase is the key protease, synthesized as an inactive form in cells, which is converted to its active form during the initial phase of apoptosis by self-proteolysis or by cleavage with other proteases. In untreated (control) HeLa cells, 98.99% of cells were found to be non-apoptotic (Fig. 23A), whereas around 45% of cells were apoptotic in caspase 3 assay after 16 h treatment with Ag PLGA NPs (Fig. 3.23B). Thus, the overall results demonstrated that the protein immobilized Ag PLGA NPs were more effective in order to cause the apoptosis mediated cells death than their individual components, possibly to complementary effects.

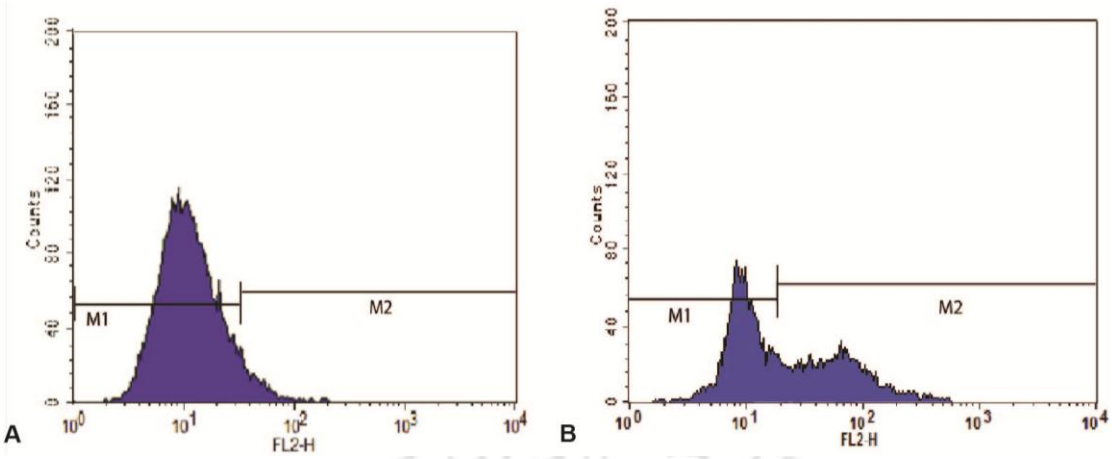

Fig 3.23. Caspase 3 analysis of **(A)** untreated HeLa cells **(B)** and HeLa cells treated with Ag PLGA NPs composite.

3.4 Conclusion

This chapter reported cloning, expression, purification of human IFNγ. Recombinant GST tagged protein was purified and showed its potential in activating macrophages cells through ROS generation. Further, the recombinant IFNγ was found to block cell cycle mostly at G1 phase of HeLa cells, but did not cause any cell death. The recombinant IFNγ was immobilized on the composite PLGA NPs together with Ag NPs, where PLGA NPs provided stability to the protein and the Ag NPs have potentiated anticancer activity of the recombinant IFNγ. The anti-cell proliferative activity was measured by MTT assay. The recomninant IFNγ protein was shown to be protected from protease degradation in the composite nanoparticles. The combination of IFNγ and Ag NPs eventually led to induction of apoptosis to the cancer cells. Thus, the composite NPs mediated delivery of this clinically important cytokine opens up a new regimen in cancer therapy, which could minimize the repetitive doses and reduce the amount of chemotherapeutic drugs.

3.5 References

1. Amatore, C., Arbault, S., and Koh, A.C.W. (2010). Simultaneous detection of reactive oxygen and nitrogen species released by a single macrophage by triple potential-step chronoamperometry. Anal. Chem. *82*, 1411–1419.
2. Bae, Y.H., and Park, K. (2011). Targeted drug delivery to tumors: myths, reality and possibility. J Control Release *153*, 198–205.
3. Billiau, A., and Matthys, P. (2009). Interferon-gamma: a historical perspective. Cytokine Growth Factor Rev. *20*, 97–113.
4. Bradford, M.M. (1976). A rapid and sensitive method for the quantitation of microgram quantities of protein utilizing the principle of protein-dye binding. Anal. Biochem. *72*, 248–254.
5. Brandacher, G., Winkler, C., Schroecksnadel, K., Margreiter, R., and Fuchs, D. (2006). Antitumoral activity of interferon-gamma involved in impaired immune function in cancer patients. Curr. Drug Metab. *7*, 599–612.
6. Cho, K., Wang, X., Nie, S., Chen, Z.G., and Shin, D.M. (2008). Therapeutic nanoparticles for drug delivery in cancer. Clin. Cancer Res. *14*, 1310–1316.
7. Danhier, F., Ansorena, E., Silva, J.M., Coco, R., Le Breton, A., and Préat, V. (2012). PLGA-based nanoparticles: an overview of biomedical applications. J Control Release *161*, 505–522.
8. Danhier, F., Ucakar, B., Magotteaux, N., Brewster, M.E., and Préat, V. (2010). Active and passive tumor targeting of a novel poorly soluble cyclin dependent kinase inhibitor, JNJ-7706621. Int J Pharm *392*, 20–28.
9. Dinarvand, R., Cesar de Morais, P., and D'Emanuele, A. (2012). Nanoparticles for Targeted Delivery of Active Agents against Tumor Cells. Journal of Drug Delivery *2012*, 1–2.
10. Dinarvand, R., Sepehri, N., Manoochehri, S., Rouhani, H., and Atyabi, F. (2011). Polylactide-co-glycolide nanoparticles for controlled delivery of anticancer agents. Int J Nanomedicine *6*, 877–895.
11. Dong, Z., Zhang, C., Wei, H., Sun, R., and Tian, Z. (2005). Impaired NK cell cytotoxicity by high level of interferon-gamma in concanavalin A-induced hepatitis. Can. J. Physiol. Pharmacol. *83*, 1045–1053.
12. Dunn, G.P., Old, L.J., and Schreiber, R.D. (2004). The immunobiology of cancer immunosurveillance and immunoediting. Immunity *21*, 137–148.
13. Eruslanov, E. and Kusmartsev, S., in Advanced Protocols in Oxidative

Stress II, ed. D. Armstrong, Humana Press, Totowa, NJ, 2010, vol. 594, pp. 57–72.

14. Farokhzad, O.C., and Langer, R. (2009). Impact of nanotechnology on drug delivery. ACS Nano *3*, 16–20.
15. Ghosh, S., Rasheedi, S., Rahim, S.S., Banerjee, S., Choudhary, R.K., Chakhaiyar, P., Ehtesham, N.Z., Mukhopadhyay, S., and Hasnain, S.E. (2004). Method for enhancing solubility of the expressed recombinant proteins in Escherichia coli. BioTechniques *37*, 418, 420, 422–423.
16. Girdlestone, J., and Wing, M. (1996). Autocrine activation by interferon-gamma of STAT factors following T cell activation. Eur. J. Immunol. *26*, 704–709.
17. Gopinath, P., Gogoi, S.K., Chattopadhyay, A., and Ghosh, S.S. (2008). Implications of silver nanoparticle induced cell apoptosis for in vitro gene therapy. Nanotechnology *19*, 075104.
18. Gopinath, P., Gogoi, S.K., Sanpui, P., Paul, A., Chattopadhyay, A., and Ghosh, S.S. (2010). Signaling gene cascade in silver nanoparticle induced apoptosis. Colloids Surf B Biointerfaces *77*, 240–245.
19. Havlis, J., Thomas, H., Sebela, M., and Shevchenko, A. (2003). Fast-response proteomics by accelerated in-gel digestion of proteins. Anal. Chem. *75*, 1300–1306.
20. Ikeda, H., Old, L.J., and Schreiber, R.D. (2002). The roles of IFN gamma in protection against tumor development and cancer immunoediting. Cytokine Growth Factor Rev. *13*, 95–109.
21. Kano, A., Watanabe, Y., Takeda, N., Aizawa, S., and Akaike, T. (1997). Analysis of IFN-gamma-induced cell cycle arrest and cell death in hepatocytes. J. Biochem. *121*, 677–683.
22. Kerényi, L., and Gallyas, F. (1973). [Errors in quantitative estimations on agar electrophoresis using silver stain]. Clin. Chim. Acta *47*, 425–436.
23. Khemani, M., Sharon, M., and Sharon, M. (2012). Encapsulation of Berberine in Nano-Sized PLGA Synthesized by Emulsification Method. ISRN Nanotechnology *2012*, 1–9.
24. Lammers, T., Kiessling, F., Hennink, W.E., and Storm, G. (2012). Drug targeting to tumors: principles, pitfalls and (pre-) clinical progress. J Control

Release *161*, 175–187.

25. Lange, F., Rateitschak, K., Fitzner, B., Pöhland, R., Wolkenhauer, O., and Jaster, R. (2011). Studies on mechanisms of interferon-gamma action in pancreatic cancer using a data-driven and model-based approach. Mol. Cancer *10*, 13.
26. Lange, F., Rateitschak, K., Fitzner, B., Pöhland, R., Wolkenhauer, O., and Jaster, R. (2011). Studies on mechanisms of interferon-gamma action in pancreatic cancer using a data-driven and model-based approach. Mol. Cancer *10*, 13.
27. Minasian, L.M., Motzer, R.J., Gluck, L., Mazumdar, M., Vlamis, V., and Krown, S.E. (1993). Interferon alfa-2a in advanced renal cell carcinoma: treatment results and survival in 159 patients with long-term follow-up. J. Clin. Oncol. *11*, 1368–1375.
28. Mosmann, T. (1983). Rapid colorimetric assay for cellular growth and survival: application to proliferation and cytotoxicity assays. J. Immunol. Methods *65*, 55–63.
29. Murakami, H., Kobayashi, M., Takeuchi, H., and Kawashima, Y. (1999). Preparation of poly(DL-lactide-co-glycolide) nanoparticles by modified spontaneous emulsification solvent diffusion method. Int J Pharm *187*, 143–152.
30. Park, D.-W., Kim, S.-S., Nam, M.-K., Kim, G.-Y., Kim, J., and Rhim, H. (2011). Improved recovery of active GST-fusion proteins from insoluble aggregates: solubilization and purification conditions using PKM2 and HtrA2 as model proteins. BMB Rep *44*, 279–284.
31. Peer, D., Karp, J.M., Hong, S., Farokhzad, O.C., Margalit, R., and Langer, R. (2007). Nanocarriers as an emerging platform for cancer therapy. Nat Nanotechnol *2*, 751–760.
32. Petrov, S., Nacheva, G., and Ivanov, I. (2010). Purification and refolding of recombinant human interferon-gamma in urea-ammonium chloride solution. Protein Expr. Purif. *73*, 70–73.
33. Roy-Ghanta, S., and Orange, J.S. (2010). Use of cytokine therapy in primary immunodeficiency. Clin Rev Allergy Immunol *38*, 39–53.
34. Sahoo, A.K., Sk, M.P., Ghosh, S.S., and Chattopadhyay, A. (2011). Plasmid DNA linearization in the antibacterial action of a new fluorescent Ag nanoparticle-paracetamol dimer composite. Nanoscale *3*, 4226–4233.

35. Samuel, C.E. (2001). Antiviral actions of interferons. Clin. Microbiol. Rev. *14*, 778–809, table of contents.
36. Schroder, K., Hertzog, P.J., Ravasi, T., and Hume, D.A. (2004). Interferon-gamma: an overview of signals, mechanisms and functions. J. Leukoc. Biol. *75*, 163–189.
37. Segura, S., Espuelas, S., Renedo, M.J., and Irache, J.M. (2005). Potential of albumin nanoparticles as carriers for interferon gamma. Drug Dev Ind Pharm *31*, 271–280.
38. Smyth, D.R., Mrozkiewicz, M.K., McGrath, W.J., Listwan, P., and Kobe, B. (2003). Crystal structures of fusion proteins with large-affinity tags. Protein Sci. *12*, 1313–1322.
39. Tao, H., Liu, W., Simmons, B.N., Harris, H.K., Cox, T.C., and Massiah, M.A. (2010). Purifying natively folded proteins from inclusion bodies using sarkosyl, Triton X-100, and CHAPS. BioTechniques *48*, 61–64.
40. Vajo, Z., Fawcett, J., and Duckworth, W.C. (2001). Recombinant DNA technology in the treatment of diabetes: insulin analogs. Endocr. Rev. *22*, 706–717.
41. Vij, N., Min, T., Marasigan, R., Belcher, C.N., Mazur, S., Ding, H., Yong, K.-T., and Roy, I. (2010). Development of PEGylated PLGA nanoparticle for controlled and sustained drug delivery in cystic fibrosis. J Nanobiotechnology *8*, 22.
42. Yang, D., Elner, S.G., Bian, Z.-M., Till, G.O., Petty, H.R., and Elner, V.M. (2007). Pro-inflammatory cytokines increase reactive oxygen species through mitochondria and NADPH oxidase in cultured RPE cells. Exp. Eye Res. *85*, 462–472.
43. Yergey, A.L., Coorssen, J.R., Backlund, P.S., Jr, Blank, P.S., Humphrey, G.A., Zimmerberg, J., Campbell, J.M., and Vestal, M.L. (2002). De novo sequencing of peptides using MALDI/TOF-TOF. J. Am. Soc. Mass Spectrom. *13*, 784–791.

CHAPTER 4

Coculture assay of breast cancer cells with macrophages in presence of recombinant cytokines

Chapter 4

4.1 Introduction

Cancer comprises changes that include suistaining proliferative signaling, resisting cell death, enabled replicative immortality, resisting growth supressors, activating invasion and metastasis, increased angiogenesis, genome instability, reprogramming in cellular energy metabolism and most importantly evading immune destruction (Hanahan *et al*, 2011). There are some natural immune regulators, which continuously monitor these complex changes in tumour microenvironment and have been emerged as natural co-ordinators between tumour and immune system, like interferons. Among them, IFNγ has a pivotal role in exerting anti tumour response (Dunn *et al*, 2006). IFNγ activates tumour immune escape mechanism by activating various cell types including macrophages. Macrophages resides in human body as monocytes in unstimulated condition. Any pathogenic challenges implement a series of changes in cytokine level which converts normal monocytes to its phagocytic form which in turn exerts many cytotoxic and phagocytic effect (Klimp *et al*, 2002). Normally, macrophages can be converted in two different subtypes which is essential for the body homeostatis (Classen *et al*, 2009). M1 subtype, also known as classical macrophages are the cytotoxic form ,which is gained by the effect of interferons (Dalton *et al*,1993; Huang *et al*, 1993). This M1 subtype conversion initiates the generation of many proteolytic enzymes which causes cytotoxicity. This subtype is essential for the clearance of apoptotic load for the maintainance of host defence sytem. Classically activated macrophages can elicit tumour tissue disruption (Sica *et al*, 2012; Mantovani *et al*, 2002). It has also been reported that tumour progression is associated with phenotype switch from M1 to M2 macrophages (Zaynagetdinov *et al*, 2011). M2 subtype of macrophage is regenerative in nature and helps in maintaiance of cellular integrity and cytoskeleton development including cancer cells, so they are called as tumour associated macrophages or alternative macrophages (Sica *et al*, 2012). Cancer progression spreads in 3 phases: Elimination, Equilibrium and Expansion phase. In the first phase body cytotoxic cells are able to destroy mutated cancerous cells while in second equilibrium phase, cancer cells make a pace with normal body cells while in third and malignant form of cancer is most dangerous as the cancer cells spreads inside the body freely and work as a free radical for the

initiation of tumours at different sites in the body (Prendergast *et al*, 2008; Teng *et al*, 2008). The question arises here is, what happened to host immune sytem, so that from the second phase of equilibrium, they don't consider cancer cells as nonself and allow them to grow and spread. Cancer cells secretes many signal molecules which masks the normal defensive effect by immune cells. In this respect, macrophages, which are the most important phagocytic cells of body also help cancer cells for its progression in M2 form stimulated by IL-4/IL-13 (Sica *et al*, 2012). Signal responsible for M2 conversion are secreted more through cancer cells but if we can change the milieu of the cancer surrounding by appropriate molecules, like TLR and IFNγ which not only recruits macrophages towards tumour, but also potentiate them as cytotoxic M1 form to enable better regression in tumours at its equilibrium and elimination phase (Schreiber *et al*, 2011) by these classically activated macrophages. This cytotoxic effect can be lead by rationalizing a complex series for destruction process; one of them is ROS mediated DNA damage in reponse to M1 phenotype (Sica *et al*, 2012). The signature feature of classically activated macrophages are the production of nitric oxide (NO) while alternatively activated macrophages fails to produce it (Mosser *et al*, 2003). Reports show an inhibitory effect of NO on cancer invasion (Wang *et al*, 2007) and proliferation (Tate *et al*, 2012).

M1 phenotypes has some silent characteristics in production of proinflammatory cytokines, increased production of reactive oxygen and nitrogen intermediates and having tumorocidal effect. Considering about all these problems and challenges, we have initiated an easy and quick FACS based approach to observe the combined effect of two cytokines in a coculture of tumor cells along with macrophage cells. These two recombinant cytokines are GMCSF and IFNγ, in which GMCSF helps in the proliferation of macrophages, while the IFNγ helps in the activation of macrophages in its cytotoxic M1 form.

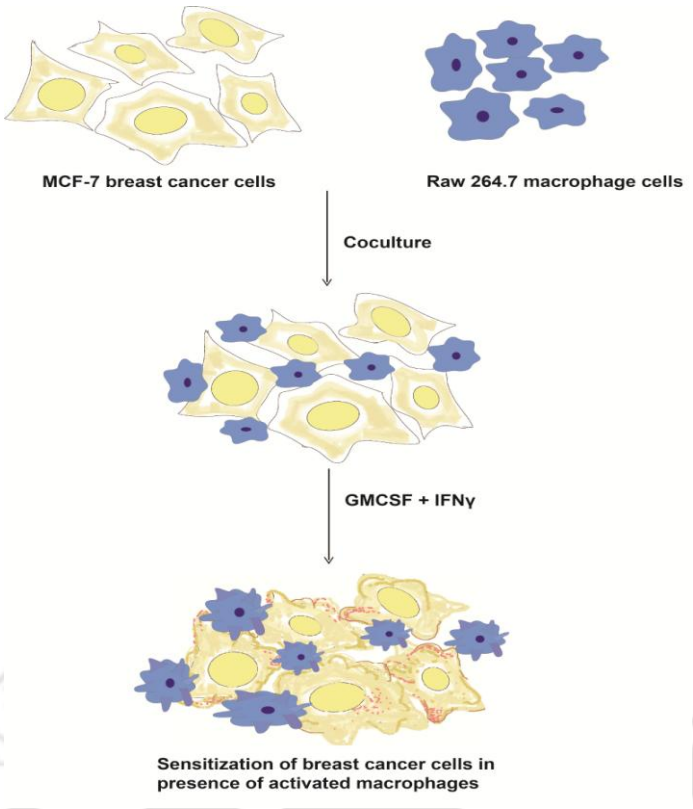

Flowdiagram 4.1. Coculture assay for MCF-7 and Raw 264.7 cells in presence of recombinant cytokines GMCSF and IFNγ.

4.2 Outline of Work

- Experimental results in the chapter 2 showed that GMCSF acted as a proliferative agent for both MCF-7 (breast cancer) as well as Raw 264.7 macrophages cells in a dose dependent manner. As the proliferative effect of GMCSF protein was more prominent over macrophages cells at low protein concentration (20 ng/mL) whereas no significant proliferation of MCF-7 was found at this protein concentration.
- In chapter 3, IFNγ protein was tested for its anti-cell proliferative effect on different cancer cell lines and among them, MCF-7 was found to be more suseptible, which renders cell growth retardation by blocking cell cycle.
- In this chapter, the reactive oxygen species (ROS) generating capacity of the recombinant IFNγ protein on MCF-7 and Raw 264.7 cells showed that Raw 264.7 cells were capable to generate more ROS in presence of recombinant IFNγ protein, while no significant ROS production was seen in MCF-7 cells. It

should be mentioned here that production of ROS by IFNγ activates macrophages for exerting its cytotoxic effect.

- Results for nitric oxide (NO) generating capacity of Raw 264.7 macrophages in response to IFNγ, indicated that they are possibly activated in cytotoxic M1 subtype.
- Coculture of MCF-7 (breast cancer) with Raw 264.7 (macrophages) have been established at ratio of 1: 20 cells.
- For coculture expriment of MCF-7 with Raw 264.7 cells, the MCF-7 cells were stained with CFSE to distinguish them in FACS based analysis from Raw 264.7 cells. Then the whole cell population was stained with 50 µg/mL of PI. The compromised cells would be shifted to (+,+) or (+,-) quadrant by uptaking PI (similar to the AnnexinV-PI assay).
- MCF-7 and Raw 264.7 cells were found to be susceptible by doxorubicin, in a closer range of 10 µM. Arround 50% cells were being compromised in both of the cells with the response of doxorubicin at 10 µM.

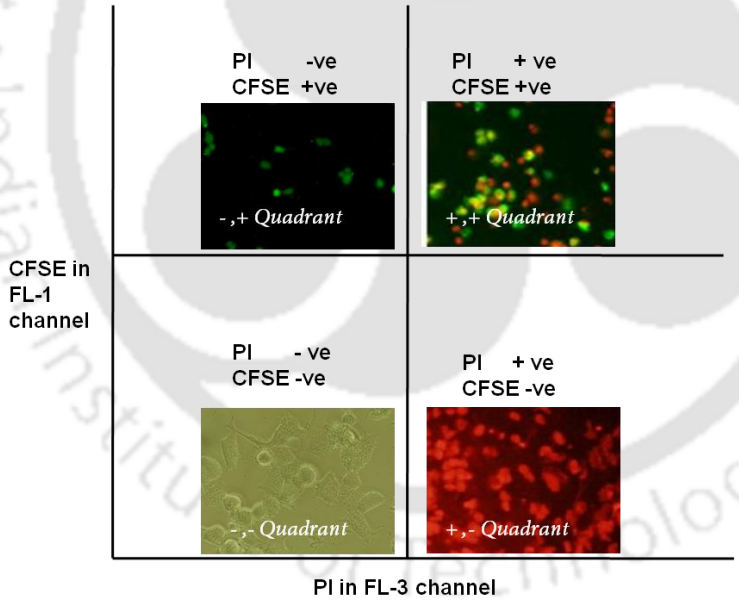

Scheme 4.1. A graphical presentation of the FACS based coculture experiment with two different colours for CFSE and PI stained cells. The (+) and (-) means CFSE, PI stained or unstained cells.

4.3 Materials and Methods

4.3.1 Cell Culture:

MCF-7 and Raw 264.7 cells were obtained from National Centre for Cell Science (NCCS), India. The cells were periodically cultured in DMEM media supplemented with 10% FBS, 20 U/mL penicillin and 50 mg/mL streptomycin in 5% CO_2 humidity at 37°C.

4.3.2 Measurement of ROS generated by recombinant IFNγ on MCF-7 cells and Raw 264.7 cells:

To determine the activity of recombinant IFNγ purified protein in generation of ROS, 5 µM of dichloro fluorescein (DCFDA, Sigma) was added on MCF-7 and Raw 264.7 cells, after 24 h of treatment with recombinant the IFNγ protein. The samples were analysed by flow cytometer (FacsCalibur, BD Biosciences, NJ) at excitation wavelength of 488 nm and emission wavelengths of 530 nm. The fluorescence data were recorded with the CellQuest program (BD Biosciences) for 15,000 cells in each sample.

4.3.3 Cell cycle analysis:

MCF-7 cells were treated with the recombinant IFNγ protein for 24 h and the cell cycle was analyzed as mentioned in Chapter 3 materials and methods section.

4.3.4 Nitric oxide determination:

The production of NO with response to recombinant IFNγ treatment on Raw 264.7 cells was determined by spectrophotometric analysis. For this purpose, 1×10^4 Raw 264.7 cells and 1×10^4 MCF-7 cells were seeded in 96 well plate/well (in 100 µL media/well) and a combination of 1×10^5 Raw cells with 1×10^5 MCF-7 cells were seeded in 35 mm plate in 1 mL media. In coculture of Raw 264.7 cells along with MCF-7 cells, it was taken into consideration that the ratio of cells: media should be the same as that of Raw 264.7 untreated control cells. Further, the cells were treated with recombinant IFNγ (100 ng/mL) and allowed to grow for next 6 h in this conditioned media. After this incubation period, 100 µL of conditioned media was

taken in an empty well of 96 well plate and supplemented with equal volume of Griess reagent (Sigma). This mixture was incubated in room temperature for 15 min before the absorbance was taken at 550 nm. Sodium nitrite was used as a standard for measuring the amount of released NO in the medium. The amount of NO released by treated cells was expressed as relative fold increase to compare with untreated control cells (considered as 100 %). Similar experiments were performed for the mixed cell population of Raw 264.7 and MCF-7 when cells were seeded in ratio of 1:20.

4.3.5 CFSE staining:

MCF-7 cells were harvested with trypsin and incubated with 1 mL of CFSE solution (10 µM of CFSE in PBS) for 5 minutes at 20°C. Afterwards, the cells were washed with 10 volume of HI-FBS PBS (5% FBS in PBS) at room temperature and sedimented by centrifugation at 300 g. The pellet was dissolved in 1 mL PBS and finally analyzed by flow cytometer.

4.3.6 Coculture:

The CFSE stained MCF-7 cells were counted and the 2×10^5 cells seeded alongwith 1×10^4 Raw 264.7 cells to maintain 20:1 ratio in 60 mm dish. Cells were allowed to attach and grow for another 24 h before any further treatment.

4.3.7 Protein therapy:

The GMCSF exhibited a proliferative effect on MCF-7 as well as Raw 264.7 cells. However, the proliferative effect was more prominent with Raw 264.7 cells even at low protein concentration as compare to MCF-7 cells. Therefore, the coculture cells were intially treated with purified GMCSF protein (20 ng/mL) and then the mix cell population was also incubated with purified IFNγ protein (100 ng/mL) as well as combination of both cytokine.

4.4 Results and Discussions

4.4.1 Activity study of the recombinant IFNγ:

Macrophage cells are known to produce high amount of reactive oxygen species (ROS) in response to IFNγ (Amatore *et al*, 2010). ROS activate macrophages into their cytotoxic form, which is responsible for scavenging effect of macrophage cells. This phenomenon is a well-established bioassay for testing functional activity of IFNγ (Yang *et al*, 2007). In this case, the mouse macrophage (Raw 264.7) and the MCF-7 cells were treated with purified recombinant IFNγ protein for 24 h, and then ROS was measured by FACS analysis using 2, 7-dichlorofluoresceindiacetate (DCFDA) staining method (Eruslanov *et al*, 2010). The non-fluorescent DCFDA freely diffuses into the cells through the plasma membrane and converts to green fluorescent DCFH due to intracellular oxidation by ROS. Thus, the amount of fluorescence intensity of DCFH produced is directly correlated with the amount of ROS production inside treated cells. The FACS results demonstrated that Raw 264.7 cells treated with recombinant IFNγ protein generated ROS, which was evident from a prominent shift of fluorescence intensity in the FL-1H channel as compared to the untreated cells (Fig. 4.1A), while there was no peak shifting in MCF-7 cells in response to the purified IFNγ (Fig. 4.1B). The results revealed that recombinant IFNγ obtained from bacterial expression host retained its functional activity, which is capable of generating ROS in macrophages cells.

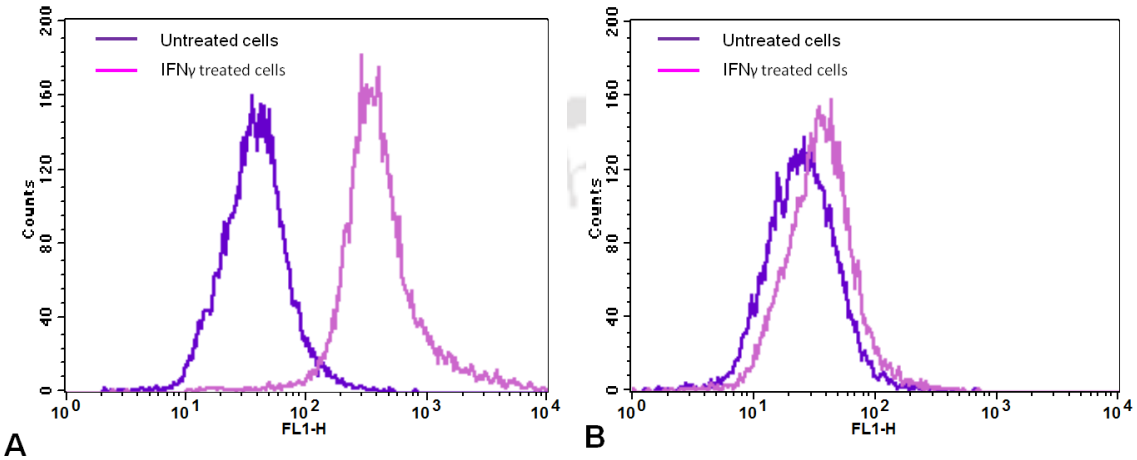

Fig 4.1. ROS estimation by DCFDA assay **A.** Raw 264.7 cells **B.** MCF-7 cells

4.4.2 NO estimation:

The production of NO was confirmed by the relative estimation of NO in untreated Raw 264.7 control cells versus IFNγ treated Raw 264.7 by spectroscopic analysis. At around 5.5 fold increase in NO content with response to IFNγ treatment in Raw 264.7 cells was noted. Further significant increase in NO was also noted in mixed cell population of MCF-7 and Raw 264.7 cells, which signifies the capability of M1 macrophage population for generating NO in mixed cell population (Fig. 4.2).

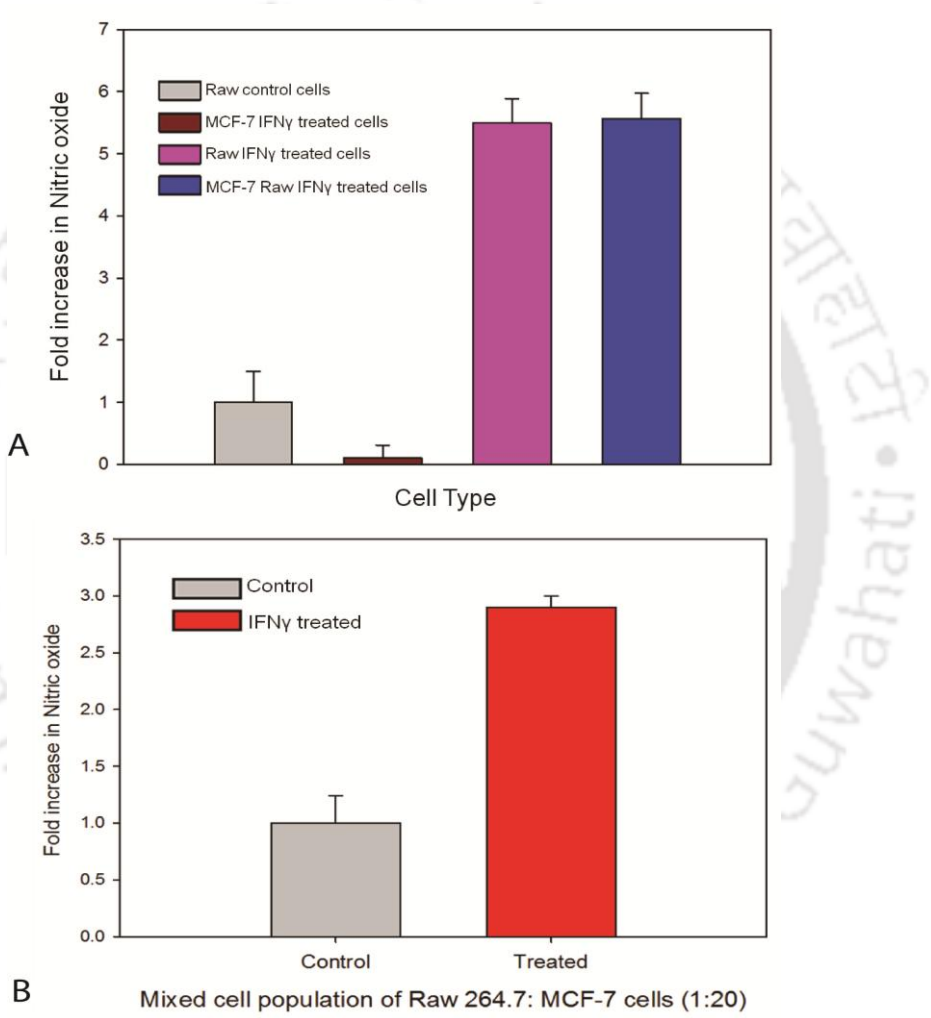

Fig 4.2. Griess based assay for Nitric oxide estimation

4.4.3 Cell cycle analysis of IFNγ treated MCF-7 cells:

Cell cycle analysis of recombinant IFNγ treated MCF-7 cells revealed a prominent cell cycle blockage in G1 phase of the treated cells (Fig. 4.3).

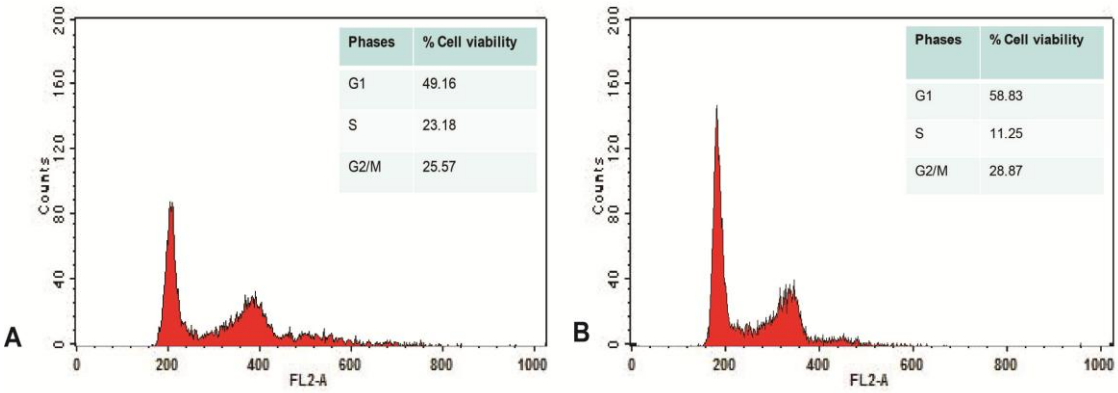

Fig 4.3. Histogram analysis **(A)** Control MCF-7 cells **(B)** IFNγ treated MCF-7 cells

4.4.4 Coculture assay:

In coculture experiment, the MCF-7 cells were seeded with Raw 264.7 cells. Dual staining by FACS was presented and the cell viability of each cell type was presented in percentage (even in control). The following sequence of experiments was performed to execute the whole set of experiments. The (+) and (-) symbols denotes whether the cells have uptaken the dyes or not.

Untreated Unstained MCF-7 and Raw 264.7 cells:

For double staining control experiments, the CFSE was represented in FL-1 channel at Y axis and PI in FL-3 channel at X axis. The CFSE unstained cells were present at the left lower quadrant (-,-) (Fig. 4.4A).

MCF-7 [PI (-), CFSE (+)] cells:

MCF-7 cells stained with CFSE as well as PI. Since the MCF-7 cells were uncompromised, so the cell membrane was intact and most of the cells (99.99%) showed only CFSE positive signal in the left upper CFSE positive quadrant (-, +), where PI was negative (Fig. 4.4B).

MCF-7 [PI (+), CFSE (+)] cells treated with IFNγ:

Treatment of MCF-7 cells with IFNγ led to the cell damage. So the CFSE stained cells were shifted to the CFSE and PI positive quadrant to the right upper panel. Around 20% of MCF-7 were found to be both CFSE and PI positive (+, +) after

treatment with IFNγ by FACS analysis. It indicated that IFNγ caused damage to MCF-7 cells as shown in figure 3 by producing ROS. The remaining cells populations resided in the same (-, +) quadrant (Fig. 4.4C).

Raw 264.7 [PI (-), CFSE (-)] cells:

The Raw 264.7 cells were stained with PI but not with CFSE. The cells were undamaged and thus did not take up PI stain. The FACS analysis showed 99.9% of the cells remained in the lower left quadrant (-,-) (Fig. 4.4D).

Raw 264.7 [PI (+), CFSE (-)] cells treated with IFNγ:

Treatment of IFNγ on Raw 264.7 cells showed negligible effect on cell death. Around 3% cells were found to be PI positive and shifted to (+,-) quadrant, while the remaining were in (-,-) quadrant (Fig. 4.4E).

Cells in coculture experiments:

MCF-7 [PI (-), CFSE (+)] and Raw 264.7 [PI (-), CFSE (-)] cells:

In a mixed culture of MCF-7 cells and Raw 264.7 cells were grown in normal cell culture media, Almost all MCF-7 cells were in (-, +) quadrant, while all Raw 264.7 cells were present in the lower quadrant (-,-) for both CFSE and PI negative. This indicated that cell were healthy in coculture conditions (Fig. 4.4F).

MCF-7 [PI (+), CFSE (+)] and Raw 264.7 [PI (+), CFSE (-)] cells treated with IFNγ:

In this experiment, the purified IFNγ (100 ng/mL) was added to the mixed cell population. FACS analysis showed that 33% of MCF-7 cells were (+, +) and 4% of Raw 264.7 cells were (+,-), which exhibited the damaged cell population. The percentage of damaged cells were significantly more in MCF-7 than Raw 264.7 cells in coculture condition, which indicated that IFNγ was more effective on MCF-7 cells when it was challenged along with macrophages. In the comparative studies 20% death of MCF-7 cells was seen by IFNγ treatment, while in coculture the death was exceeded by 13%. Around 4% of cell death in Raw 264.7 cells has also been observed (Fig. 4.4G).

MCF-7 [PI (+), CFSE (+)] and Raw 264.7 [PI (-), CFSE (-)] cells treated with both GMCSF and IFNγ:

Anti-cell proliferative effect of IFNγ on MCF-7 cells was demonstrated. However, the recombinant IFNγ had little effect on Raw 264.7 cells. MTT assay results in Chapter 2 showed a effective proliferative role of recombinant GMCSF protein on Raw 264.7 cells at its low concentration than MCF-7 cells. It has been reported that the phagocytic macrophages could be able to clear apoptotic load after targeting any benign tumour with therapeutic drugs and thereby, enhanced the efficacy of the treatment. However, one more hurdle is that the therapeutic drugs also target immune cells and macrophages. To address this challenge, the methodologies could be adopted to rescue the macrophages in this adverse condition after therapy. Thus, the recombinant GMCSF protein was added to the IFNγ treated mixed cell population. FACS analysis resulted in the similar percentage of viable MCF-7 cells while a less cell death was recorded in Raw 264.7 cells in response to IFNγ. Only negligible 1.09% of Raw 264.7 cells were dead and interestingly the total ratio of Raw 264.7 cells in coculture was increased from 1:20 to 1.15 (Fig. 4.4H).

Effect of chemotherapeutic drug Doxorubicin in Coculture:

MCF-7 [PI (+), CFSE (+)] cells treated with doxorubicin:

After 24 h treatment with doxorubicin (10 µM), FACS analysis was performed on the mixed population. Around 36% of MCF-7 cells were moved to upper right quadrant which was positive for both PI and CFSE compromised cells (+, +) (Fig. 4.4I).

Raw 264.7 [PI (+), CFSE (-)] cells treated with doxorubicin:

After 24 h treatment with doxorubicin (10 µM) around 32% of macrophages cells were moved to the lower right quadrant (+,-) which was for PI positive damaged cells (Fig. 4.4J).

MCF-7 [PI (+), CFSE (+)] and Raw 264.7 [PI (+), CFSE (–)] cells treated with both IFNγ and doxorubicin:

This experiment mimics a complex situation where cancer cells can be targeted with two or more therapeutic modules, such as chemotherapeutic agent, macrophages and

anti-tumour cytokine IFNγ. For this experiment, MCF-7 cells and Raw 264.7 macrophages cells were seeded in 1:1 ratio. In this mixed cell population, after 24 h treatment with doxorubicin and IFNγ, about 49% of MCF-7 and 34% of Raw 264.7 cells were found dead by FACS analysis (Fig. 4.4K).

MCF-7 [PI (+), CFSE (+)] and Raw 264.7 [PI (-), CFSE (–)] cells treated with IFNγ and doxorubicin and GMCSF:

This experiment has been performed to rescue macrophages from the side effect of chemotherapeutic drugs during cancer therapy, so they could retrieve proper immune response. The mixed culture of MCF-7 cells and Raw 264.7 cells (1:1) treated with doxorubicin and IFNγ simultaneously, exhibited significant cell death for both cell types as evident by FACS analysis. Hence, in order to reduce death of macrophages, the recombinant GMCSF was added to the mixed population at the time of treatment. Results showed a significant decrease in cell death for the macrophages (14.88% cells were dead), while no considerable difference in cell viability of MCF-7 cells (43%) was seen (Fig. 4.4L). It implied that GMCSF helped in recovering the treated macrophages in the mixed culture population. This could be an avenue to recover macrophages during chemotherapeutic treatment of cancer.

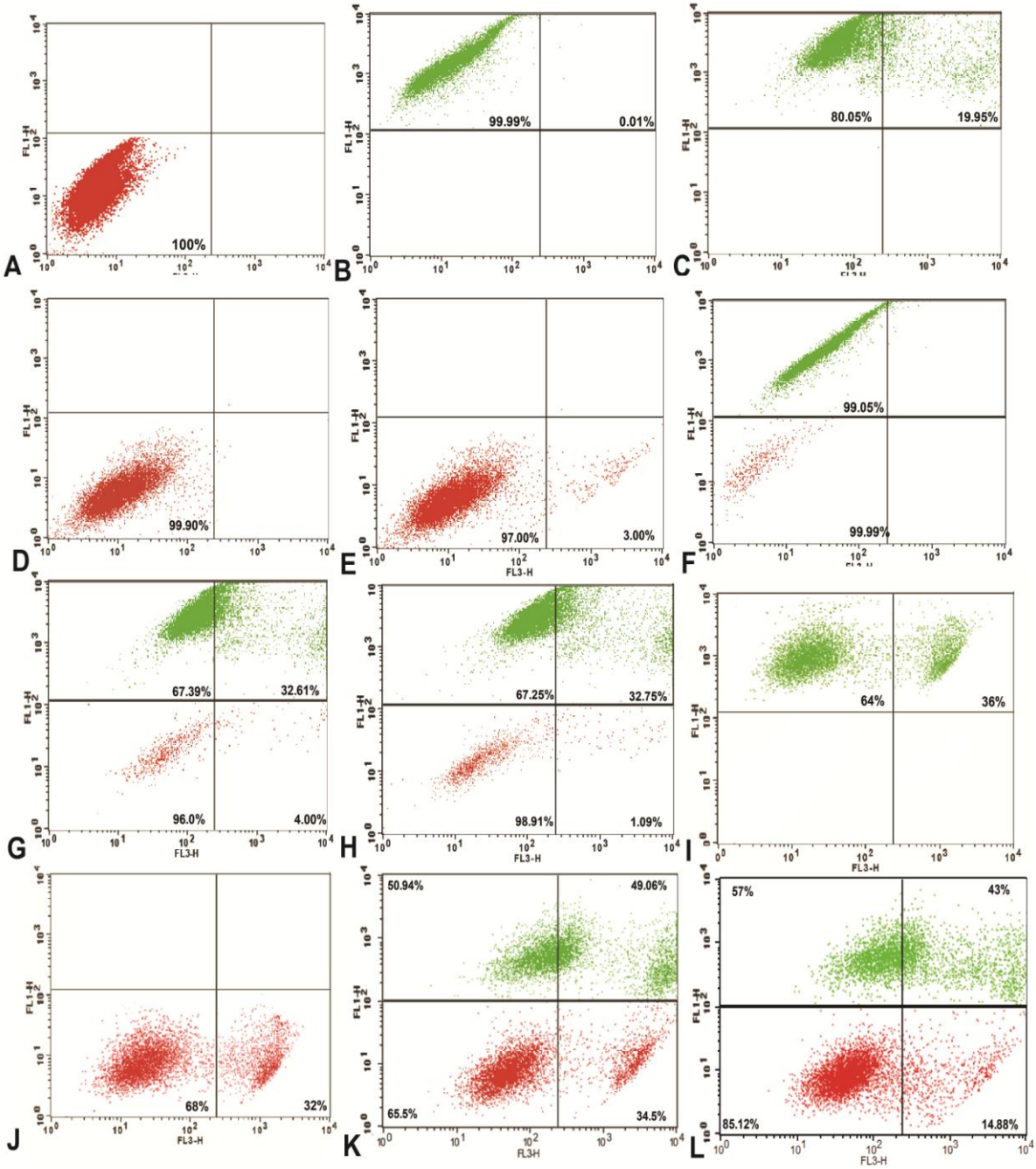

Fig 4.4. Dot plot for coculture population. **A.** MCF-7 and Raw 264.7 unstained control cells **B.** PI (-), CFSE (+) MCF-7 control cells **C.** IFNγ treated PI (+), CFSE (+) MCF-7 cells **D.** PI (-), CFSE (-) Raw 264.7 control cells **E.** IFNγ treated PI (+), CFSE (-) Raw 264.7 cells **F.** Mixed population of [PI (-), CFSE (+)] MCF-7 cells and [PI (-) CFSE (-)] Raw 264.7 cells **G.** Mixed population of [PI (+), CFSE (+)] MCF-7 cells and [PI (+) CFSE (-)] Raw 264.7 cells treated with IFNγ **H.** Mixed population of [PI (+), CFSE (+)] MCF-7 cells and [PI (-) CFSE (-)] Raw 264.7 cells treated with GMCSF and IFNγ **I.** Doxorubicin treated [PI (+), CFSE (+)] MCF-7 cells **J.** Doxorubicin treated [PI (+), CFSE (-)] Raw 264.7 cells **K.** MCF-7 [PI (+), CFSE (+)] and Raw 264.7 [PI (+) CFSE (–)] cells treated with both IFNγ and doxorubicin **L.** MCF-7 [PI (+), CFSE (+)] and Raw 264.7 [PI (-), CFSE (–)] cells treated with IFNγ and doxorubicin and GMCSF.

Table 4.1. Tabular presentation of viable and dead cells in mixed cell population of MCF-7 and Raw 264.7 macrophages in presence of recombinant cytokines and drugs

SL No.	Culture Condition	Cell type	PI stained	CFSE stained	Treatment	Live cells (%)	Dead cells (%)
1	Single	MCF-7	-	+	-	99.99	0.01
2	Single	MCF-7	+	+	IFNγ	80.05	19.95
3	Single	Raw 264.7	-	-	-	99.90	0.10
4	Single	Raw 264.7	+	-	IFNγ	97.00	3.00
5	Mixed	MCF-7 and Raw 264.7	-	-	-	100	0
6	Mixed	MCF-7 and Raw 264.7	-	+	-	99.05	0.95
			-	-	-	99.99	0.01
7	Mixed	MCF-7 and Raw 264.7	+	+	IFNγ	67.39	32.61
			+	-		96	4
8	Mixed	MCF-7 and Raw 264.7	+	-	GMCSF and IFNγ	67.25	32.75
			-	-		98.91	1.09
9	Single	MCF-7	+	+	Doxorubicin	64	36
10	Single	Raw 264.7	+	-	Doxorubicin	68	32
11	Mixed	MCF-7 and Raw 264.7	+	+	Doxorubicin and IFNγ	50.94	49.06
			+	-		65.5	34.5
12	Mixed	MCF-7 and Raw 264.7	+	+	Doxorubicin GMCSF IFNγ	57	43
			-	-		85.12	14.88

4.5. Conclusion

In this chapter an easy and quick flow cytometry based method was established for finding the effect of recombinant cytokines in mixed cell population. The coculture assay was establihed for growing cancer cells with macrophages. Addition of recombinant IFNγ produced significant reactive oxygen species which could damage the MCF-7 cancer cells, but there was little effect on the macrophages. In coculture experiment, addition of recombinant GMCSF protected the damage of macrophages either in presence of IFNγ or in combination of both. Moreover, doxorubicin based coculture results revealed that macrophages were rescued from the negative effect of drugs by the administration of proliferative GMCSF cytokine. Hence, this FACS based approach can easily be employed to test the effect of cytokines or drugs in combination on the cell growth using simple coculture based experiments.

4.6. References

1. Amatore, C., Arbault, S., and Koh, A.C.W. (2010). Simultaneous detection of reactive oxygen and nitrogen species released by a single macrophage by triple potential-step chronoamperometry. Anal. Chem. *82*, 1411–1419.
2. Classen, A., Lloberas, J., and Celada, A. (2009). Macrophage Activation: Classical Vs. Alternative. In Macrophages and Dendritic Cells, N.E. Reiner, ed. (Totowa, NJ: Humana Press), pp. 29–43.
3. Dalton, D.K., Pitts-Meek, S., Keshav, S., Figari, I.S., Bradley, A., and Stewart, T.A. (1993). Multiple defects of immune cell function in mice with disrupted interferon-gamma genes. Science *259*, 1739–1742.
4. Dunn, G.P., Koebel, C.M., and Schreiber, R.D. (2006). Interferons, immunity and cancer immunoediting. Nat. Rev. Immunol. *6*, 836–848.
5. Eruslanov, E., and Kusmartsev, S. (2010). Identification of ROS using oxidized DCFDA and flow-cytometry. Methods Mol. Biol. *594*, 57–72.
6. Hanahan, D., and Weinberg, R.A. (2011). Hallmarks of cancer: the next generation. Cell *144*, 646–674.
7. Huang, S., Hendriks, W., Althage, A., Hemmi, S., Bluethmann, H., Kamijo, R., Vilcek, J., Zinkernagel, R.M., and Aguet, M. (1993). Immune response in mice that lack the interferon-gamma receptor. Science *259*, 1742–1745.
8. Klimp, A.H., de Vries, E.G.E., Scherphof, G.L., and Daemen, T. (2002). A potential role of macrophage activation in the treatment of cancer. Crit. Rev. Oncol. Hematol. *44*, 143–161.
9. Mantovani, A., Sozzani, S., Locati, M., Allavena, P., and Sica, A. (2002). Macrophage polarization: tumor-associated macrophages as a paradigm for polarized M2 mononuclear phagocytes. Trends Immunol. *23*, 549–555.
10. Mosser, D.M. (2003). The many faces of macrophage activation. Journal of Leukocyte Biology *73*, 209–212.
11. Prendergast, G.C. (2008). Immune escape as a fundamental trait of cancer: focus on IDO. Oncogene *27*, 3889–3900.
12. Schreiber, R.D., Old, L.J., and Smyth, M.J. (2011). Cancer immunoediting: integrating immunity's roles in cancer suppression and promotion. Science *331*, 1565–1570.
13. Sica, A., and Mantovani, A. (2012). Macrophage plasticity and polarization: in vivo veritas. Journal of Clinical Investigation *122*, 787–795.

14. Tate Jr., D.J. (2012). Interferon-Gamma-Induced Nitric Oxide Inhibits the Proliferation of Murine Renal Cell Carcinoma Cells. International Journal of Biological Sciences 1109–1120.
15. Teng, M.W.L., Swann, J.B., Koebel, C.M., Schreiber, R.D., and Smyth, M.J. (2008). Immune-mediated dormancy: an equilibrium with cancer. J. Leukoc. Biol. *84*, 988–993.
16. Wang, F., Zhang, R., Xia, T., Hsu, E., Cai, Y., Gu, Z., and Hankinson, O. (2007). Inhibitory effects of nitric oxide on invasion of human cancer cells. Cancer Lett. *257*, 274–282.
17. Yang, D., Elner, S.G., Bian, Z.-M., Till, G.O., Petty, H.R., and Elner, V.M. (2007). Pro-inflammatory cytokines increase reactive oxygen species through mitochondria and NADPH oxidase in cultured RPE cells. Exp. Eye Res. *85*, 462–472.
18. Zaynagetdinov, R., Sherrill, T.P., Polosukhin, V.V., Han, W., Ausborn, J.A., McLoed, A.G., McMahon, F.B., Gleaves, L.A., Degryse, A.L., Stathopoulos, G.T., *et al*. (2011). A critical role for macrophages in promotion of urethane-induced lung carcinogenesis. J. Immunol. *187*, 5703–5711.

CHAPTER 5

Overexpression studies of recombinant cytokines in cancer cells.

Chapter 5

5.1 Introduction

Pleitropicity in the behaviour of cytokines (GMCSF and IFNγ) has brought more attention towards their activity study in different environment. In this regard, their overexpression study is more preferable as they provide a homogenous platform to see the effect of overexpressed protein. Generally, CSFs are well tolerated in patients, with some side effects because of rapid proliferation of myeloid cells. Among all CSFs, GMCSF is a well established cytokine marketed under the tradename of Sargramostim and Morgramostim and it is commonly being used after chemotherapy in acute myeloid leukemia, bone marrow transplantation, transplantation of organ to decrease the chances of graft rejection etc (Mezzano *et al*, 2000). GMCSF is well tolerable but sometimes it also exerts severe side effect as uncontrolled increase in myeloid cell number may also be deadly. But this cytokine behaves pleiotropically, its effect is dose dependent as well as based on the surroundings. GMCSF overexpression study also reveals its pleitropic role and its overexpression upto 150 fold. Increase in the basal level of this cytokine implies many biological changes such as enlarged and histologically abnormal liver and spleen, increased number and activation state of peripheral blood granulocyte and macrophages (Bauer *et al*, 1977). Inspite of all the problems associated with this overexpressed cytokine level, the livestock was found to be alive. The overexpression of CSFs was not always found to be deterioratic, for example in mice lung it enhances the survival in hyperoxia condition upto 70% (Li *et al*, 1991). Thus, any feasible model of overexpression provides a platform to understand the potential role of these cytokines in disease and health, which could futher lead to the development of disease resistant livestocks. Here a model system was generated, where GMCSF was stably transfected in a cell line, which showed enhanced sensitivity against the purified recombinant GMCSF protein. MCF-7 cells were being proliferated in response to recombinant GMCSF protein *in vitro*.

On the other hand, there are only few reports available regarding the overexpression studies of proinflammatory cytokine IFNγ. The antitumour activity exerted by IFNγ showed its potential in tumour targeting (Tu *et al*, 2011). Here IFNγ was overexpressed in neuroblastoma U87MG cells, a cell line less sensitive towards many

anticancer drugs. In order to achieve proper sensitivity of this cell line towards chemotherapy, overexpression of this anti tumour IFNγ cytokine in U87MG neuroblastoma cells was performed. Scheme 5.1 shows a schematic representation for the work done in this chapter.

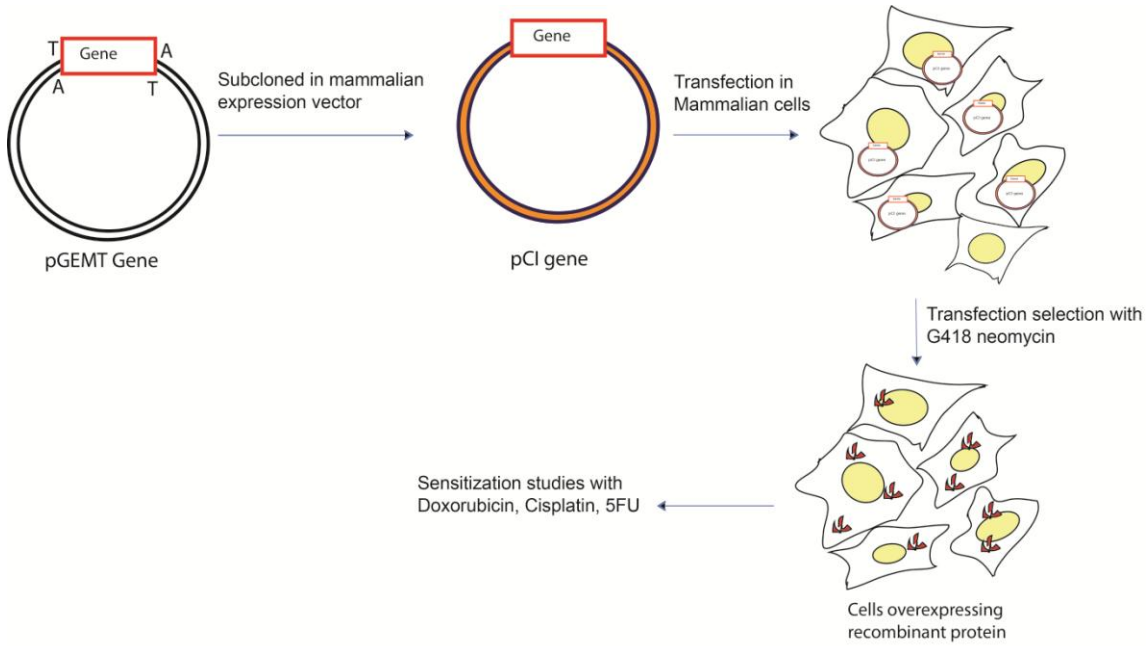

Scheme 5.1 Strategy of work in cytokine over expressing cancer cells

5.2 Materials and Methods

5.2.1 Cloning of gene into pCI neo mammalian expression vector:

GMCSF and IFNγ genes were subcloned from their pGEMT Easy construsts (reported in Chapter 2 and Chapter 3 respectively), into pCI neo mammalian expression vector. Following gene specific forward and reverse primers, with *Xho I* and *Not I* sites in the overhangs, were used for amplification of GMCSF and IFNγ genes, repectively:

Forward primer 5' GCC TCG AGA TGT GGC TGC AGA GCC TG 3'

Reverse primer 5' GAG CGG CCG CTC ACT CCT GGA CTG GCT 3'

Forward primer 5' GCC TCG AGA TGA AAT ATA CAA GTT A 3'

Reverse primer 5' CAG CGG CCG CTT ACT GGG ATG CTC TT 3'

PCR reaction was performed and the amplicons were checked by agarose gel electrophoresis. The desired fragments were eluted from gel. All protocols have been described in detail in the chapter 2, materials and methods section.

5.2.2 Generation of stable cell lines:

The pCI-GMCSF plasmid was transfected into MCF-7 cells by Electro Square Porator ECM 830 (BTX, Harvard Apparatus) electroporator. Cells were trypsinized and washed with DMEM containing 10% FBS. Cells were again washed with DMEM containing 2.0% FBS without antibiotic and resuspended at a density of 1×10^8. About 400 µL of the cell suspension was incubated with 25 µg of pCI neo-vector at room temperature for 5 min and further electroporated at 170 volt for 60 ms. After electroporation, the cells were resuspended in 10% FBS in DMEM with antibiotic and seeded in a 6 well plate. Electroporated cells were maintained at 5% CO_2 at 37°C. After 48 h of transfection, the electroporated cells were selected with 600 µg/mL of G418 (Sigma) for stable transformants and the media was changed periodically after 72 h. In the presence of G418, majority of cells died within 10-12 days. Only stably transfected cells were able to cope up with antibiotic neomycin because of the presence of neomycin phosphotransferase gene. The CMV promoter allowed strong and constitutive expression of desired gene product so the transfected cells survived in presence of antibiotic. Further, transfected cells were maintained in 400 µg/mL of G418.

For transfecting IFNγ in pCI neo mammalian expression vector (Promega), firstly U87MG (1×10^6) cells were seeded in the plate. Further, 1 µg of pCI IFNγ plasmid was incubated with 2 µL of lipofectamine solution (Invitrogen) in 90 µL of serum free media without antibiotic. And this mixture was added to 1 mL of serum free media. Media was taken out from the plate and cells were washed with PBS, before addition of the serum free media having composite of DNA and lipofectamine. Cells were kept with this composite for next 24 h in incubator and later on media was replaced by serum media and the cells were allowed to grow in incubator at 37°C.

5.2.3 Extraction of proteins from mammalian cells:

Isolation of total protein from mammalian cell lines was done by RIPA buffer (Sigma), which contained proteases inhibitors as well as cell membrane disrupting

reagents. Media was discarded from cell culture plate and the cells were washed with PBS to remove the residual media. About 500 µL of RIPA buffer was added to 35 mm plate and the cells were taken out simply by repetitive pipetting. At this step, cells can be stored at -20°C for a week or could proceed further by centrifugation for 10 min at 10,000 rpm at 4°C. The supernatant was collected, which contains the cellular proteins. This sample was subjected to SDS-PAGE analysis. Lowry's method was employed for protein estimation.

5.2.4 Estimation of Protein:

Endogenous expression of recombinant protein was estimated by Lowry's method. BSA (Himedia, India) was used as standard control protein. BSA was dissolved in the same RIPA buffer (Sigma) in which cell lysate proteins were present. About 500 µL of complex forming reagent (2% Na_2CO_3 in 0.1 N NaOH: 2% Potassium Sodium Tartarate: 1% $CuSO_4.5H_2O$) was added with 100 µL of diluted crude protein lysate. After 10 min of incubation at room temperature, the reaction mixture was added with 50 µL of freshly prepared diluted Folin reagent (Folin reagent: H_2O=1:1) and vortexed for 10 seconds. This total mixture was incubated at room temperature for 30 min in dark. After 30 min of incubation, 200 µl reaction mixture of each sample was transferred into 96 well plate for measuring optical density at 660 nm in ELISA reader (Perkin Elmer 2030 Multilabel reader) (Lowry *et al*, 1951).

5.2.5 Westeren Blot:

Western blot was performed to analyse the expression of recombinant protein in stably transfected cells. Cells were disrupted and the concentrated cell extract was resolved by 12% SDS PAGE and electroblotted over PVDF membrane (0.2 µM Milipore, USA) for 4 h using semidry blot transfer appratus (G. E Healthcare). Trasfer was confirmed by Ponceau S staining (0.1% Ponceau stain in 5% Acetic acid), which was further washed with PBST (PBS containing 0.1% Tween 20) to remove the stain. Further membrane was blocked with 5% BSA in PBST for 2 h. Thereafter, the membrane was incubated with primary dilution of antibody in 5% BSA in PBST for 2 h at room temperature. After removing primary antibody, the membrane was washed gently with PBST and again incubated with Horse radish peroxidase conjugated 2° Ab for 1 h at room temperature. Then the blot was washed throughly with PBST, the

signal was developed with chemiluminescence (Super Signal West Dura, Thermo Scientific) and imaged with gel documented system (Gel Logic System 1500, Kodak).

5.2.6 Cell Viability Assay:

To measure cell viability, MTT assay (Himedia) was performed. The detailed protocol has been described in the chapter 3, materials and methods section (Mosmann *et al*, 1983). About 1×10^4 cells were seeded in each well of 96 well plate. After 24 h the stably transfected cells as well as untransfected control cells were treated with different chemotherapeutic drugs and allowed to grow for next 24 h to examine their sensitivity for these drugs. At the specified time, 8 µL of MTT (Himedia, 5 mg/mL in PBS) was added in each well and kept in 5% CO_2 incubator for 2 h at 37°C. For measuring, the optical density media was replaced by DMSO, so that the end product of MTT became soluble in organic solvent. OD was measured at 550 nm with background subtraction at 650 nm.

5.2.7 Cell Cycle Analysis:

After treatment with different reagents, cell cycle was analyzed by FACS with propidium iodide staining. After 24 h of cell seeding in 6 well plate (~10^5 cells/well), the cells were taken for treatment. At specific time points, cells were taken out by trypsinization and suspended in 1 mL media (DMEM with 10% FBS) for centrifugation at 500 g at 4°C for 5 minutes. Supernatant was discarded and pellet was resuspended in ice cold fixation solution (70% ice cold ethanol in PBS) with intermittent vortexing. For FACS analysis, the cells were pelleted down by centrifugation, supernatant was discarded and pellet was resuspended in DNA staining solution (50 µg/mL PI, 200 µg/mL RNase A, 0.05% Triton X 100 in PBS). Cell cycle profile analysis was performed with 20,000 cells on a FACS Calibur flow cytometer using the Cell quest analysis program (Becton Dickinson). Cell cycle was analysed by Modfit LT (Verity Software). Fluorescence intensities of PI stained cells were measured in FL-2 channel in linear mode. (Riccardi *et al*, 2006).

5.2.8 Carboxyfluorescein succinimidyl ester (CFSE) assay:

CFSE assay was used to calculate the doubling time of cells. Detailed protocol for CFSE staining has been mentioned in chapter 3 materials and methods.

Subsequently, labeled cells were seeded in 6 well plates (~10^5 cells/well). At the same time, sample was run for zero hour analysis by flow cytometry. Upto 72 hours, the cells were harvested, washed, and analyzed by flow cytometry by 24 h interval using BD Biosciences FACS Calibur flow cytometer. Data was acquired and analyzed using CellQuest software (BD Biosciences). Measurements for CFSE were made in FL-1 channel in log mode and data for 20,000 cells were collected in each case. Because the cell population was homogenous with unimodal CFSE fluorescence histograms, a simple model was used to calculate average doubling time. Assuming that all cells are dividing and there is no cell death during the study, the mean doubling time, $\langle T_d \rangle = T/\log_2 (\langle Fo \rangle / \langle F_T \rangle)$; where, $\langle F_0 \rangle$ = geometric mean fluorescence intensity at zero hour and $\langle F_T \rangle$= geometric mean fluorescence intensity at T h (Quah *et al*, 2007).

5.2.9 Semiquantitative PCR analysis for cyclins study:

For setting up a PCR for cyclins study, total RNA was isolated from MCF-7 and GMCSF stably transfected MCF-7 cells. The detailed protocol has been described in chapter 2, materials and methods section. PCR condition was also same as mentioned there with 27 amplification cycles. The product was analysed using agarose gel electrophoresis. The fold change in expression was estimated by volume analysis of Image lab 4.1 software of Molecular Imager Chemidoc^{TM} XRS^{+} system.

5.3 Results and Discussions

5.3.1 Cloning of GMCS IFNγ in pCI neo mammalian expression vector:

Human GMCSF and IFNγ were subcloned into mammalian expression vector from their pGEMT Easy constructs. Firstly, these genes were amplified with their respective gene specific primers. The PCR product were analysed and the specific bands were eluted from agarose gel. Eluted products were double digested with *Xho I* and *Not I* to generate compatible ends to clone in pCI neo backbone. The digested pCI neo plasmid backbone and PCR products were purified and ligted. The ligation product was transformed into bacterial competent cells and the transformed colony

was screened by colony PCR. The recombinant plasmids were isolated from the positively screened colonies and digested with *Xho I* and *Not I* which released the legitimate band of 435 bp for GMCSF and 501 bp for IFNγ from the recombinant pCI neo-GMCSF and pCI neo IFNγ constructs, respectively as shown in Fig 5.5A and 5.5B.

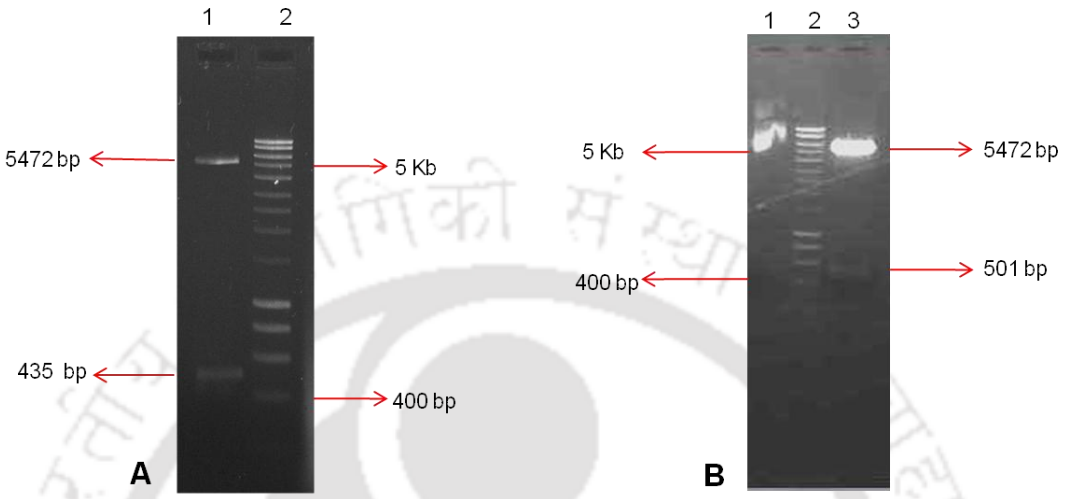

Fig 5.5. restriction digestion profile of the recombinant clones with *Xho I, Not I* **(A)** Lane 1: 435 bp release of GMCSF from pCI neo GMCSF construct, Lane 2: Hyperladder (NEB) **(B)** Lane 1: Undigested pCI IFN γ plasmid, Lane 2: Hyperladder (NEB), Lane 3: 501 bp release of IFNγ fragment from the pCI neo IFNγ construct.

5.3.2 Semiquantitative RT-PCR to check overexpression of GMCSF and IFNγ:

The overexpression of GMCSF in GMCSF transfected MCF-7 stable cells and that of IFNγ in IFNγ transfected U87MG stable cells were checked by semiquantitaive RT PCR. The procedure for RNA isolation and cDNA preparation has already been described in materials and methods section of chapter 2. The overexpression of full length GMCSF and IFNγ was checked by PCR of 26 cycles of amplification. Legitimate band for GMCSF (435 bp) in MCF-7 cells (Figure 6A) and IFNγ (501 bp) in U87MG cells (Fig. 5.6B) were observed after gel eletrophoresis.

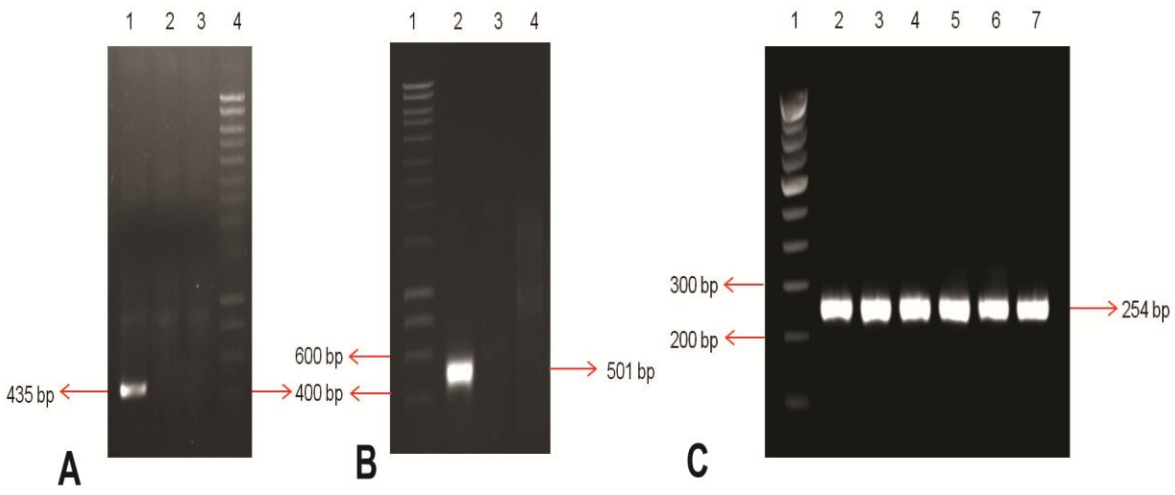

Fig 5.6. PCR analysis transgenes **(A)** Overexpression study for GMCSF in transfected MCF-7 stable cells; Lane 1: GMCSF transfected MCF-7 stable cells, Lane 2: untransfected MCF-7 cells, Lane 3: pCI neo backbone transfected MCF-7 control cells, Lane 4: Marker, **(B)** Overexpression study for IFNγ in trasnfected stable U87MG cells; Lane 1: Marker, Lane 2: IFNγ transfected U87MG stable cells, Lane 3: untransfected U87MG cells, Lane 4: pCI neo backbone transfected U87MG control cells **(C)** β actin analysis as loading control in; Lane 1: 100 bp Marker, Lane 2: GMCSF transfected MCF-7 stable cells, Lane 3: MCF-7 cells, Lane 4: pCI neo backbone transfected MCF-7 control cells, Lane 5: IFNγ transfected U87MG stable cells, Lane 6: U87MG cells, Lane 7: pCI neo backbone transfected U87MG control cells.

5.3.3 Western Blots:

Western blot analysis revealed that GMCSF protein was overexpressed in GMCSF trasnfected MCF-7 stable cells (Figure 7A). Similarly, IFNγ protein was overexpressed in IFNγ transfected stable U87MG cells (Fig. 5.7B). The β actin was used as internal control protein for this analysis.

Fig 5.7. Western blot analysis of **(A)** Lane 1: Anti GMCSF Western in MCF-7 cells, Lane 2: Anti GMCSF Western in GMCSF transfected MCF-7 stable cells, Lane 3: β actin in MCF-7 cells, Lane 4: β actin in GMCSF transfected MCF-7 stable cells **(B)** Lane 1: Anti IFNγ Western in U87MG cells, Lane 2: Anti IFNγ Western in IFNγ

transfected U87MG stable cells, Lane 3: β actin in U87MG cells, Lane 4: β actin in IFNγ transfected U87MG stable cells.

5.3.4 Cell Viability Assay:

To observe the effect of different chemotherapeutic drugs on transfected cell lines, the cell viability of IFNγ transfected U87MG stable cells and GMCSF transfected MCF-7 stable cells was measured against their untransfected control and pCI backbone transfected control cells with drug treatment. The pCI neo vector backbone transfected MCF-7 and U87MG cells were taken as control to examine the effect of desired gene. However, no significant change in cell viability was observed in case of IFNγ transfected U87MG stable cells as compare to their control cells, after treatment with doxorubicin, cisplatin and 5FU (Fig. 5.8D, 5.8E, 5.8F). A considerable cell viability difference was obsereved in GMCSF transfected MCF-7 stable cells as compared to the control cells. Viability of GMCSF transfected MCF-7 stable cells was reduced to 25% with respect to their untransfected control cells, which showed that GMCSF transfected stable cells were more sensitive towards chemotherapeutic drugs, like doxorubicin, cisplatin and 5FU (Fig. 5.8A, 5.8B, 5.8C). Doxorubicin treatment from 1 to 100 µM showed a significant change in cell viability in GMCSF transfected MCF-7 stable cells with a maximum difference of 25% after 10 µM drug addition (Fig. 5.8A). Cisplatin treated cells showed even more sensitization of GMCSF transfected MCF-7 stable cells cells at lower drug concentration. IC_{50} was found to be 10 µg/mL, whereas for the MCF-7 control cells IC_{50} value was achieved at 25 µg/mL (Fig. 5.8B). In case of 5FU treatment the GMCSF transfected MCF-7 stable cells showed IC_{50} at 4.5 µM though the untransfected control cells have IC_{50} at 9 µM along with pCI neo plasmid backbone transfected control cells (Fig. 5.8C).

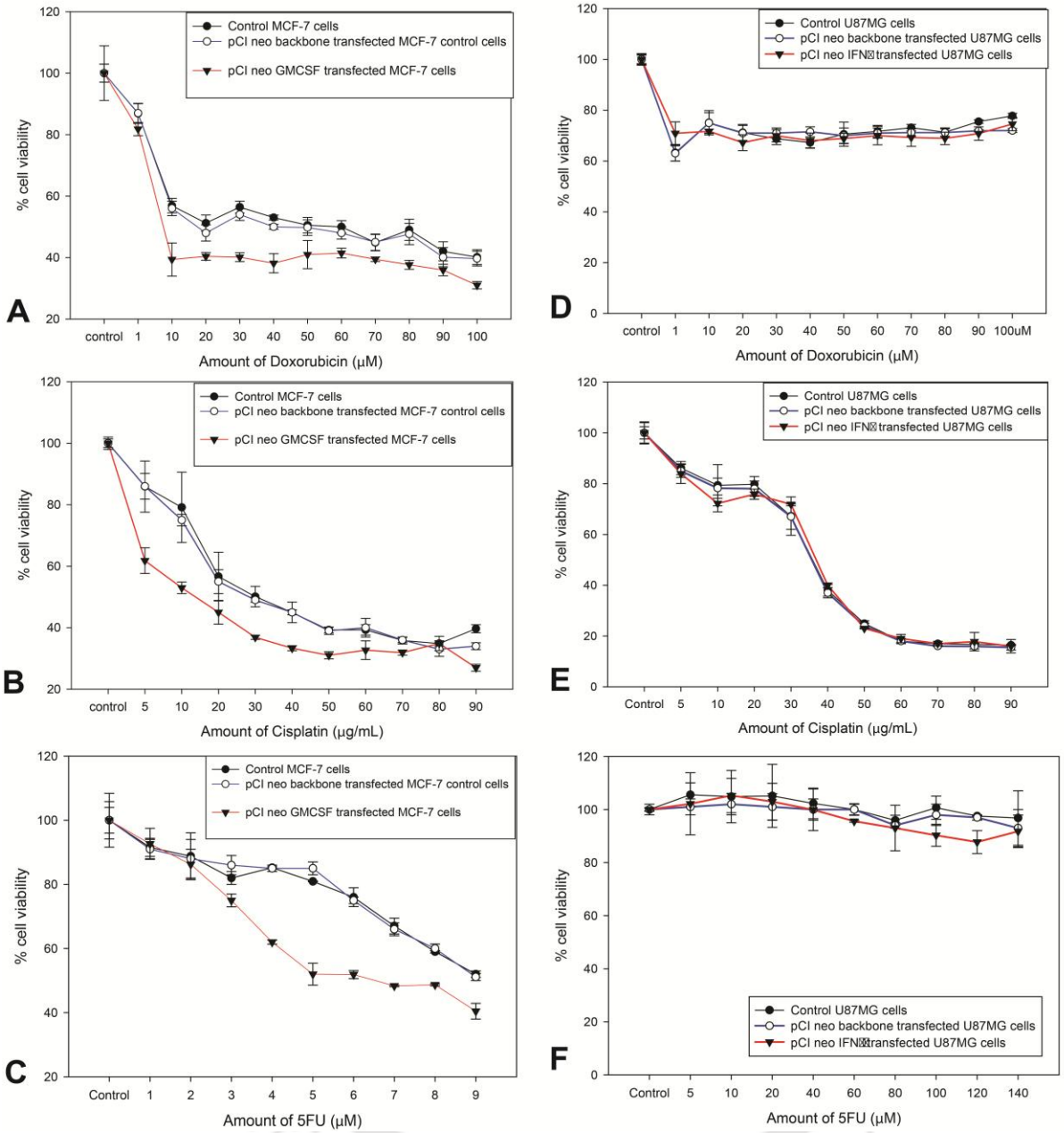

Fig 5.8. Cell viability analysis by MTT assay in **(A)** GMCSF transfected MCF-7 stable cells treated with doxorubicin along with respective control cells **(B)** Cisplatin treated GMCSF transfected MCF-7 stable cells treated along with respective control cells **(C)** 5FU treated GMCSF transfected MCF-7 stable cells along with control cells **(D)** IFNγ transfected U87MG cells treated with doxorubicin alon with respective control cells **(E)** Cisplatin treated IFNγ transfected U87MG cells along with control U87MG cells **(F)** IFNγ transfected U87MG cells treated with 5FU along with respective control cells.

5.3.5 Cell cycle analysis:

MTT assay results indicated a significant effect on GMCSF transfected MCF-7 stable cells. Further, it was important to check the cell cycle of the drug treated cells to delineate different phases of cells. FACS results showed that the various chemotherapeutic drugs were blocking different phases of cell cycle in 48 h. The block was more prominent in GMCSF transfected MCF-7 stable cells as compared to its control MCF-7 cells. Doxorubicin blocked G2 phase, cisplatin blocked S phase and 5FU blocked G1 phase more significantly in GMCSF transfected MCF-7 stable cells (Fig. 5.9).

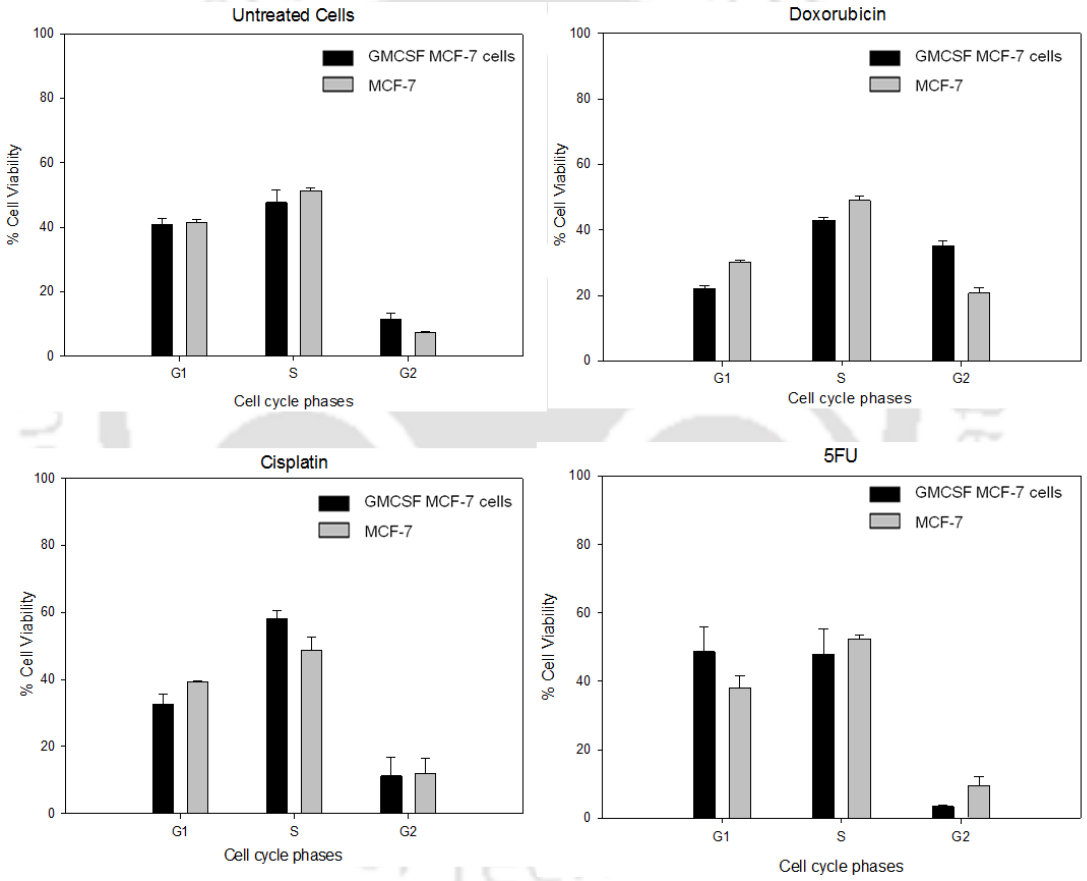

Fig 5.9. FACS based cell cycle analysis of GMCSF transfected MCF-7 stable cells as compared to control MCF-7 cells **(A)** Untreated cells **(B)** 5 FU treated cells **(C)** Cisplatin treated cells and **(D)** Doxorubicin treated cells. The values are represented as mean ± SD of three individual experiments with $p < 0.005$.

5.3.6 CFSE based doubling time calculation:

Doubling time calculation was performed for GMCSF transfected MCF-7 stable cells as the cell viability data indicated its more sensitization towards chemotherapeutic drugs and the cell cycle data indicated significant blocking in various cell cycle phases by these drugs as compared to their control MCF-7 cells. The results showed decrease in doubling time of GMCSF transfected cells (i.e. 26.686 h) with respect to MCF-7 control cells (29.42 h).

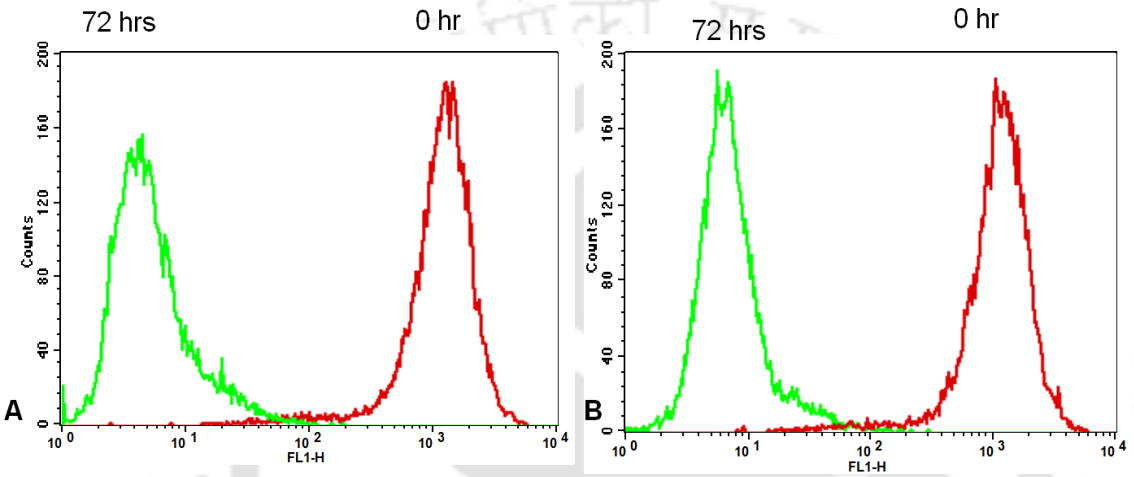

Fig 5.10. CFSE based proliferation analysis by doubling time calculation through flow cytometry in **(A)** MCF-7 cells **(B)** GMCSF transfected MCF-7 stable cells.

5.3.7 Analysis of Cyclins:

Cyclin concentration varies with the progression of cell cycles in different phases. This whole process is helped by CDKs (cyclin dependent kinases). Thus, cyclins provide an indicative way to know more about the progress of cell cycle, check points and its underlying pathway. Hence, semiquantitaive RT PCR was performed to check the expression of various cyclins using the protocols described in chapter 3. It was found that expression of cyclin D1, E1 and B1 were increased in level upto two folds in GMCSF overexpressed cells, while cyclin A2 level was unaltered. But intrestingly after drug treatment, all cyclins were deregulated.

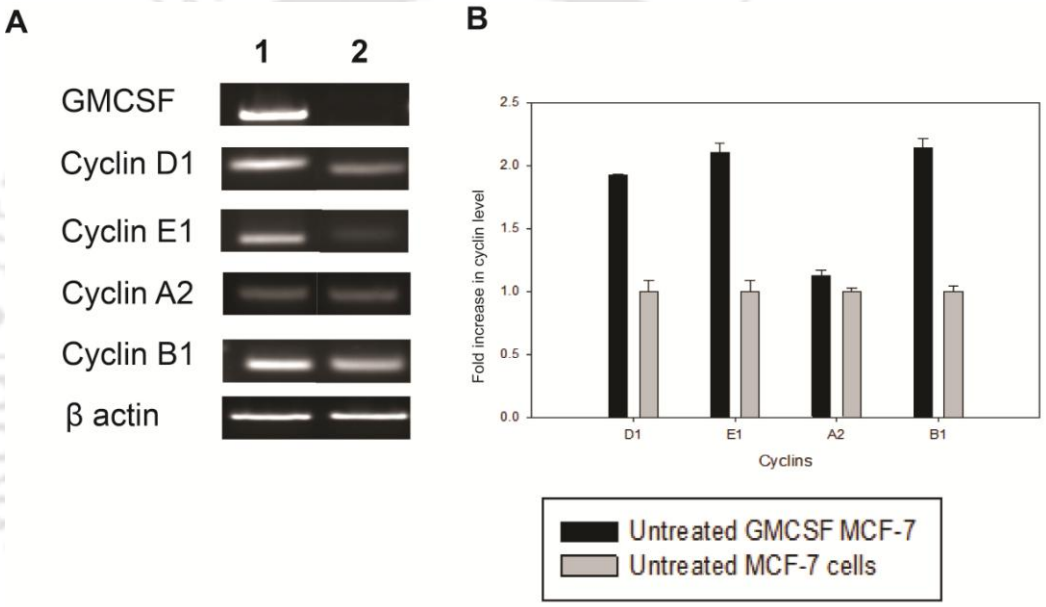

Fig 5.11. Cyclin expression profile of untreated cells by semiquantitative RT PCR **(A)** RT PCR analysis with different primers. Lane 1: GMCSF overexpressed MCF-7 stable cells, Lane 2: MCF-7 cells **(B)** Bar represents fold increase in the transcripts level. All data was presented as mean ±S.D. and statistical analysis was done by one way ANOVA in Sigma plot. Data were statistically significant with $p<0.05$.

In case of doxorubicin treated GMCSF transfected MCF-7 stable cells, cyclin D and B level were decreased significantly. The level of cyclin E did not altered much. Cyclin Al, which is responsible for S to G2 phase transition, was also not changed in all treated and untreated cell types (GMCSF transfected MCF-7 stable cells and MCF-7 cells).

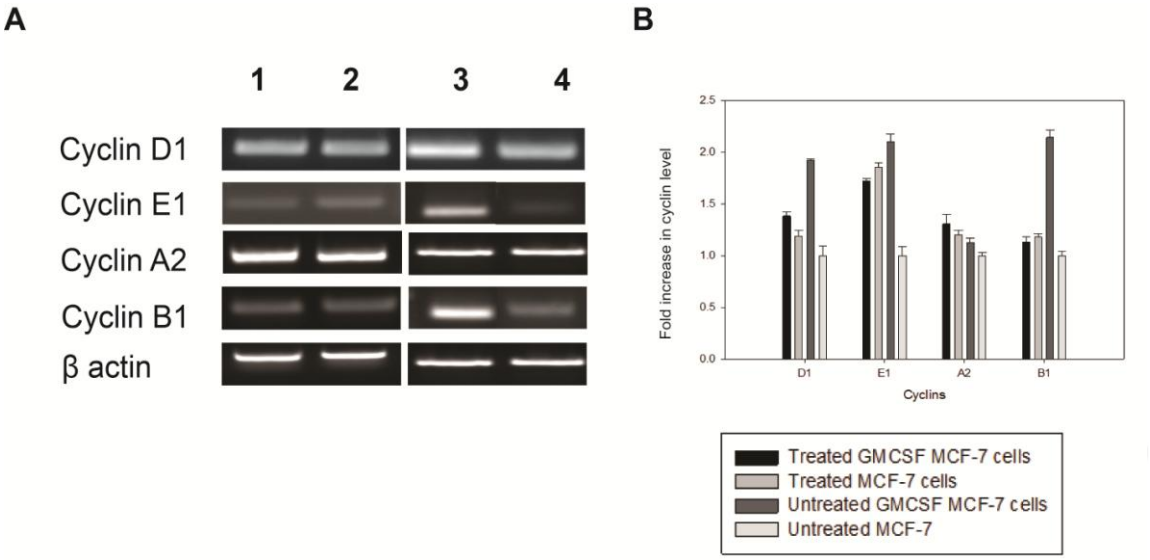

Fig 12. Cyclin expression profile of doxorubicin treated cells by semiquantitative RT PCR **(A)** RT-PCR analysis with different set of primers. Lane 1: GMCSF overexpressed MCF-7 cells, Lane 2: MCF-7 cells **(B)** Bar represents fold increase in transcripts level. All data has presented as mean ±S.D. and statistical analysis was done by one way ANOVA in Sigma plot. Data were statistically significant with $p<0.05$.

In cisplatin treated GMCSF MCF-7 cells, cyclin D, E and B level was decreased significantly, while the level of cyclin A ,which is the signature of blocking of the cells in S phase, was increased abruptly similar to cisplatin treated control MCF-7 cells and this result was also validated by cell cycle data also.

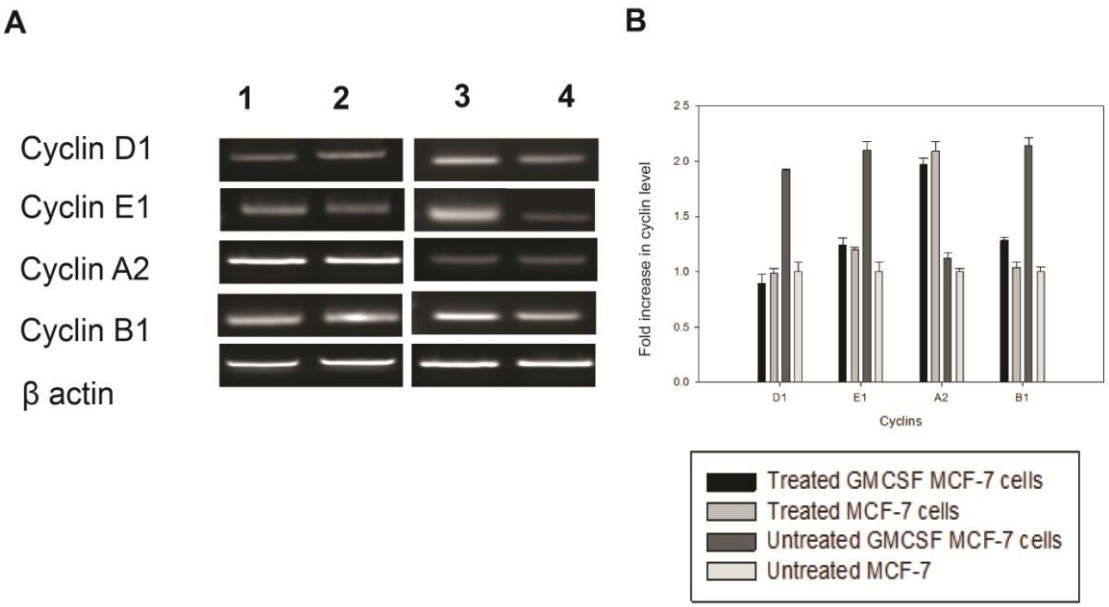

Fig 5.13. Cyclin expression profile of Cisplatin treated cells by semiquantitative RT PCR **(A)** RT PCR analysis with different set of primers. Lane 1: GMCSF overexpressed MCF-7 cells, Lane 2: MCF-7 cells **(B)** Bar represents fold increase in transcripts level. All data has presented as mean ±S.D. and statistical analysis was done by one way ANOVA in Sigma plot. Data were statistically significant with $p<0.05$.

For 5 FU treated cells, there was a prominent increase in cyclin E level in GMCSF overexpressed cells as compared to the treated control MCF-7 cells (2 fold) (Chung *et al*, 2010). Level of cyclin A2 was similar to that of the treated control cells, but there was no effect on the level of cyclin D1, B1 in GMCSF overexpressed cells after drug treatment.

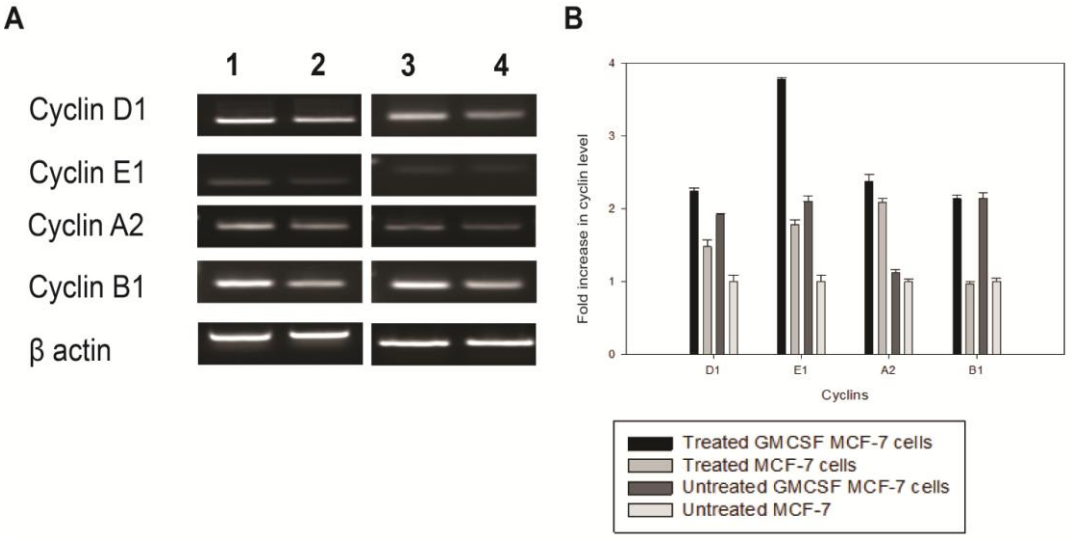

Fig 5.14. Cyclin expression profile of 5FU treated cells by semiquantitative RT PCR **(A)** PCR analysis with different set of primers. Lane 1: GMCSF overexpressed MCF-7 cells, Lane 2: MCF-7 cells **(B)** Bar represents fold increase in transcripts level. All data has presented as mean ±S.D. and statistical analysis was done by one way ANOVA in Sigma plot. Data were statistically significant with $p<0.05$.

Experimental results showed that overexpression of a proliferative cytokine in cancer cells elevated the level of cyclins could possibly shorten the cell doubling time. However, the cells became sensitized to drugs and as a result significant decrease in cell viability was observed in response to treatment of chemootherapeutic drugs. Chemotherapeutic drugs were also more effective in blocking cell cyle phases in GMCSF overexpressing cells by reducing and deregulating various cyclin expressions.

5.4 Conclusion

In this chapter, the effect of homogenously overexpressed cytokine GMCSF in cancer cells were studied. Experimental data showed more sensitization of GMCSF overexpressed breast cancer cells toward chemotherapeutic drugs, such as cisplatin, doxorubicin and 5FU. However, IFNγ overexpressing neuroblastoma cells did not show any such drug sensitization. Cell cycle analysis of GMCSF overexpressing cells a significant blockage to cell cycle as compared to MCF-7 control cells after drug treatment. The cyclin expressions of GMCSF overexpressed cells was also elevated, which reduced the cell doubling time. Thus in this section an incresed drug sensitization of GMCSF overexpressed MCF-7 cells was reported. Thus, this overexpression model can be explored to test the drug sensitization involving signaling molecules.

5.5 References

1. Bauer, K. (1977). Degradation of hypothalamic hormones. Naunyn Schmiedebergs Arch. Pharmacol. *297 Suppl 1*, S55–56.

2. Chung, H., Chaudhry, J., Lopez, C.G., and Carethers, J.M. (2010). Cyclin E and histone H3 levels are regulated by 5-fluorouracil in a DNA mismatch repair-dependent manner. Cancer Biology & Therapy *10*, 1147–1156.

3. Li, D.Y., Eberspächer, J., Wagner, B., Kuntzer, J., and Lingens, F. (1991). Degradation of 2,4,6-trichlorophenol by Azotobacter sp. strain GP1. Appl. Environ. Microbiol. *57*, 1920–1928.
4. Lowry, O.H., Rosebrough, N.J., Farr, A.L., and Randall, R.J. (1951). Protein measurement with the Folin phenol reagent. J. Biol. Chem. *193*, 265–275.
5. Mezzano, S.A., Droguett, M.A., Burgos, M.E., Ardiles, L.G., Aros, C.A., Caorsi, I., and Egido, J. (2000). Overexpression of chemokines, fibrogenic cytokines, and myofibroblasts in human membranous nephropathy. Kidney International *57*, 147–158.
6. Mosmann, T. (1983). Rapid colorimetric assay for cellular growth and survival: application to proliferation and cytotoxicity assays. J. Immunol. Methods *65*, 55–63.
7. Quah, B.J.C., Warren, H.S., and Parish, C.R. (2007). Monitoring lymphocyte proliferation in vitro and in vivo with the intracellular fluorescent dye carboxyfluorescein diacetate succinimidyl ester. Nat Protoc *2*, 2049–2056.
8. Riccardi, C., and Nicoletti, I. (2006). Analysis of apoptosis by propidium iodide staining and flow cytometry. Nat Protoc *1*, 1458–1461.
9. Tu, S.P., Quante, M., Bhagat, G., Takaishi, S., Cui, G., Yang, X.D., Muthuplani, S., Shibata, W., Fox, J.G., Pritchard, D.M., *et al*. (2011). IFN- Inhibits Gastric Carcinogenesis by Inducing Epithelial Cell Autophagy and T-Cell Apoptosis. Cancer Research *71*, 4247–4259.

CHAPTER 6

Conclusion and Future Prospects

Conclusions and Future Prospects

The main focus of the present dissertation has been to develop two different recombinant cytokines using rDNA technology and understand their interaction with cancer cells with an aim of pursuing their therapeutic implications.

In the current thesis, the FDA approved important cytokines viz GMCSF an IFNγ were cloned and expressed in bacterial system. The main work was focused on purification, characterization of these two recombinant cytokines, and their effects on cancer cells alone or in combination with chemotherapeutic drugs. The cytokines were purified to homogeneity by affinity column chromatography technique. The proliferative action of the recombinant GMCSF and the anti-cell proliferative effect of the recombinant IFNγ loaded composite nanoparticles on cancer cell lines were examined. Mixed population of macrophages and cancer cells in presence of recombinant GMCSF and IFNγ exhibited preferential activation of macrophages and prominent killing of cancer cells. Lastly, stable cell lines over-expressing these cytokines were more sensitized towards chemotherapeutic drugs.

The importance of recombinant therapeutic proteins, their cloning strategy, purification and functional activities were described in the chapter 1. The chapter 1 also illustrated important polymeric nanoparticles for protein stabilization, role of cytokines as adjuvant and immune surveillance in cancer therapy, importance of recombinant cytokines and anticancer drugs in combination therapy.

The cloning of GMCSF cytokine from ACHN (renal carcinoma) cells and its purification by affinity chromatography has been reported in chapter 2. The chapter described characterization of recombinant GMCSF by MALDI spectroscopy, Western blot, and circular dichroism spectra analysis. The dose dependent cell proliferative activity of the recombinant GMCSF on MCF-7 (human breast cancer), THP-1 (human leukemia), U87MG (human neuroblastoma) and Raw 264.7 (mouse macrophages) cells and its *in silico* structural conformation analysis were elucidated in this chapter.

Next, chapter 3 reported the cloning and functional significance of IFNγ of human origin. The chapter illustrates the methods for cloning of cytokine IFNγ from human blood cDNA, detergent solubilization of protein from inclusion bodies, and its purification by affinity chromatography. The chapter also reported characterization of the recombinant IFNγ by MALDI mass spectroscopy and Western blot analysis. Most importantly, the recombinant IFNγ was stabilized in the composite PLGA

nanoparticles loaded with Ag NPs (GST IFNγ-Ag PLGA NPs), which showed profound anti-cancer effects of recombinant IFNγ protein and silver nanoparticles (Ag NPs). Experimental results depicted complementary effects of the composite nanoparticles, where the recombinant IFNγ had blocked the cell cycle and allowed cell surface receptor targeting; on the other hand, the Ag NPs had induced apoptosis. Thus, the combination of the duos led to efficient induction of apoptosis in cancer cells.

The combined effect of two recombinant GMCSF and IFNγ in mixed cell population of macrophage cells (Raw 264.7) and breast cancer cells **(**MCF-7) has been reported in chapter 4. The combined function of the recombinant cytokines was examined for proliferation and activation of macrophage cells, and subsequent generation of ROS, which in turn kills the cancer cells. The GMCSF treated MCF-7 cells were mixed with the macrophages and treated with recombinant IFNγ and GMCSF simultaneously. GMCSF allowed the macrophages to remain proliferative, whereas, the recombinant IFNγ generated ROS to trigger cancer cell death. FACS based assay showed efficient MCF-7 cell death in the mixed population indicating possible role of these two recombinant cytokines duos in controlling growth of cancer cells. FACS analysis exhibited 15-20% of cancer cell death in presence of IFNγ protein. The effect was augmented upto 25-30% in the mixed cell culture condition with macrophages. Again, to mimic the condition of chemotherapy in solid tumor, the cells in coculture conditions were treated with doxorubicin, which showed substantial cancer cell death. Addition of purified GMCSF, as a potent growth proliferating agent retrived survival of macrophages in presence of doxorubicin. This work concluded that such approach may be explored to treat solid tumor with chemotherapeutic drugs along with adjuvant cytokine to augment phagocytic effect of macrophages and suppressed tumor growth efficiently.

Generation of the cell lines over-expressing GMCSF and IFNγ have been reported in the chapter 5. The GMCSF overexpressing MCF-7 cells and IFNγ overexpressing U87MG cells were developed. The chapter reported the effects of chemotherapeutic drugs, doxorubicin, 5FU and cisplatin on these two cytokine over-expressing cells. However, IFNγ over-expressing cells did not show any significant change in cell viability, but GMCSF over expressing cells were more sensitized towards the drugs. This observation was explained by cell cycle analysis and semi -quantitative measurement of cyclins expression of the drug treated cells. Experimental results

exhibited preferential cell cycle blockage of GMCSF overexpressing cells in presence of doxorubicin, cisplatin and 5FU.

This current study leaves plenty of scope to address by these recombinant cytokines in combination therapy.

Future prospects:

- Recombinant GMCSF and IFNγ cytokines may be explored in combination therapy.
- Recombinant IFNγ cytokine delivered by nanoparticles as therapeutic agent.
- Delineation of molecular pathways to explore use of recombinant GMCSF and IFNγ along with chemotherapeutic drugs.
- Molecular events involved in the increased sensitization of GMCSF overexpressing cells may be explored.
- Combined effect of cytokines and drugs may be examined in co-culture methods.

Appendix

SRL, India reagents: Acetic acid, Ammonium acetate, Ammonium persulphate (APS), Bis-acrylamide, Boric acid, Bromophenol blue, Chloroform, Di-sodium hydrogen phosphate, Ethanol, Ethylene di-amine tetra acetic acid, Formaldehyde, Glucose, Glycerol, Hydrochloric acid, Isopropyl alcohol, Isoamyl alcohol, Methanol, Potassium acetate, Potassium chloride, Potassium di hydrogen phosphate, Sulphuric acid, Sodium chloride, Sodium lauryl sulphate.

Himedia, India 3-[4, 5- dimethylthiazol-2-yl]-2, 5-diphenyltetrazolium bromide (MTT), Ampicillin**,** Bovine serum albumin (BSA).

Molecular biology grade reagents from Sigma Aldrich, USA: 2,3-bis-(2-methoxy-4-nitro-5-sulfophenyl)-2H- tetrazolium-5-carboxanilide (XTT), 2,7 Dichloro fluorescein diacetate (DCFDA), 5 Fluorouracil (5FU), Acrylamide, Agarose electrophoresis grade, Bradford reagent, Carboxyfluorescein succinimidyl ester (CFSE), Diethylpyrocarbonate (DEPC), Dimethylsulphoxide, G418, Glutathione-agarose beads, Isopropyl β-D-1-thiogalactopyranoside (IPTG), Lysozyme, Magnesium chloride hexahydrate, Polyethylene glycol 8000, Polyvinyl alcohol, Ponceau S, Phenol, Reduced glutathione, RIPA buffer, Sarkosyl, Sodium bicarbonate, Tris saturated phenol, Trypsin-EDTA, Trizma base (Tris), Triton X-100, Tween 20, Tetra methyl ethylene diamine (TEMED), Tri reagent.

Merck, India: 5-bromo-4-chloro-3-indolyl-β-D-galactopyranoside (X-gal), β-mercaptoethanol, Glycine, Glutaraldehyde, Methanol, **S**odium acetate, Sodium carbonate, Sodium thiosulphate, PCR Master mix.

Pfizer, India: Cisplatin (1 mg/mL)

Parental Drugs, India: Doxorubicin

Amresco, USA: (3,3' diaminobenzidine) DAB, dithiothreitol (DTT), Ribonuclease A.

Qiagen, India: Protease (7.5 AU), Gel extraction kit.

Bacterial culture medium from: Luria Bertani (LB) Broth, Bacteriological agar powder, ampicillin sodium salt, chloramphenicol, tetracycline from **Himedia, India**.

Mammalian cell culture medium and components: Dulbecco's modified Eagle's media (DMEM) and Penicillin-Sterptomycin antibiotic solution from **Sigma**, fetal calf serum- from **PAA**.

Enzymes: *Not I, Bam HI, Xho I, Eco RI*, - from **NEB**, **UK**. T4 DNA ligase from-**Promega,U.S.A.**, Reverse transcriptase from **Fermentas, Lithuania**, Red Taq polymerase **(Bioline, UK**).

Blotting Membranes and Filters: PVDF membrane (0.2 µm) from **Milipore, U.S.A.**, 3mm filter paper from **Whatman, USA**.

DNA and protein markers: Hyperladder DNA marker (200 bp to 10 kb), Protein marker, Broad range (2-212 kDa), Color plus prestained protein marker (7-170 kDa) **(New England Biolabs, USA),**
dNTPs, $MgCl_2$ **(Bioline, UK),** 100 bp ladder **(Bangalore Genei, India).**

Plastic and Glasswares: PCR tubes - from **Axygen, USA**; micro pipette tips, micro centrifuge tubes, petri dishes and other plastic wares- from **Tarson Products Pvt. Ltd., India**. Glasswares- from **Borosil International, India**.

Cell lines: All the cell lines were procured from National Centre for Cell Science, Pune, India.

Primary antibodies: Mouse anti human IFNγ antibody (554549), Rat anti human GMCSF antibody (554503), PE conjugated rabbit anti Caspase-3 antibody **(BD Pharmingen, USA),** Rabbit anti human β actin **(Cell Signalling Technologies, USA).**

Secondary antibodies: Goat anti-mouse HRP conjugated IgG **(Sigma),** anti-rabbit HRP conjugated IgG **(Cell Signalling Technologies, USA),** Goat anti rat HRP conjugated polyclonal antibody **(Calbiochem, Merck, India).**

Plasmids
pGEMT Easy (Amp^r) *E.coli* cloning vector with *Eco RI* site **(Promega, USA)**
pCI neo (Amp^r in bacteria, Neo^r in mammalian cells) Mammalian expression vector **(Promega, USA)**
pGEX4T2 (Amp^r) MCS in bacterial expression vector **(GE Healthcare, Sweden)**

Table 1. Buffers and their constituents:

Phosphate buffered saline	137 mM NaCl, 2.68 mM KCl, 7.98 mM Na_2HPO4, 1.4 mM KH_2PO4, pH 7.4
TSS buffer for transformation	10% (w/v) PEG 8000, 0.6% (w/v) $MgCl_2.6H_2O$, 5% (v/v) DMSO in LB media
Tris-acetate EDTA (TAE) 50X (100 mL)	24.2 g Tris base, 5.71 mL of glacial acetic acid, 10 mL of 0.5 M EDTA (pH 8.0)
Acetate buffer	1 M ammonium acetate and 0.077% (v/v) glacial acetic acid in sterile distilled water, pH 4.2
Alkaline lysis solution I	50 mM glucose, 25 mM Tris-Cl (pH-8.0), EDTA (10 mM)
Alkaline lysis solution II	0.2 N NaOH, (freshly diluted from 10 N stock), 1% (w/v) SDS
Alkaline lysis solution III	5 M potassium acetate (60 mL), glacial acetic acid (11.5 mL), water (28.5 mL)
4X protein loading dye (for 10 mL)	2.0 ml 1M Tris-HCl (pH 6.8), 0.8 g SDS, 4.0 ml 100% glycerol, 0.4 mL 14.7 M β-mercaptoethanol, 8 mg bromophenol blue in water
6X DNA loading dye	0.25 (%)(w/v) bromophenol blue, 0.25% (w/v) xylene cyanol FF, 30% (v/v) glycerol in H_2O
Cleaning buffer 1(pH-8.5)	0.1 M boric acid, 0.5 M NaCl, adjust the pH 8.5 with sodium hydroxide
Cleaning buffer 1(pH-4.5)	0.1 M sodium acetate, 0.5 M NaCl, pH 4.5 with acetic acid
Polyacrylamide solution (30%)	29.2% (w/w) acrylamide, 0.8% (w/w) N,N'-methylenebisacrylamide
GMCSF inclusion body dissolving Solution I	10 mM phosphate buffer saline (PBS), 1 mM PMSF, 1 mM EDTA, 1% Triton X-100
GMCSF inclusion body dissolving Solution II	50 mM TrisCl, 5 mM EDTA and 2% Triton X-100
GMCSF inclusion body dissolving Solution III	50 mM TrisCl containing 1% Na deoxycholate, 0.5 mM EDTA
Lysis Buffer for purifying GST IFNγ protein	50 mM Tris pH 8.0 with 1% of sarkosyl, 1 mM PMSF, 1 mM EDTA

Table 2. Primers list:

GMCSF pGEMT Easy primer	Forward: 5' ATGTGGCTGCAGAGCCTGCTG 3' Reverse: 5' TCACTCCTGGACTGGCTCCCA 3'
GMCSF pGEX4T2 primer	Forward: 5' GTGGATCCATGTGGCTGCAGAGCCT 3' Reverse: 5' GACTCGAGTCACTCCTGGACTGGCTC 3'
GMCSF pCI neo primer	Forward: 5' GCCTCGAGATG GGCTGCAGAGCCTG 3' Reverse: 5' GAGCGGCCGCTCACTCCTGGACTGGCT 3'
IFNγ pGEMT Easy primer	Forward: 5' ATGTGGCTGCAGAGCCTGCTG 3' Reverse: 5' TCACTCCTGGACTGGCTCCCA 3'
IFNγ pGEX4T2 primer	Forward: 5' GCGGATCCATGAAATATACAAGTTAT 3' Reverse: 5' GACTCGAGTTACTGGGATGCTCTTC 3'
IFNγ pCI neo primer	Forward: 5' GCCTCGAGATGAAATATACAAGTTA 3' Reverse: 5' CAGCGGCCGCTTACTGGGATGCTCTT 3'
Cyclin D1	Forward: 5' CGCCCCACCCCTCCAG 3' Reverse: 5' CGCCCAGACCCTCAGACT 3'
Cyclin E1	Forward: 5' CGCCCAGACCCTCAGACT 3' Reverse: 5' CGCCCAGACCCTCAGACT 3'
Cyclin A2	Forward: 5' CGCCCAGACCCTCAGACT 3' Reverse: 5' CGCCCAGACCCTCAGACT 3'
Cyclin B1	Forward: 5' CGCCCAGACCCTCAGACT 3' Reverse: 5' CGCCCAGACCCTCAGACT 3'
β actin	Forward: 5' CGCCCAGACCCTCAGACT 3' Reverse : 5' CGCCCAGACCCTCAGACT 3'

List of publications:

1. Nidhi Chaubey, Amaresh Kumar Sahoo, Arun Chattopadhyay, Siddhartha Sankar Ghosh (2014). Silver nanoparticle loaded PLGA composite nanoparticles for improving therapeutic efficacy of recombinant IFNγ by targeting cell surface *Biomaterials Science*, DOI:10.1039/C3BM60251F.

2. Nidhi Chaubey, Siddhartha Sankar Ghosh (2013). Molecular cloning, Purification and Functional implications of recombinant GST tagged hGMCSF cytokine, *Applied Biochemistry Biotechnology*, 169(5):1713-26.

3. Nidhi Chaubey, Siddhartha Sankar Ghosh. Pleotropic effects of cytokines in cancer. (Manuscript under preparation)

4. **Nidhi Chaubey**, Siddhartha Sankar Ghosh. *In vitro* effect of cytokines in a mixed cell population of cancer cells with macrophages. (Manuscript under preparation)

Conferences:

1. **World Congress on Biotechnology-2012, 4-6th May, Hyderabad.**

Cloning, Expression, Purification and Functional aspects of recombinant GST tagged GMCSF cytokine. Nidhi Chaubey, Siddhartha Sankar Ghosh.

2. **Carcinogenesis 2012, 19-21th November, New Delhi.**

GST tagged IFNγ: Cloning, Expression, Purification and Functional aspects of recombinant cytokine. Nidhi Chaubey, Siddhartha Sankar Ghosh.

3. **Society of Biological Chemists 2012, 8-11th November, Kolkata.**

Recombinant GST-tagged Human Granulocyte Macrophage Colony Stimulating Factor (GST-hGMCSF) in Combination Therapy. Nidhi Chaubey, Siddhartha Sankar Ghosh.

4. **FICS 2012, 2-3rd, December, IIT Guwahati.**

Recombinant IFNγ encapsulated polymeric nanoparticles in cancer therapy.
Nidhi Chaubey, Amaresh Kumar Sahoo, Siddhartha Sankar Ghosh.